Covariate-assisted Sparse Tensor Completion

Hilda S Ibriga and Will Wei Sun

Purdue University

Abstract

We aim to provably complete a sparse and highly-missing tensor in the presence of covariate information along tensor modes. Our motivation comes from online advertising where users' click-through-rates (CTR) on ads over various devices form a CTR tensor that has about 96% missing entries and has many zeros on non-missing entries, which makes the standalone tensor completion method unsatisfactory. Beside the CTR tensor, additional ad features or user characteristics are often available. In this paper, we propose Covariate-assisted Sparse Tensor Completion (`COSTCO`) to incorporate covariate information for the recovery of the sparse tensor. The key idea is to jointly extract latent components from both the tensor and the covariate matrix to learn a synthetic representation. Theoretically, we derive the error bound for the recovered tensor components and explicitly quantify the improvements on both the reveal probability condition and the tensor recovery accuracy due to covariates. Finally, we apply `COSTCO` to an advertisement dataset consisting of a CTR tensor and ad covariate matrix, leading to 23% accuracy improvement over the baseline. An important by-product is that ad latent components from `COSTCO` reveal interesting ad clusters, which are useful for better ad targeting.

Key Words: clustering, high-dimensional statistics, low-rank tensor completion, non-convex optimization, sparsity

[i]Hilda S Ibriga is a PhD candidate of Statistics at Purdue University. Will Wei Sun is Assistant Professor of Krannert School of Management at Purdue University. Contact email: sun244@purdue.edu

1 Introduction

Low-rank tensor completion aims to impute missing entries of a partially observed tensor by forming a low-rank decomposition on the observed entries. It has been widely used in various scientific and business applications, including recommender systems (Symeonidis et al., 2008; Karatzoglou et al., 2010; Bi et al., 2018), neuroimaging analysis (Zhou et al., 2013; Wang et al., 2017; Tang et al., 2020), signal processing (Papalexakis et al., 2016; Sidiropoulos et al., 2017), social network analysis (Hoff, 2015; Jing et al., 2020), personalized medicine (Luo et al., 2017; Wang et al., 2019), and time series analysis (Chen et al., 2019). We refer to the recent surveys on tensors for more real applications (Song et al., 2019; Bi et al., 2020). In spite of its popularity, it is also well known that when the missing percentage of the tensor is very high, a standalone tensor completion method often fails at yielding desirable recovery results. Fortunately, in many real applications, we also have access to some side covariate information. In this paper, we aim to complete a sparse and highly-missing tensor in the presence of covariate information along tensor modes.

Our motivation originates from online advertising application, where advertisement (ad) information is usually described by both users' click behavior data and ad characteristics data. More formally, the users' click data refer to as the click-through rate (CTR) of the ads, quantifying the user click behavior on different ads, various platforms, different devices or over time etc. The CTR data is therefore often represented as a tensor of three or four modes, e.g., the user $\times$ ad $\times$ device tensor shown in Figure 1. The ad characteristic data on the other hand is usually represented in the form of a matrix which contains context information for each ad. Typically in online advertising not all users are presented with all ads, thus creating many missing data in the CTR tensor. Moreover, users typically engage with a small subset of the ads that are presented to them. Low rates of ads engagement is a common phenomenon in online advertising which begets a highly sparse CTR tensor (many zero entries) with high percentage of missing entries. For instance, in our real data shown in Section 6, the ad CTR tensor has 96% missing entries and is highly sparse with only 40% of the revealed entries being nonzero. We show in Sections 5 and 6 that methods using a standalone tensor completion often fail at recovering the missing entries of a tensor with such missing percentage. On the contrary the ad characteristic data is usually relatively complete and dense. It therefore becomes advantageous to incorporate the ad characteristic information in a model to recover the missing entries of the CTR tensor. The structure of the sparse CTR tensor with missing entries

coupled with the ad characteristic data is illustrated in Figure 1. As shown in Figure 1 the two sources of data; CTR tensor and ad covariates matrix are coupled along the ad mode.
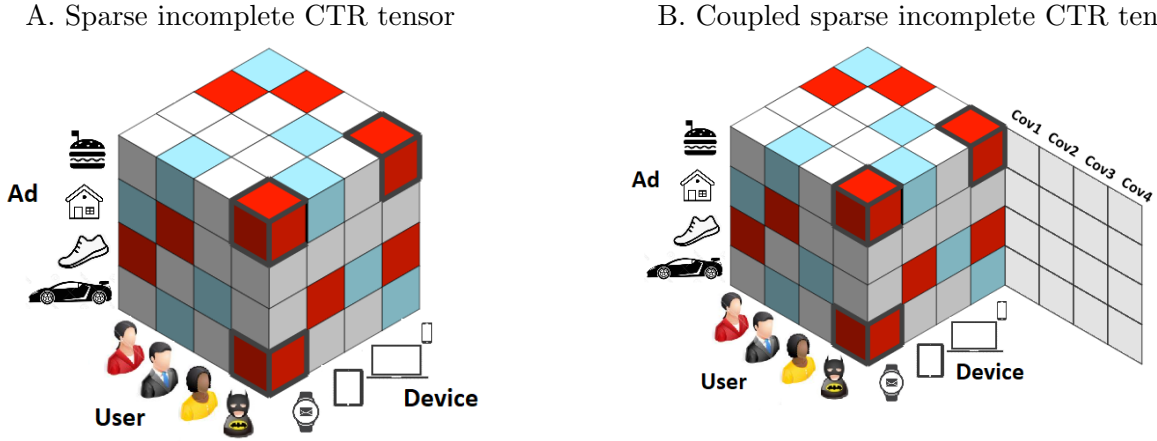
A. Sparse incomplete CTR tensor
B. Coupled sparse incomplete CTR tensor

Figure 1: A. sparse (user × ad × device) CTR tensor with missing entries; B. sparse CTR tensor with missing entries coupled with matrix of ad covariates. The red cells represent missing entries; blue cells represent zeros, grey cells represent non-zero entries.

In this article, we propose Covariate-assisted Sparse Tensor Completion (COSTCO) to recover missing entries in highly sparse tensor with a large percentage of missing entries. Under the low-rank assumption on both the tensor and the covariate matrix, we assume the latent components corresponding to the coupled mode are shared by both the tensor and matrix decomposition. This model encourages a synthetic representation of the coupled mode by leveraging the additional covariate information into tensor completion. We formulate the parameter estimation as a non-convex optimization with sparsity constraints, and propose an efficient sparse alternating least squares approach with an extra refinement step. Our algorithm jointly extracts latent features from both tensor and the covariate matrix and uses covariate information to improve the recovery accuracy of the recovered tensor components. We showcase through extensive numerical studies that our COSTCO is able to successfully recover entries for a tensor even with 98% missing entries.

In addition to the above methodological contributions, we also make theoretical contributions to the understanding of how side covariate information affects the performance of tensor completion. In particular, we derive the non-asymptotic error bound for the recovered tensor components and explicitly quantify the improvements on both the reveal probability condition and the tensor recovery accuracy due to additional covariate information. We show that COSTCO allows for a relaxation on

the lower bound of the reveal probability p compared to that required in tensor completion with no covariates, see Assumption 5 for details. In the extreme case where all tensor modes are coupled with covariate matrices, we can still recover the tensor entries even when the reveal probability of the tensor is close to zero. Moreover, we present the statistical errors for the shared tensor component (corresponding to the coupled mode) and non-shared tensor components separately to demonstrate the gain brought in through the coupling of covariates information in the model. We show that given some mild assumptions on noise levels and condition numbers, our COSTCO guarantees an improved recovery accuracy for the shared component. Unlike existing theoretical analysis on low-rank tensors which assumes the error tensor to be Gaussian, we do not impose any distributional assumption on the error tensor or the error matrix. Our theoretical results depends on the error term only through its sparse spectral norm.

Finally, we apply our COSTCO to the advertising data from a major internet company to demonstrate its practical advantages. COSTCO makes use of both ad CTR tensor and ad covariate matrix to extract the latent component which leads to about 23% accuracy improvement in recovering the missing entries when compared to the standalone sparse tensor completion method. Moreover, an important by-product from our COSTCO is to use the recovered ad latent components for better ad clustering. Ad clustering is an essential task for targeted advertising that helps lead useful ad recommendation for online platform users. Cluster analysis on our ad latent components reveals interesting and new clusters that link different product industries which are not formed in existing clustering methods. Such findings could directly help the marketing team to strategize the ad planing procedure accordingly for better ad targeting.

1.1 Related work and paper organization

Tensor completion with side information: The simultaneous extraction of latent information from multiple sources of data can be interpreted as a form of data fusion (Lin et al., 2009; Koren et al., 2009; Acar et al., 2011, 2013; Haghighat et al., 2016; Zhou et al., 2017; Li et al., 2018; Kishan et al., 2018; Choi et al., 2019; Huang et al., 2020; Li et al., 2020; Xue and Qu, 2020). Among them, there are a few work related to tensor completion with side information. The most related work to our approach is the gradient-based all-at-once optimization method proposed by Acar et al. (2011) which updates the matrix and tensor components all at once. We compare it in our experiments and find that it is consistently inferior to our COSTCO. Zhou et al. (2017) proposed a Riemannian

conjugate gradient descent algorithm to solve the tensor completion problem in the presence of side information. However, this procedure does not address the tensor completion problem in the presence of high percentage of missing entries combined with a high sparsity level. Choi et al. (2019) developed a fast and scalable algorithm for the estimation of shared latent features in coupled tensor matrix model. However, their approach does not allow missing entries and only works for complete data. Importantly, all the aforementioned works did not provide any theoretical analysis for their methods. Kishan et al. (2018) proposed a convex coupled tensor-matrix completion method through the use of coupled norms and derived its excess risk bound. In a more general setting, Huang et al. (2020) applied the tensor ring decomposition method on the coupled tensor-tensor problem and derived the excess risk bound. However, the methods considered in these two works do not account for noise in the tensor or matrix, i.e., their model is noiseless, nor do they consider the sparse tensor case. To the best of our knowledge, our work is the first provably method that is tailored for completing a highly sparse and highly missing tensor in the presence of covariate information.

Tensor completion with theoretical guarantees: Our theoretical analysis is related to a list of recent theoretical work in standalone tensor completion that does not incorporate covariate information (Jain and Oh, 2014; Zhang, 2019; Xia and Yuan, 2019; Cai et al., 2019; Xia et al., 2021). In particular, Jain and Oh (2014) provided recovery guarantee for symmetric and orthogonal tensors with missing entries, but did not explore recovery for the tensor completion with coupled covariates nor did they address the case of the non-orthogonal, noisy and sparse tensor. Zhang (2019) established a sharp recovery error for a special tensor completion problem, where the missing pattern was not uniformly missing but followed a cross structure. Xia and Yuan (2019) proved exact recovery for the noiseless tensor completion problem under a uniform random sampling schema. Unlike our analysis which is based on the CP model, they do not address the noisy tensor case and analyze the completion problem under the Tucker model representation which leads to different assumptions than those required in our case. In their recent work, Xia et al. (2021) proposed a two-step algorithm (a spectral initialization method followed by the power method) for the noisy Tensor completion case and established the optimal statistical rate in low-rank tensor completion. Different from our model, they assumed the error tensor to be subgaussian and did consider sparsity in tensor completion. Cai et al. (2019) also independently proposed a provable two stage algorithm (initialization followed by gradient descent) for the noisy tensor completion problem. These two works provide ground breaking theoretical contributions to tensor completion. Importantly, none

of the aforementioned work accommodates the inclusion of covariate information in the tensor completion model. The coupled sparse tensor and matrix formulation in our COSTCO poses unique difficulties in the theoretical analysis. The unequal weights of the tensor and matrix prevent us to obtain a close-form solution for the alternative least squares problem compared to the traditional tensor completion. Moreover, the presence of non-orthogonality, general noise, and sparsity in our model introduce additional challenges. These make our theoretical analysis far from a simple extension to the standard tensor completion problem as it calls for new techniques and assumptions.

Paper organization: The rest of the paper is organized as follows. Section 2 reviews some notations, basic definitions of algebra of tensors. Section 3 presents our model, the optimization problem and our algorithm along with procedures for initialization and parameter tuning. Section 4 presents the main theoretical results. Section 5 contains a series of simulation studies. Section 6 applies our algorithm to an advertisement data set to illustrate its practical advantages. All proof details, lemmas and additional simulation results are left in the supplemental material.

2 Notation and Preliminaries

In this section, we introduce some notation, and review some background on tensors. Throughout the paper we denote tensors by Euler script letters, e.g., $\mathcal{T}, \mathcal{E}$. Matrices are denoted by boldface capital letters, e.g., $\mathbf{A}, \mathbf{B}, \mathbf{C}$; vectors are represented with boldface lowercase letters, e.g., $\mathbf{a}, \mathbf{v}$, and scalars are denoted by lowercase letters, e.g., a, λ. The $n \times n$ identity matrix $\mathbf{I}_n$ is simply written as $\mathbf{I}$ when the dimension can be easily implied from the context.

Following Kolda and Bader (2009), we use the term tensor to refer to a multidimensional array; a concept that generalizes the notion of matrices and vectors to higher dimensions. A first-order tensor is a vector, a second-order tensor is a matrix and a third-order tensor is a three dimensional array. Each order of a tensor is referred to as a mode. For example a matrix (second-order tensor) has two modes with mode-1 and mode-2 being the dimensions represented by the rows and columns of the matrix respectively. Let $\mathcal{T} \in \mathbb{R}^{n_1 \times n_2 \times n_3}$ be a third-order non-symmetric tensor. We denote its (i, j, k)th entry as $\mathcal{T}_{ijk}$. A tensor fiber refers to a higher order analogue of matrix row and column and is obtained by fixing all but one of the indices of the tensor. For the tensor $\mathcal{T}$ defined above, the mode-1 fiber is given by $\mathcal{T}_{:jk}$; the mode-2 fiber by $\mathcal{T}_{i:k}$ and mode-3 fiber by $\mathcal{T}_{ij:}$. Next the slices of the tensor $\mathcal{T}$ are obtained by fixing all but two of the tensor indices. For example the frontal, lateral and horizontal slices of the tensor $\mathcal{T}$ as denoted as $\mathcal{T}_{::k}$, $\mathcal{T}_{:j:}$ and $\mathcal{T}_{i::}$.

6

We define three different types of tensor vector products. For vectors $\mathbf{u} \in \mathbb{R}^{n_1}, \mathbf{v} \in \mathbb{R}^{n_2}, \mathbf{w} \in \mathbb{R}^{n_3}$, the mode-1, mode-2 and mode-3, tensor-vector product is a matrix defined as a combinations of tensor slices: $\mathcal{T} \times_1 \mathbf{u} = \sum_{i=1}^{n_1} \mathbf{u}_i \mathcal{T}_{i::}$, $\mathcal{T} \times_2 \mathbf{v} = \sum_{j=1}^{n_2} \mathbf{v}_j \mathcal{T}_{:j:}$, $\mathcal{T} \times_3 \mathbf{w} = \sum_{k=1}^{n_3} \mathbf{w}_k \mathcal{T}_{::k}$. The tensor multiplying two vectors along its two modes is a vector defined as: $\mathcal{T} \times_2 \mathbf{v} \times_3 \mathbf{w} = \sum_{j,k} \mathbf{v}_j \mathbf{w}_k \mathcal{T}_{:jk}$, $\mathcal{T} \times_1 \mathbf{u} \times_2 \mathbf{v} = \sum_{i,j} \mathbf{u}_i \mathbf{v}_j \mathcal{T}_{ij:}$, $\mathcal{T} \times_1 \mathbf{u} \times_3 \mathbf{w} = \sum_{i,k} \mathbf{u}_i \mathbf{w}_k \mathcal{T}_{i:k}$. Finally the tensor-tensor product is a scalar defined as $\mathcal{T} \times_1 \mathbf{u} \times_2 \mathbf{v} \times_3 \mathbf{w} = \sum_{i,j,k} \mathbf{u}_i \mathbf{v}_j \mathbf{w}_k \mathcal{T}_{ijk}$.

We denote $\|\mathbf{M}\|$ and $\|\mathbf{M}\|_F$ to be the spectral norm and the Frobenius norm of a matrix $\mathbf{M}$, respectively. The spectral norm of a tensor $\mathcal{T}$ is defined as

$$\|\mathcal{T}\| := \sup_{\|\mathbf{u}\|_2 = \|\mathbf{v}\|_2 = \|\mathbf{w}\|_2 = 1} \left| \mathcal{T} \times_1 \mathbf{u} \times_2 \mathbf{v} \times_3 \mathbf{w} \right|, \tag{1}$$

and its Frobenius norm is $\|\mathcal{T}\|_F := \left(\sum_{i,j,k} \mathcal{T}_{ijk}^2 \right)^{1/2}$. Define the sparse spectral norm of a matrix $\mathbf{M}$ as $\|\mathbf{M}\|_{<d_1>} := \sup_{\|\mathbf{u}\|_2 = 1, \|\mathbf{u}\|_0 = d_1} \|\mathbf{M} \times_1 \mathbf{u}\|_2$ and the sparse spectral norm of a tensor $\mathcal{T}$ as

$$\|\mathcal{T}\|_{<d_1,d_2,d_3>} := \sup_{\substack{\|\mathbf{u}\|_2 = \|\mathbf{v}\|_2 = \|\mathbf{w}\|_2 = 1 \\ \|\mathbf{u}\|_0 = d_1, \|\mathbf{u}\|_0 = d_2, \|\mathbf{u}\|_0 = d_3}} \left| \mathcal{T} \times_1 \mathbf{u} \times_2 \mathbf{v} \times_3 \mathbf{w} \right|,$$

where $d_1 < n_1$, $d_2 < n_2$, $d_3 < n_3$. When $d_1 = d_2 = d_3 = d$, we simplify $\|\mathcal{T}\|_{<d,d,d>}$ as $\|\mathcal{T}\|_{<d>}$.

Given a third-order tensor $\mathcal{T} \in \mathbb{R}^{n_1 \times n_2 \times n_3}$, we denote its CP decomposition as

$$\mathcal{T} = \sum_{r \in [R]} \lambda_r \mathbf{a}_r \otimes \mathbf{b}_r \otimes \mathbf{c}_r, \tag{2}$$

where $[R]$ indicates the set of integer numbers $\{1, \ldots, R\}$, and $\otimes$ denotes the outer product of two vectors. For example, the outer product of three vectors $\mathbf{a}_r \in \mathbb{R}^{n_1}$, $\mathbf{b}_r \in \mathbb{R}^{n_2}$ and $\mathbf{c}_r \in \mathbb{R}^{n_3}$ forms a third order tensor of dimension $n_1 \times n_2 \times n_3$ whose $(i, j, k)^{\text{th}}$ entry is equal to $a_{ri} \times b_{rj} \times c_{rk}$ where a_{ri} is the ith entry of $\mathbf{a}_r$. In (2), $\mathbf{a}_r, \mathbf{b}_r, \mathbf{c}_r$ are of unit norm; that is $\|\mathbf{a}_r\|_2 = \|\mathbf{b}_r\|_2 = \|\mathbf{c}_r\|_2 = 1$ for all $r \in [R]$; $\lambda_r \in \mathbb{R}^+$ is the rth decomposition weight of the tensor. We denote matrices $\mathbf{A} \in \mathbb{R}^{n_1 \times R}$, $\mathbf{B} \in \mathbb{R}^{n_2 \times R}$ and $\mathbf{C} \in \mathbb{R}^{n_3 \times R}$ whose columns are $\mathbf{a}_r, \mathbf{b}_r$ and $\mathbf{c}_r$ for $r \in [R]$ respectively as,

$$\mathbf{A} = [\mathbf{a}_1, \mathbf{a}_2, \ldots, \mathbf{a}_R] \quad \mathbf{B} = [\mathbf{b}_1, \mathbf{b}_2, \ldots, \mathbf{b}_R] \quad \mathbf{C} = [\mathbf{c}_1, \mathbf{c}_2, \ldots, \mathbf{c}_R].$$

3 Methodology

In this section we introduce our sparse tensor completion model when the covariate information is available and propose a non-convex optimization for parameter estimation. Our algorithm employs an alternative updating approach and incorporates a refinement step to boost the performance.

3.1 Model

We observe a third-order tensor $\mathcal{T} \in \mathbb{R}^{n_1 \times n_2 \times n_3}$ and a covariate matrix $\mathbf{M} \in \mathbb{R}^{n_1 \times n_v}$ corresponding to the feature information along the first mode of the tensor $\mathcal{T}$. Here, without loss of generality, we consider the case where the tensor has three modes and the tensor and the matrix are coupled along the first mode. Our method can be easily extended to the case where more than one mode of the tensor has a covariates matrix.

Let Ω be the subset of indexes of the tensor $\mathcal{T}$ for which entries are not missing. We define a projection function $P_\Omega(\mathcal{T})$ that projects the tensor onto the observed set Ω, such that

$$[P_\Omega(\mathcal{T})]_{ijk} = \begin{cases} \mathcal{T}_{ijk} & \text{if } (i,j,k) \in \Omega \\ 0 & \text{otherwise.} \end{cases} \tag{3}$$

We assume a noisy observation model, where the observed tensor and matrix are noisy versions of their true counterparts. That is,

$$P_\Omega(\mathcal{T}) = P_\Omega(\mathcal{T}^* + \mathcal{E}_T); \quad \mathbf{M} = \mathbf{M}^* + \mathcal{E}_M, \tag{4}$$

where $\mathcal{E}_T$ and $\mathcal{E}_M$ are the error tensor and the error matrix respectively; $\mathcal{T}^*$ and $\mathbf{M}^*$ are the true tensor and the true matrix which are assumed to have low-rank decomposition structures (Kolda and Bader, 2009),

$$\mathcal{T}^* = \sum_{r \in [R]} \lambda_r^* \mathbf{a}_r^* \otimes \mathbf{b}_r^* \otimes \mathbf{c}_r^*; \quad \mathbf{M}^* = \sum_{r \in [R]} \sigma_r^* \mathbf{a}_r^* \otimes \mathbf{v}_r^*, \tag{5}$$

where λ_r^* and $\sigma_r^* \in \mathbb{R}^+$, and $\mathbf{a}_r^* \in \mathbb{R}^{n_1}, \mathbf{b}_r^* \in \mathbb{R}^{n_2}, \mathbf{c}_r^* \in \mathbb{R}^{n_3}$ and $\mathbf{v}_r^* \in \mathbb{R}^{n_v}$ with $\|\mathbf{a}_r^*\|_2 = \|\mathbf{b}_r^*\|_2 = \|\mathbf{c}_r^*\|_2 = \|\mathbf{v}_r^*\|_2 = 1$ for all $r \in [R]$. As motivated from the online advertisement application, we impose an important sparsity structure on the tensor and matrix components $\mathbf{a}_r^*, \mathbf{b}_r^*, \mathbf{c}_r^*$ and $\mathbf{v}_r^*$ such that they belong to the set $\mathcal{S}(n, d_i)$ with $i = 1, 2, 3, v$, where

$$\mathcal{S}(n, d_i) \quad := \quad \left\{ \mathbf{u} \in \mathbb{R}^{n_i} \,\Big|\, \|\mathbf{u}\|_2 = 1, \sum_{j=1}^{n_i} 1_{\{\mathbf{u}_j \neq 0\}} \leq d_i \right\}. \tag{6}$$

The values d_i for $i = 1, 2, 3, v$ are considered to be the true sparsity parameters for the tensor and matrix latent components.

Given a tensor $\mathcal{T}$ with many missing entries and a covariate matrix $\mathbf{M}$, our goal is to recover the true tensor $\mathcal{T}^*$ as well as its sparse latent components. We formulate the model estimation as a joint sparse matrix and tensor decomposition problem. This comes down to finding a sparse and

low-rank approximation to the tensor and matrix that are coupled in the first mode.

$$\min_{\mathbf{A},\mathbf{B},\mathbf{C},\mathbf{V}} \left\{ \|P_\Omega(\mathcal{T}) - P_\Omega\big(\sum_{r\in[R]} \lambda_r \mathbf{a}_r \otimes \mathbf{b}_r \otimes \mathbf{c}_r\big)\|_F^2 + \|\mathbf{M} - \sum_{r\in[R]} \sigma_r \mathbf{a}_r \otimes \mathbf{v}_r\|_F^2 \right\} \tag{7}$$

subject to $\|\mathbf{a}_r\|_2 = \|\mathbf{b}_r\|_2 = \|\mathbf{c}_r\|_2 = \|\mathbf{v}_r\|_2 = 1, \|\mathbf{a}_r\|_0 \leq s_1, \|\mathbf{b}_r\|_0 \leq s_2, \|\mathbf{c}_r\|_0 \leq s_3, \|\mathbf{v}_r\|_0 \leq s_v.$

Here s_i, $i = 1, 2, 3, v$, are the sparsity parameters and can be tuned via a data-driven way. The problem in (7) is a non-convex optimization when considering all parameters at once, however the objective function is convex in each parameter while other parameters are fixed. Such multi-convex property motivates us to consider an efficient alternative updating algorithm.

3.2   Algorithm

In order to solve the optimization problem formulated in (7), we use an Alternating Least Squares (ALS) approach and incorporate an extra refinement step as introduced in Jain and Oh (2014). In each iteration of ALS, all but one of the components are fixed and the optimization problem reduces to a convex least squares problem. In order to enforce ℓ_0 norm penalization in the optimization, we apply a truncation step after each component update similar to that used in Sun et al. (2017); Zhang and Han (2019); Hao et al. (2020). For a vector $\mathbf{u} \in \mathbb{R}^n$ and an index set $F \subseteq [n]$ we define Truncate$(\mathbf{u}, F)$ such that its i-th entry is

$$[\text{Truncate}(\mathbf{u}, F)]_i = \begin{cases} \mathbf{u}_i & \text{if } i \in F \\ 0, & \text{otherwise.} \end{cases}$$

For a scalar $s < n$, we denote Truncate$(\mathbf{u}, s)=$Truncate$(\mathbf{u}, \text{supp}(\mathbf{u}, s))$, where supp$(\mathbf{u}, s)$ is the set of indices of $\mathbf{u}$ which have the largest s absolute values. For example, consider $\mathbf{u} = (0.1, 0.2, 0.5, -0.6)^\top$, we have supp$(\mathbf{u}, 2) = \{3, 4\}$ and Truncate$(\mathbf{u}, 2) = (0, 0, 0.5, -0.6)^\top$. Note that existing sparse tensor models encourage the sparsity either via a Lasso penalized approach (Pan et al., 2019), dimension reduction approach (Li and Zhang, 2017), or sketching (Xia and Yuan, 2021). We extend the truncation-based sparsity approach in traditional high-dimensional vector models (Wang et al., 2014a,b) and tensor factorization (Sun et al., 2017; Zhang and Han, 2019; Hao et al., 2020) to the tensor completion problem. As shown in Wang et al. (2014b); Sun et al. (2017), the truncation-based sparsity approach often leads to improved estimation performance in practice.

   Our COSTCO in Algorithm 1 takes a matrix $\mathbf{M}$ and a tensor $\mathcal{T}$ with missing entries as input and computes the components of the matrix and tensor. Due to the non-convexity of the optimization

---

Algorithm 1 COSTCO: Covariate-assisted Sparse Tensor Completion for Solving (7)

1: **Input:** Observed tensor $P_\Omega(\mathcal{T}) \in \mathbb{R}^{n_1 \times n_2 \times n_3}$, observed matrix $\mathbf{M} \in \mathbb{R}^{n_1 \times n_v}$, maximal number of iterations τ, tolerance tol, rank R, and cardinality (s_1, s_2, s_3, s_v).

2: Initialize $(\lambda_1, \ldots, \lambda_r), (\mathbf{A}, \mathbf{B}, \mathbf{C}), (\sigma_1, \ldots \sigma_r), \mathbf{V}$.

3: $\mathbf{a}_r, \mathbf{b}_r, \mathbf{c}_r, \mathbf{v}_r \leftarrow$ the rth columns of $\mathbf{A}, \mathbf{B}, \mathbf{C}$ and $\mathbf{V}$ respectively, $\forall r \in [R]$

4: **While** $t \leq \tau$ and $\left(\frac{\|\mathbf{A}_{old}-\mathbf{A}\|_F}{\|\mathbf{A}_{old}\|_F} + \frac{\|\mathbf{B}_{old}-\mathbf{B}\|_F}{\|\mathbf{B}_{old}\|_F} + \frac{\|\mathbf{C}_{old}-\mathbf{C}\|_F}{\|\mathbf{C}_{old}\|_F} \right) \geq tol,$

5:      $\mathbf{A}_{old} \leftarrow \mathbf{A}, \quad \mathbf{B}_{old} \leftarrow \mathbf{B}, \quad \mathbf{C}_{old} \leftarrow \mathbf{C}, \quad \mathbf{V}_{old} \leftarrow \mathbf{V}$

6:      **For** $r = 1, \ldots, R$

7:          $\text{res}_T \leftarrow P_\Omega(\mathcal{T}) - P_\Omega(\sum_{m \neq r} \lambda_m \mathbf{a}_m \otimes \mathbf{b}_m \otimes \mathbf{c}_m) \quad$ and $\quad \text{res}_M \leftarrow \mathbf{M} - \sum_{m \neq r} \sigma_m \mathbf{a}_m \otimes \mathbf{v}_m$

8:          $\widetilde{\mathbf{a}}_r \leftarrow \frac{\lambda_r \text{res}_T(\mathbf{I}, \mathbf{b}_r, \mathbf{c}_r) + \sigma_r \text{res}_M \mathbf{v}_r}{\lambda_r^2 P_\Omega(\mathbf{I}, \mathbf{b}_r^2, \mathbf{c}_r{}^2) + \sigma_r^2}$

9:          $\widetilde{\mathbf{a}}_r \leftarrow \text{Truncate}(\widetilde{\mathbf{a}}_r, s_1), \quad \mathbf{a}_r \leftarrow \widetilde{\mathbf{a}}_r / \|\widetilde{\mathbf{a}}_r\|_2$

10:         $\widetilde{\mathbf{b}}_r \leftarrow \frac{\text{res}_T(\mathbf{a}_r, \mathbf{I}, \mathbf{c}_r)}{P_\Omega(\mathbf{a}_r^2, \mathbf{I}, \mathbf{c}_r^2)}, \quad \widetilde{\mathbf{c}}_r \leftarrow \frac{\text{res}_T(\mathbf{a}_r, \mathbf{b}_r, \mathbf{I})}{P_\Omega(\mathbf{a}_r^2, \mathbf{b}_r^2, \mathbf{I})} \quad$ and $\quad \widetilde{\mathbf{v}}_r \leftarrow \text{res}_M^\top \mathbf{a}_r$

11:         $\widetilde{\mathbf{b}}_r \leftarrow \text{Truncate}(\widetilde{\mathbf{b}}_r, s_2) \quad \widetilde{\mathbf{c}}_r \leftarrow \text{Truncate}(\widetilde{\mathbf{c}}_r, s_3), \quad \widetilde{\mathbf{v}}_r \leftarrow \text{Truncate}(\widetilde{\mathbf{v}}_r, s_v)$

12:         $\lambda_r \leftarrow \|\mathbf{c}_r\|_2, \quad \sigma_r \leftarrow \|\mathbf{v}_r\|_2$

13:         $\mathbf{b}_r \leftarrow \widetilde{\mathbf{b}}_r / \|\widetilde{\mathbf{b}}_r\|_2, \quad \mathbf{c}_r \leftarrow \widetilde{\mathbf{c}}_r / \|\widetilde{\mathbf{c}}_r\|_2, \quad \mathbf{v}_r \leftarrow \widetilde{\mathbf{v}}_r / \|\widetilde{\mathbf{v}}_r\|_2$

14:      **End For**

15: **End While**

---

problem, there could be multiple local optima. In our algorithm we initialize the tensor and matrix components using the procedure in Section 3.2.1 which is shown through extensive simulations to provide good starting values for tensor and matrix component. Line 6 of the algorithm has an inner loop on $r \in [R]$ which loops on each tensor rank. This inner loop on r performs an "extra refinement" step that was first introduced in Jain and Oh (2014) for tensor completion; and is, therein, proved to improve the error bounds of tensor recovery. The main component updates are performed in Lines 8 and 10 which are solutions to the least squares problem while other parameters are fixed. Note that the horizontal double line in Lines 8 and 10 indicate element-wise fraction and the squaring in the denominator applies entry-wise on the vectors. After obtaining these non-sparse components, Lines 9 and 11 perform the truncation operator to encourage the sparsity on the latent components. The detailed derivation of this algorithm is shown in Lemma 1 in the supplementary material. Finally, the algorithm stops if either the maximum number of iterations τ is reached or the normalized Frobenius norm difference of the current and previous components are below a threshold tol.

Figure 2 is an illustration of COSTCO which reveals the intuition behind the working of Algorithm 1. As the percentage of missing entries in the tensor increases, recovering the tensor components using only the observed tensor entries leads to a reduction in the accuracy of the recovered tensor
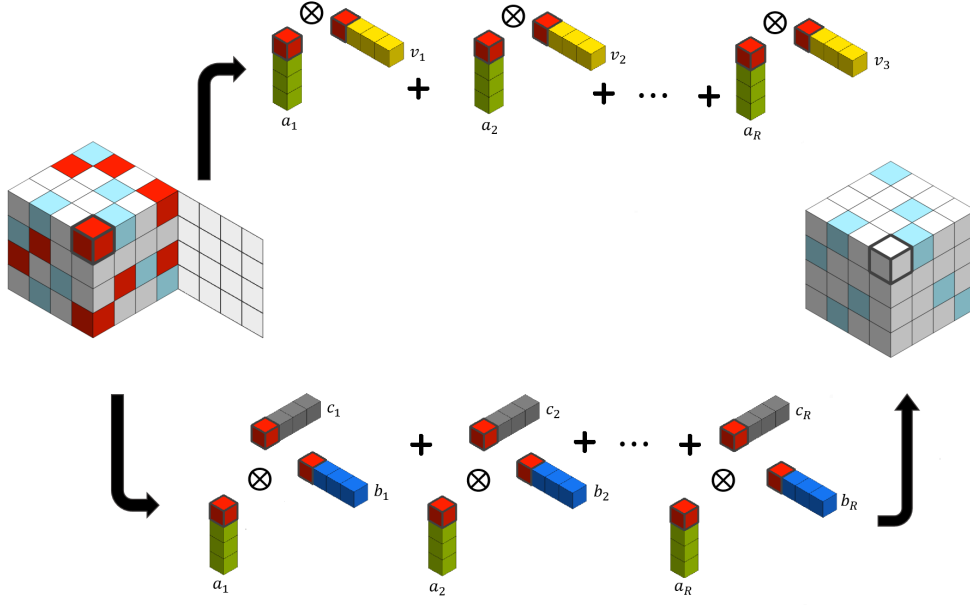
Figure 2: Illustration of COSTCO showing recovery procedure for missing entries through joint tensor matrix decomposition; red cells represent missing entries. The tensor and matrix are coupled along the first mode and the components $\mathbf{a}_r$, $r \in [R]$ are shared by the tensor and matrix decomposition.

components. However, with COSTCO, we leverage the additional latent information coming from the matrix of covariates on the shared mode. The signal obtained from the matrix contributes in improving the recovery of the shared components and indirectly that of the non-shared components as well. This observation is reflected on Line 8 of Algorithm 1 for the shared component update, where we see in the denominator that even when $P_\Omega(\mathbf{I}, \mathbf{b}_r^2, \mathbf{c}_r{}^2)$ is close to zero (meaning most entries of the tensor are missing) the denominator remains a non-zero value due to the signal from covariate matrix. In this case we are still able to estimate the shared component $\mathbf{a}_r$. This would not be the case without the addition of the covariates matrix information, where the denominator for the update would only be $P_\Omega(\mathbf{I}, \mathbf{b}_r^2, \mathbf{c}_r{}^2)$ which is close to zero. Therefore, a standalone tensor completion algorithm would become unstable. In the more general case where all three modes of the tensor are coupled to their own covariates matrices, it is easy to see from the illustration in Figure 2 that the missing percentage of the tensor could be close to 100%. This is because in such case, the covariates matrix components could still be used in the algorithm to recover the tensor components for all three modes and therefore recover the tensor entries.

3.2.1 Initialization Procedure

This subsection presents details about the method used for the initialization procedure on Line 2 of Algorithm 1. Unlike matrix completion, success in designing an efficient and accurate algorithm for the tensor completion problem is contingent to starting with a good initial estimate. In fact the convergence rate of low-rank tensor algorithms is typically written as a function of the tensor components weights as well as the initialization error (Anandkumar et al., 2014a; Jain and Oh, 2014; Sun et al., 2017; Cai et al., 2019; Xia et al., 2021). It is therefore imperative to design an initialization procedure efficient enough to help rule out local stationary points.

We use to our advantage, the fact that in our model, the tensor and matrix share at least one mode and use the singular value decomposition (SVD) (Stewart, 1990; Ipsen, 1998) of the observed matrix $\mathbf{M}$ to initialize the shared components of the tensor $\mathbf{A}$ along with the matrix weights $\sigma_1, \cdots, \sigma_R$ and matrix component $\mathbf{V}$ respectively. We then use the robust tensor power method (RTPM) from Anandkumar et al. (2014a) to initialize the non-shared components $\mathbf{B}$ and $\mathbf{C}$ and the tensor weights. This is done by setting all missing entries in the tensor to be zero before running RTPM. In practice we show in our simulations in section 5 that this is an adequate initialization procedure and produces much better initials compared to a random initialization scheme. In the more general case where all tensor modes have covariate matrices, the SVD on the covariate matrices can be used to initialize all the tensor components. In this case, the RTPM for non-shared components initialization would not be needed.

3.2.2 Rank and Cardinality Tuning

Our `COSTCO` method relies on two key parameters: the rank R and the sparsity parameters. It has been shown that exact tensor rank calculation is a NP-hard problem (Kolda and Bader, 2009). In this subsection, following the tuning method in Allen (2012); Sun et al. (2017), we provide a BIC-type criterion to tune these parameters in practice. Given a pre-specified set of rank values $\mathcal{R}$ and a pre-specified set of cardinality values $\mathcal{S}$, we choose the parameters which minimizes

$$
\begin{aligned}
BIC = \log & \left(\frac{\|P_\Omega\big(\mathcal{T} - \sum_{r \in [R]} \lambda_r \mathbf{a}_r \otimes \mathbf{b}_r \otimes \mathbf{c}_r\big)\|_F^2}{n_1 n_2 n_3} + \frac{\|\mathbf{M} - \sum_{r \in [R]} \sigma_r \mathbf{a}_r \otimes \mathbf{v}_r\|_F^2}{n_1 n_v} \right) \\
& + \frac{\log(n_1 n_2 n_3 + n_1 n_v)}{(n_1 n_2 n_3 + n_1 n_v) \sum_{r \in [R]} (\|\mathbf{a}\|_0 + \|\mathbf{b}\|_0 + \|\mathbf{c}\|_0 + \|\mathbf{v}\|_0)}
\end{aligned}
\tag{8}
$$

To further speed up the computation, in practice we tune these parameters sequentially. That is, we first fix $s_i = n_i$ and tune the rank R via (8). Then given the tuned rank, we tune the sparsity parameters. This tuning procedure works very well through simulation studies in Section 5.

4   Theoretical Analysis

In this section, we derive the error bound of the recovered tensor components obtained from Algorithm 1. We present the recovery results for the estimated shared components $\mathbf{a}_r$ and non-shared tensor components $\mathbf{b}_r$ and $\mathbf{c}_r$ separately to highlight the sharp improvement in recovery accuracy resulting from incorporating the covariate information.

The theory is presented in two phases, first we focus on a simplified case in which the true tensor and matrix components $\mathbf{a}_r^*, \mathbf{b}_r^*, \mathbf{c}_r^*$ and $\mathbf{v}_r^*$ are non-sparse and both tensor and matrix weights are equal (i.e, $\sigma_r^* = \lambda_r^*$, $\forall r \in [R]$). Presenting this simplified case allows us to showcase clearly the interplay between the reveal probability, the tensor and matrix dimensions as well as how the noises in the tensor and matrix affect the statistical and computational errors of the algorithm. In the second case, we then present the results for the general scenario where the tensor and matrix weights are allowed to be unequal and the tensor and matrix components are assumed to be sparse.

4.1   Case 1: Non-sparse Tensor and Matrix with Equal Weights

Before presenting the theorem for the simplified case, we introduce assumptions on the true tensor $\mathcal{T}^*$ and matrix $\mathbf{M}^*$ on the identifiability and incoherence. Denote $n := \max{(n_1, n_2, n_3, n_v)}$.

Assumption 1: (Tensor and matrix structure)

i. Assume $\mathcal{T}^*$ and $\mathbf{M}^*$ are specified as in equation (5) with unique low-rank decomposition up to a permutation, and assume rank $R = o(n^{1/2})$ and $\lambda_r^* = \sigma_r^*$ (equal weight), $\forall r \in [R]$.

ii. The entries of the decomposed components for both $\mathcal{T}^*$ and $\mathbf{M}^*$ satisfy the μ-mass condition,

$$\max_r \{\|\mathbf{a}_r^*\|_\infty, \|\mathbf{b}_r^*\|_\infty, \|\mathbf{c}_r^*\|_\infty, \|\mathbf{v}_r^*\|_\infty\} \leq \frac{\mu}{\sqrt{n}},$$

where μ is a constant.

iii. The components across ranks for both $\mathcal{T}^*$ and $\mathbf{M}^*$ meet the incoherence condition,

$$\max_{i \neq j} \left\{|\langle \mathbf{a}_i^*, \mathbf{a}_j^* \rangle|, |\langle \mathbf{b}_i^*, \mathbf{b}_j^* \rangle|, |\langle \mathbf{c}_i^*, \mathbf{c}_j^* \rangle|, |\langle \mathbf{v}_i^*, \mathbf{v}_j^* \rangle|\right\} \leq \frac{c_0}{\sqrt{n}},$$

where c_0 is a constant.

We briefly discuss the utility of the above listed assumptions. Assumption $(1i)$ is a common assumption in the tensor decomposition literature to ensure the identifiability (Kolda and Bader, 2009; Anandkumar et al., 2014a; Jain and Oh, 2014; Sun et al., 2017). It imposes the condition that the tensor admits a low rank CP decomposition which is unique. This is the case of the undercomplete tensor decomposition, where the rank of the tensor is assumed to be lower than the dimension of the component. The assumption $\lambda_r^* = \sigma_r^*$ is a simplification of the problem which allows us to simplify the derivation and sharpen the convergence rate compared to that in the general non-equal weight case in Section 4.2. Assumption $(1ii)$ ensures that the mass of the tensor is not contained in only a few entries and is necessary if one hopes to recover any of the non-share components of the tensor with acceptable accuracy. Assumption $(1iii)$ is related to the non-orthogonality of the tensor components and imposes a soft orthogonality condition on the tensor and matrix components. That is, the tensor components are allowed to be correlated only to a certain degree. Anandkumar et al. (2014b) and Sun et al. (2017) show that such a condition is met when the tensor and matrix component are randomly generated from a Gaussian distribution. Both the μ-mass condition and the incoherence conditions have been commonly assumed in low-rank tensor models (Anandkumar et al., 2014a; Jain and Oh, 2014; Sun et al., 2017; Cai et al., 2019; Xia and Yuan, 2019; Cai et al., 2020).

Assumption 2: (Reveal probability) Denote $\lambda_{min}^* := \min\limits_{r \in [R]}\{\lambda_r^*\}$ and $\lambda_{max}^* := \max\limits_{r \in [R]}\{\lambda_r^*\}$. We assume that each entry (i, j, k) of the tensor $\mathcal{T}^*$ for all $i \in [n_1]$, $j \in [n_2]$ and $k \in [n_3]$ is observed with equal probability p which satisfies,

$$p \geq \frac{CR^2\mu^3\lambda_{max}^{*2}\log^2(n)}{(\lambda_{min}^* + \sigma_{min}^*)^2 n^{3/2}},$$

where C is a constant.

Assumption 2 guarantees that the tensor entries are revealed uniformly at random with probability p. The lower bound on p is an increasing function of the tensor rank since recovering tensors with a larger rank is a harder problem which requires more observed entries. The bound on p is also an increasing function of the μ-mass parameter since a larger μ-mass parameter in Assumption $(1ii)$ indicates a smaller signal in each tensor entry and hence more reveal entries for accurate component recovery would be needed. Moreover, the bound on p is a decreasing function of the tensor component dimension n and relates as $n^{-3/2}$ up to a logarithm term. This is the optimal dependence on the dimension in tensor completion literature (Jain and Oh, 2014; Xia and Yuan,

14

2019). Most importantly, the lower bound on p is relaxed when the minimal weight $\lambda^*_{\min}$ of the tensor or the minimal weight $\sigma^*_{\min}$ of the matrix increases. This reflects a critical difference when compared to the lower bound condition required in traditional tensor completion (Jain and Oh, 2014; Xia and Yuan, 2019) which corresponds to the case $\sigma^*_{\min} = 0$. It shows the advantage of coupling the matrix of covariates for the tensor completion. This new lower bound on p translates to requiring less observed entries for the tensor recovery in the presence of covariates. Note that in the present simplified case $\sigma^*_r = \lambda^*_r$, we still choose to write $\sigma^*_{\min}$ explicitly in the lower bound condition to showcase the effect of the covariate information. The improvement on p over existing literature will be clearer in Assumption 5 for the general non-equal weight case.

Assumptions 3 (Initialization error) Define the initialization errors for the tensor components as $\epsilon_{0_T} := \max_{r \in [R]}\{\|\mathbf{a}^0_r - \mathbf{a}^*_r\|_2, \|\mathbf{b}^0_r - \mathbf{b}^*_r\|_2, \|\mathbf{c}^0_r - \mathbf{c}^*_r\|_2, \frac{|\lambda^0_r - \lambda^*_r|}{\lambda^*_r}\}$ and the initialization error for the matrix components as $\epsilon_{0_M} := \max_{r \in [R]}\{\|\mathbf{v}^0_r - \mathbf{v}^*_r\|_2, \frac{|\sigma^0_r - \sigma^*_r|}{\sigma^*_r}\}$. Assume that

$$\epsilon_0 := \max\{\epsilon_{0_T}, \epsilon_{0_M}\} \leq \frac{\lambda^*_{min}}{100 R \lambda^*_{max}} - \frac{c_0}{3\sqrt{n}}. \tag{9}$$

Here the component $c_0/\sqrt{n}$ is due to the non-orthogonality of the tensor components. When the components are orthogonal, we allow a larger initialization error. This observation aligns with the common knowledge in tensor recovery as the problem is known to be harder for non-orthogonal tensor factorization (Anandkumar et al., 2014b). Similarly, a larger rank R of the tensor leads to a harder problem and a stronger condition on the initialization error. Under Assumption (1i) $R = o(n^{1/2})$, when the condition number $\lambda^*_{max}/\lambda^*_{min} = O(1)$, this initial condition reduces to $\epsilon_0 = O(1/R)$. As shown in Anandkumar et al. (2014b); Jain and Oh (2014), the robust tensor power method initialization procedure used in our Algorithm satisfies $O(1/R)$ error bound.

Theorem 1 (Non-sparse tensor and matrix components with equal weights). *Assuming Assumptions 1, 2 and 3 are met. After running $\Omega\left(\log_2\left(\frac{(p(63/64)+1)\lambda^*_{min}\epsilon_0}{p(65/64)\|\mathcal{E}_T\|+\|\mathcal{E}_M\|} \vee \frac{\lambda^*_{min}\epsilon_0}{\|\mathcal{E}_T\|}\right)\right)$ iterations of Algorithm 1 with $s_i = n_i$, for $i = 1, 2, 3, v$, we have*

- **Shared Component $\mathbf{a}_r$:**

$$\max_{r \in [R]} (\|\mathbf{a}_r - \mathbf{a}^*_r\|_2) = \mathcal{O}\left(\frac{p(65/64)\|\mathcal{E}_T\| + \|\mathcal{E}_M\|}{[p(63/64)+1]\lambda^*_{min}}\right), \tag{10}$$

where $\|\mathcal{E}_T\|$, $\|\mathcal{E}_M\|$ is the spectral norm of the error tensor and error matrix, respectively.

- **Non-Shared Components $\mathbf{b}_r$, $\mathbf{c}_r$:**

$$\max_{r \in [R]} \left(\|\mathbf{b}_r - \mathbf{b}^*_r\|_2, \|\mathbf{c}_r - \mathbf{c}^*_r\|_2, \frac{|\lambda_r - \lambda^*_r|}{\lambda^*_r}\right) = \mathcal{O}\left(\frac{\|\mathcal{E}_T\|}{\lambda^*_{min}}\right). \tag{11}$$

15

Theorem 1 indicates that the shared component error is a weighed average of the spectral norm of the error tensor and error matrix. Whereas the non-shared component error is simply a function of the error tensor. In the extreme case in which the covariates matrix $\mathbf{M}$ is noiseless, then the recovery error of the shared component becomes $\frac{p(65/64)\|\mathcal{E}_T\|}{[p(63/64)+1]\lambda^*_{min}}$ which is much smaller than the recovery error of the non-shared component $\frac{\|\mathcal{E}_T\|}{\lambda^*_{min}}$. Moreover even in the case in which the coupled covariates matrix is not noiseless, since $p \leq 1$ we notice an improvement in the statistical error of the recovered shared component compared to that of the non-shared components as long as the spectral norm of the error matrix is in the same magnitude of or smaller than that of the error tensor. This is usually the case in practice. To see it, recall that $\mathcal{E}_M \in \mathbb{R}^{n_1 \times n_v}$ and $\mathcal{E}_T \in \mathbb{R}^{n_1 \times n_2 \times n_3}$, hence when entries of $\mathcal{E}_M$ and $\mathcal{E}_T$ are of the same scale, $\|\mathcal{E}_M\|$ is much smaller than $\|\mathcal{E}_T\|$ as n_v is much smaller than $n_2 \times n_3$ in our real application. In Theorem 2 for the general weight case, we will explicitly showcase the improvement of the shared component error over traditional tensor completion methods due to the additional covariate information.

4.2   Case 2: Sparse Tensor and Matrix with General Weights

We now present the result for the general case with low rank sparse tensor and matrix $\mathcal{T}^*$ and $\mathbf{M}^*$ and the weights of the tensor and matrix are allowed to be unequal. The theoretical analysis for the generalized case is much more challenging than that covered in Theorem 1. Unlike that in Case 1, we are no longer able to derive the closed form solution to the optimization problem in (7) for the shared tensor component. To remedy it, we construct an intermediate estimate in the analysis of the shared component recovery. Fortunately, this general result allows us to explicitly quantify the improvement due to the covariates on the missing percentage requirement and the final error bound.

The following conditions are needed for the general scenario. Recall that $d = \max\{d_1, d_2, d_3, d_v\}$ is the maximal true sparsity parameter defined in (6) and define $s := \max\{s_1, s_2, s_3, s_v\}$.

Assumption 4 (sparse tensor and matrix structure)

i. Assume $\mathcal{T}^*$ and $\mathbf{M}^*$ have the sparse structure in (5) and (6) with unique low-rank decomposition up to a permutation, and assume rank $R = o(d^{1/2})$.

ii. The entries of the decomposed components for $\mathcal{T}^*$ satisfy the following μ-mass condition

$$\max_r\{\|\mathbf{a}^*_r\|_\infty, \|\mathbf{b}^*_r\|_\infty, \|\mathbf{c}^*_r\|_\infty, \|\mathbf{v}^*_r\|_\infty\} \leq \frac{\mu}{\sqrt{d}}.$$

16

iii. The components across ranks for both $\mathcal{T}^*$ and $\mathbf{M}^*$ meet the incoherence condition,

$$\max_{i \neq j} \left\{ |\langle \mathbf{a}_i^*, \mathbf{a}_j^* \rangle|, |\langle \mathbf{b}_j^*, \mathbf{b}_i^* \rangle|, |\langle \mathbf{c}_j^*, \mathbf{c}_i^* \rangle|, |\langle \mathbf{v}_j^*, \mathbf{v}_i^* \rangle| \right\} \leq \frac{c_0}{\sqrt{d}}.$$

Notice that since the components of tensor and matrix are assumed to be sparse, the μ-mass and incoherence condition are functions of the maximum number of non-zero elements d in the tensor and matrix components rather than the dimension n. In the case in which $d \ll n$, this constitutes a milder assumption compared to Assumptions 1(ii) and 1(iii).

Assumption 5 (Reveal probability) We assume that each tensor entry (i, j, k) for all $i \in [n_1]$, $j \in [n_2]$ and $k \in [n_3]$ is observed with equal probability p which satisfies,

$$p \geq \frac{CR^2 \mu^3 \lambda_{max}^{*2} \log^2(d)}{(\lambda_{min}^* + \sigma_{min}^*)^2 d^{3/2}}. \tag{12}$$

Similar to that discussed after Assumption 2, the required lower bound on the reveal probability in (12) improves the established lower bound for the tensor completion with no covariates matrix. Specifically, Yuan and Zhang (2017); Jain and Oh (2014); Montanari and Sun (2018) show that the lower bound for non-sparse tensor completion is of the order $\frac{\lambda_{max}^{*2} \log^2(n)}{\lambda_{min}^{*2} n^{3/2}}$ while our lower bound is of the order $\frac{\lambda_{max}^{*2} \log^2(n)}{(\lambda_{min}^* + \sigma_{min}^*)^2 n^{3/2}}$ when the components are not sparse $(d = n)$. This highlight the facts that a weaker assumption on the reveal probability is required in the presence of covariates matrix than in the case with no covariates. An interesting phenomenon is that when the minimal weight of the matrix σ_{min}^* is very large, we could allow the reveal probability to be even close to zero. As demonstrated in our simulations, our COSTCO is still satisfactory even when 98% of the tensor entries are missing, while the traditional tensor completion method fails with more than 90% missing entries. Moreover, in the sparse case, the lower bound is now a decreasing function of the sparsity parameter d. This is intuitive as when d decreases, the non-zero tensor components will concentrate on fewer dimensions which makes the tensor recovery problem harder.

Assumption 6 (Initialization error) Assume that

$$\epsilon_0 := \max\{\epsilon_{0_T}, \epsilon_{0_M}\} \leq \frac{95/96 \lambda_{min}^{*2} + \sigma_{min}^{*2}}{144R(\lambda_{max}^{*2} + \sigma_{max}^{*2})} - \frac{c_0}{3\sqrt{d}}, \tag{13}$$

with ϵ_{0_T} and ϵ_{0_M} as defined in Assumption 3.

Compared to that in Assumption 3, the initialization condition for Case 2 is slightly stronger. This is reflected on two parts. First, the term $c_0/\sqrt{d}$ is due to the non-orthogonality of sparse tensor components and is larger in the sparse case. This requires a stronger condition on the

rank R as shown in Assumption (1i) in order to ensure the positivity of the right-hand side of (13). Second, the ratio $(95/96\lambda_{min}^{*2} + \sigma_{min}^{*2})/144(\lambda_{max}^{*2} + \sigma_{max}^{*2}))$ is smaller than $\lambda_{min}^*/(100\lambda_{max}^*)$ in Assumption 3. Even when $\lambda_r^* = \sigma_r^*$ and $d = n$, this condition is still slightly stronger than Assumption 3 since $\lambda_{min}^{*2}/\lambda_{max}^{*2} < \lambda_{min}^*/\lambda_{max}^*$. This additional term is due to handling the non-equal weights. Fortunately, when condition numbers $\lambda_{max}^*/\lambda_{min}^* = O(1)$ and $\sigma_{max}^*/\sigma_{min}^* = O(1)$, we have $\epsilon_0 = O(1/R)$, which is again satisfied by the initialization procedure in our Algorithm.

Theorem 2 (Sparse tensor and matrix components with general weights). *Assuming assumptions 4, 5 and 6 are met. After running* $\Omega\left(\log_2\left(\frac{[(95/96)p\lambda_{min}^{*2} + \sigma_{min}^{*2}]\epsilon_0}{(97/96)p\lambda_{max}^*\|\mathcal{E}_T\|_{<d+s>} + \sigma_{max}^*\|\mathcal{E}_M\|_{<d+s>}} \vee \frac{\lambda_{min}^*\epsilon_0}{\|\mathcal{E}_T\|_{<d+s>}\epsilon_T}\right)\right)$ *iterations of Algorithm 1 with $s_i \geq d_i$, for $i = 1, 2, 3, v$, we have*

- **Shared Component $\mathbf{a}_r$:**

$$\max_{r \in [R]} \left(\|\mathbf{a}_r - \mathbf{a}_r^*\|_2\right) = \mathcal{O}\left(\frac{(97/96)p\lambda_{max}^*\|\mathcal{E}_T\|_{<d+s>} + \sigma_{max}^*\|\mathcal{E}_M\|_{<d+s>}}{(95/96)p\lambda_{min}^{*2} + \sigma_{min}^{*2}}\right), \quad (14)$$

  where $\|\mathcal{E}_T\|_{<d+s>}, \|\mathcal{E}_M\|_{<d+s>}$ are the sparse spectral norm of error tensor $\mathcal{E}_T$ and error matrix $\mathcal{E}_M$. Remind that the sparse spectral norm is defined in Section 2.

- **Non-Shared Components $\mathbf{b}_r, \mathbf{c}_r$:**

$$\max_{r \in [R]} \left(\|\mathbf{b}_r - \mathbf{b}_r^*\|_2, \|\mathbf{c}_r - \mathbf{c}_r^*\|_2, \frac{|\lambda_r - \lambda_r^*|}{\lambda_r^*}\right) = \mathcal{O}\left(\frac{\|\mathcal{E}_T\|_{<d+s>}}{\lambda_{min}^*}\right). \quad (15)$$

Similar to that in Theorem 1, the statistical error for the shared tensor component in Theorem 2 is a weighed average of the sparse spectral norm of the error tensor $\mathcal{E}_T$ and error matrix $\mathcal{E}_M$. The key difference is that the weight is now related to $\lambda_{\max}^*$ and $\sigma_{\max}^*$ and the spectral norm is now much smaller than the non-sparse counterparts in Theorem 1 since typically $d + s < n$ and hence $\|\mathcal{E}_T\|_{<d+s>} \leq \|\mathcal{E}_T\|$. Similarly, the recovery error for the non-shared tensor component in the general case is also smaller than that in (11) due to a smaller spectral norm. This observation highlights the advantage of considering sparse tensor components. In addition, we highlight a few important scenarios in Table 1 where the error of shared tensor component is smaller than that of the non-shared component. Such scenario indicates when the additional covariate information is useful to reduce the estimation error of the tensor components. In summary, such improvement is observed when the sparse spectral norm of the error matrix is smaller than or comparable to that of the error tensor. Otherwise, it is not conclusive whether such improvement exists.

18

Table 1: Statistical error of shared tensor component in Theorem 2 under various conditions. Improvement represent improvement over the recovery error of the non-shared components

Condition Number	Noise	Statistical Error	Improve?
$\lambda_{max}^*/\lambda_{min}^* = O(1)$ & $\sigma_{max}^*/\sigma_{min}^* = O(1)$	$\|\mathcal{E}_M\|_{<d+s>} = 0$	$\mathcal{O}\left(\frac{(97/96)p\|\mathcal{E}_T\|_{<d+s>}}{(95/96)p\lambda_{min}^*+\sigma_{min}^*}\right)$	✓
	$\|\mathcal{E}_M\|_{<d+s>} = \|\mathcal{E}_T\|_{<d+s>}$	$\mathcal{O}\left(\frac{\|\mathcal{E}_T\|_{<d+s>}((97/96)p+1)}{(95/96)p\lambda_{min}^*+\sigma_{min}^*}\right)$	✓
	$\|\mathcal{E}_M\|_{<d+s>} < \|\mathcal{E}_T\|_{<d+s>}$	$\mathcal{O}\left(\frac{(97/96)p\lambda_{max}^*\|\mathcal{E}_T\|_{<d+s>}+\sigma_{max}^*\|\mathcal{E}_M\|_{<d+s>}}{(95/96)p\lambda_{min}^{*2}+\sigma_{min}^{*2}}\right)$	✓
	$\|\mathcal{E}_M\|_{<d+s>} > \|\mathcal{E}_T\|_{<d+s>}$	$\mathcal{O}\left(\frac{(97/96)p\lambda_{max}^*\|\mathcal{E}_T\|_{<d+s>}+\sigma_{max}^*\|\mathcal{E}_M\|_{<d+s>}}{(95/96)p\lambda_{min}^{*2}+\sigma_{min}^{*2}}\right)$	inconclusive

5   Simulations

In this section we evaluate the performance of our COSTCO algorithm via a series of simulations. We compare it with two competing state of the arts methods tenALSsparse by Jain and Oh (2014) and OPT by Acar et al. (2011). tenALSsparse is an alternating minimization based method for tensor completion which incorporates a refinement step in the standard ALS method. In contrast to our method, tenALSsparse does not incorporate side covariate information in tensor completion. Comparing our algorithm to tenALSsparse helps to highlight the impact of incorporating addition information through coupling with a covariate matrix. It is worth noting that the original algorithm from Jain and Oh (2014) was built for the recovery of non-sparse tensors. In order to allow a fair comparison between our algorithm and theirs, we modify their original algorithm by introducing the same truncation scheme presented in Algorithm 1 to generate the sparse version of their algorithm. The second comparison method is the OPT algorithm by Acar et al. (2011), which approaches the coupled matrix and tensor component recovery by solving for all components simultaneously using a gradient-based optimization approach. The all-at-once optimization method is known to be robust to rank mis-specification (Song et al., 2019), however it is computationally less efficient then ALS based methods specially when the tensor is highly missing (Tomasi and Bro., 2006).

In the aforementioned sections, we discuss our models and theories via a third-order tensor to simply the presentation. Note that our COSTCO is applicable to the tensor with more than three modes. In the simulation, we generate a fourth-order tensor $\mathcal{T}^* \in \mathbb{R}^{d_1 \times 30 \times 30 \times 30}$ and a matrix $\mathbf{M}^* \in \mathbb{R}^{d_1 \times 30}$. We assume that the matrix and the tensor share components across the first mode just as is the case in the aforementioned sections. In order to form the tensor $\mathcal{T}^*$ and the matrix $\mathbf{M}^*$, we draw each entry of $\mathbf{A}^* \in \mathbb{R}^{d_1 \times R}, \mathbf{B}^* \in \mathbb{R}^{30 \times R}, \mathbf{C}^* \in \mathbb{R}^{30 \times R}, \mathbf{D}^* \in \mathbb{R}^{30 \times R}$ and $\mathbf{V}^* \in \mathbb{R}^{30 \times R}$, from the

iid standard normal distribution. We enforce sparsity to the tensor components by keeping only the top 40% of the entries in each column in $\mathbf{B}^*, \mathbf{C}^*$ and $\mathbf{D}^*$ and set the rest of the entries to zero. In all of our simulations we consider the coupled modes $\mathbf{A}^*$ to be dense to mimic the real data scenario in Section 6 where the coupled matrix is dense. We define $\lambda_1^*, \ldots, \lambda_R^*$ and $\sigma_1^*, \ldots, \sigma_R^*$ as the product of the non-normalized component norms in each mode, that is, $\lambda_r^* = \|\mathbf{a}_r^*\|_2 \times \|\mathbf{b}_r^*\|_2 \times \|\mathbf{c}_r^*\|_2 \times \|\mathbf{d}_r^*\|_2$ and $\sigma_r^* = \|\mathbf{a}_r^*\|_2 \times \|\mathbf{v}_r^*\|_2$. We then normalize each of the columns of $\mathbf{A}^*, \mathbf{B}^*, \mathbf{C}^*, \mathbf{D}^*, \mathbf{V}^*$ to unit norm. To illustrate, the first mode component matrix $\mathbf{A}^*$ becomes $\mathbf{A}^* = [\frac{\mathbf{a}_r^*}{\|\mathbf{a}_r^*\|_2}, \cdots, \frac{\mathbf{a}_R^*}{\|\mathbf{a}_R^*\|_2}]$. The sparse tensor $\mathcal{T}^*$ and matrix $\mathbf{M}^*$ are then formed as $\mathcal{T}^* = \sum_{r \in [R]} \lambda_r^* \mathbf{a}_r^* \otimes \mathbf{b}_r^* \otimes \mathbf{c}_r^* \otimes \mathbf{d}_r^*$ and $\mathbf{M}^* = \sum_{r \in [R]} \sigma_r^* \mathbf{a}_r^* \otimes \mathbf{v}_r^*$. We then add noise to the tensor and matrix using the following setup $\mathcal{T} = \mathcal{T}^* + \eta_T \mathcal{N}_T \frac{\|\mathcal{T}^*\|_F}{\|\mathcal{N}_T\|_F}$ and $\mathbf{M} = \mathbf{M}^* + \eta_M \mathcal{N}_M \frac{\|\mathbf{M}^*\|_F}{\|\mathcal{N}_M\|_F}$, where $\mathcal{N}_T$ and $\mathcal{N}_M$ are a tensor and a matrix of the same size as $\mathcal{T}^*$ and $\mathbf{M}^*$ respectively, whose entries are generated from the standard normal distribution. A similar noise generation procedure has been considered in Acar et al. (2011). We simulate the uniformly missing at random pattern in the tensor data by generating entries of the reveal tensor $\mathbf{\Omega} \in \mathbb{R}^{d_1 \times 30 \times 30 \times 30}$ from the binomial distribution with reveal probability p. The sparse and noisy tensor $P_\Omega(\mathcal{T})$ with missing data is finally obtained as $P_\Omega(\mathcal{T}) = \mathcal{T} * \mathbf{\Omega}$, where $*$ is the element-wise multiplication.

To assess the goodness of fit for the tensor and tensor components recovery, we use the normalized Frobenius norm of the difference between the recovered component and the true component. We compute the tensor estimation error, the tensor component error and tensor weights error as:

$$\text{tensor error} := \|\mathcal{T}^* - \mathcal{T}\|_F / \|\mathcal{T}^*\|_F; \quad \text{component error} := \|\mathbf{U}^* - \mathbf{U}\|_F / \|\mathbf{U}^*\|_F;$$

$$\text{weight error} := \|\boldsymbol{\lambda}^* - \boldsymbol{\lambda}\|_2 / \|\boldsymbol{\lambda}^*\|_2, \tag{16}$$

where $\mathcal{T}, \mathbf{U}$, are the estimated tensor and tensor components with $\mathbf{U} \in \{\mathbf{A}, \mathbf{B}, \mathbf{C}, \mathbf{D}\}$, and $\boldsymbol{\lambda} := (\lambda_1, \cdots, \lambda_R)^\top$ is the vector of estimated tensor weights returned by Algorithm 1. In all simulations we return the mean error of 30 replicas of each experiment. Throughout all the experiments, we set the maximum number of iterations τ to be 200, the tolerance *tol* in Algorithm 1 is set to be $1e^{-7}$. To avoid bad local solutions, we conduct 10 initializations for each replicate in all methods. We set the tuning range for the rank R to be $\{1, 2, 3, 4, 5\}$. The tuning range for the sparsity is set to be $\{20\%, 40\%, 60\%, 80\%, 90\%, 100\%\}$, each value representing the percentage of non-zero entries in the latent components as performed on Lines 9 and 11 of Algorithm 1. Note that in addition to a series of simulations considered here, in Section S.4 of the supplementary material, we provide two additional simulations to investigate the practical effect of dimension size of the shared component

and the rank on our `COSTCO` algorithm.

5.1 Missing Percentage

In this first simulation we consider the case with varying levels of missing percentages. We set the dimension of the couple mode to be $d_1 = 30$ and therefore generate $P_\Omega(\mathcal{T}) \in \mathbb{R}^{30 \times 30 \times 30 \times 30}$. We set the rank to be $R = 2$ and the noise level η_T, η_M to be both 0.001. We measure the recovery error under four different settings of the reveal probability parameter $p = \{0.2, 0.1, 0.05, 0.01\}$. In other words, 80%, 90%, 95% and 99% of the tensor entries are missing in each setting. Table 2 indicate that under all varying missing probability, our `COSTCO` algorithm provides a better fit in tensor recovery relative to `tenALSsparse` and `OPT`. Notably, with a higher level of missing data, missing percentage ≥ 90 `COSTCO` significantly outperforms both `tenALSsparse` and `OPT` methods of tensor recovery. This is more evident when we compare our algorithm to `tenALSsparse` for the case where missing percentage ranges from 90% to 98%; in these scenarios the recovery error of `COSTCO` is at least 10 folds better than that of `tenALSsparse`. This agrees with the two advantages of incorporating covariate information into tensor completion as we discussed in the theoretical results: (1) allowing higher missing percentage; (2) reducing estimation errors. Moreover, we notice that the estimation error for the shared component Comp $\ddot{\mathbf{A}}$ is better than that of the non-shared components. This also aligns with the theoretical result which shows that the recovery of the couple component improves over that of non-coupled components due to additional covariate information. Finally, although `OPT` also uses coupling, it underperforms compared to `COSTCO` because the all at once optimization method suffers with unstable gradient when the missing entry percentage is large.

5.2 Noise Level

In the next set of experiments we vary the noise level parameter for the tensor η_T and noise level for the matrix η_M to test algorithms' robustness to noise. These two parameters control the signal-to-noise ratio in the model. The missing probability for these experiments is set to 90% and tensor rank and sparsity of the true tensor are set to $R = 2$ and 60% respectively.

As can be seen in Table 3, when the tensor noise η_T is greater than that of the matrix noise η_M, our algorithm outperforms the two competing methods with a large gap in recovery error. Even when the matrix has a slightly larger noise level than the tensor ($\eta_M = 0.01, \eta_T = 0.001$), `COSTCO` still outperforms the other two algorithms. It shows that in high missing data regime coupling a

Table 2: Estimation errors with varying missing percentages. Reported values are the average and standard error (in parentheses) of tensor, tensor components and weight recovery error based on 30 data replications. `COSTCO`: the proposed method; `tenALSsparse`: sparse version of the tensor completion method by Jain and Oh (2014); `OPT`: the gradient based all at once optimization method of Acar et al. (2011); symbol ($\ddot{A}$) used to put shared tensor-matrix component **A** in emphasis.

Missing Percent	Component	Estimation Error		
		`COSTCO`	`tenALSsparse`	`OPT`
80%	$\mathcal{T}$	**3.38e-05 (2.36e-12)**	3.66e-05 (2.73e-12)	3.56e-05 (2.31e-12)
	Comp $\ddot{A}$	**1.52e-05 (2.37e-12)**	2.22e-05 (3.93e-12)	**1.52e-05 (2.36e-12)**
	Comp **B**	**2.12e-05 (4.39e-12)**	2.13e-05 (3.64e-12)	2.26e-05 (5.05e-12)
	Comp **C**	**1.98e-05 (4.69e-12)**	1.99e-05 (4.83e-12)	2.24e-05 (4.35e-12)
	Comp **D**	**2.17e-05 (2.92e-12)**	2.18e-05 (2.78e-12)	2.26e-05 (2.99e-12)
	λ	1.18e-06 (4.67e-13)	**1.17e-06 (4.95e-13)**	1.18e-06 (4.67e-13)
90%	$\mathcal{T}$	**3.93e-05 (6.12e-12)**	4.47e-02 (2.71e-11)	4.94e-05 (6.07e-12)
	Comp $\ddot{A}$	**1.80e-05 (2.79e-12)**	5.65e-02 (2.74e-11)	**1.80e-05 (2.82e-12)**
	Comp **B**	**2.16e-05 (1.31e-11)**	4.84e-02 (2.02e-11)	3.17e-05 (1.31e-11)
	Comp **C**	**2.12e-05 (9.54e-12)**	4.96e-02 (3.22e-11)	3.13e-05 (9.75e-12)
	Comp **D**	**2.17e-05 (1.38e-11)**	5.79e-02 (2.00e-11)	3.18e-05 (1.39e-11)
	λ	**1.65e-06 (7.98e-13)**	4.84e-02 (8.31e-13)	1.65e-06 (7.98e-13)
95%	$\mathcal{T}$	**5.69e-05 (1.92e-11)**	1.19e-01 (8.70e-03)	6.93e-05 (1.90e-11)
	Comp $\ddot{A}$	1.92e-05 (5.60e-12)	1.44e-01 (2.01e-02)	**1.50e-05 (6.30e-12)**
	Comp **B**	**3.44e-05 (2.29e-11)**	1.28e-01 (1.61e-02)	4.45e-05 (2.30e-11)
	Comp **C**	**3.39e-05 (3.36e-11)**	1.30e-01 (1.02e-02)	4.39e-05 (3.34e-11)
	Comp **D**	**3.74e-05 (1.84e-11)**	1.40e-01 (1.39e-02)	4.74e-05 (1.80e-11)
	λ	**1.26e-06 (8.99e-13)**	1.25e-01 (1.08e-02)	1.76e-06 (8.99e-13)
98%	$\mathcal{T}$	**2.36e-02 (3.50e-11)**	5.05e-01 (1.75e-02)	5.02e-02 (1.98e-02)
	Comp $\ddot{A}$	**2.17e-02 (1.18e-11)**	6.58e-01 (2.03e-02)	6.87e-02 (2.61e-03)
	Comp **B**	**2.63e-02 (5.60e-11)**	6.18e-01 (1.29e-02)	6.31e-02 (2.95e-02)
	Comp **C**	**2.58e-02 (5.81e-11)**	5.89e-01 (1.49e-02)	6.27e-02 (3.86e-02)
	Comp **D**	**2.16e-02 (5.39e-11)**	5.94e-01 (2.16e-02)	6.96e-02 (2.03e-02)
	λ	**2.14e-02 (5.67e-13)**	5.19e-01 (1.75e-02)	5.00e-02 (2.14e-02)
99%	$\mathcal{T}$	**7.13e-01 (5.93e-11)**	9.99e-01 (5.35e-02)	8.80e-01 (2.33e-02)
	Comp $\ddot{A}$	**3.60e-01 (1.28e-10)**	1.17e+00 (1.17e-01)	4.17e-01 (4.39e-02)
	Comp **B**	**7.40e-01 (1.04e-10)**	1.14e+00 (9.65e-02)	7.94e-01 (3.70e-02)
	Comp **C**	**8.25e-01 (3.75e-11)**	1.17e+00 (9.15e-02)	9.14e-01 (3.65e-02)
	Comp **D**	**5.90e-01 (4.57e-11)**	9.77e-01 (9.83e-02)	7.12e-01 (4.51e-02)
	λ	**6.48e-01 (5.73e-11)**	9.77e-01 (6.04e-02)	8.68e-01 (2.33e-02)

matrix that has a slightly larger noise than the tensor still provides enough information to improve the tensor recovery rate. On the other hand, when the matrix noise level is much higher than that of the tensor ($\eta_M = 0.1, \eta_T = 0.001$ in Table 3), we observe that our algorithm `COSTCO` and the other coupled algorithm `OPT` are inferior compared to `tenALSsparse`. In this case, the recovery of the shared component **A** suffers the most in `COSTCO` and `OPT` and is responsible for the inferior tensor recovery error compared to `tenALSsparse` which does not use the coupled matrix. This is expected as a matrix with much larger noise than that of a tensor no longer brings in enough signals

Table 3: Estimation errors with varying noise levels of error matrix and error tensor. Reported values are the average and standard error (in parentheses) of estimation errors. `COSTCO`: the proposed method; `tenALSsparse`: sparse version of the tensor completion method by Jain and Oh (2014); `OPT`: the gradient based all at once optimization method of Acar et al. (2011).

Noise Level	Component	Estimation Error		
		`COSTCO`	`tenALSsparse`	`OPT`
	$\mathcal{T}$	**2.74e-04 (7.31e-10)**	5.37e-04 (1.00e-09)	4.74e-04 (7.31e-10)
	Comp $\ddot{\mathbf{A}}$	**1.05e-04 (2.24e-10)**	3.17e-04 (1.13e-09)	1.05e-04 (2.24e-10)
$\eta_M = 0.001$	Comp $\mathbf{B}$	**2.13e-04 (8.03e-10)**	3.10e-04 (4.72e-10)	3.13e-04 (8.03e-10)
$\eta_T = 0.01$	Comp $\mathbf{C}$	**2.15e-04 (1.33e-09)**	3.14e-04 (1.35e-09)	3.15e-04 (1.33e-09)
	Comp $\mathbf{D}$	**2.21e-04 (1.43e-09)**	3.22e-04 (1.69e-09)	3.21e-04 (1.43e-09)
	λ	**1.41e-05 (6.77e-11)**	1.48e-05 (7.44e-11)	**1.41e-05 (6.77e-11)**
	$\mathcal{T}$	**2.73e-03 (5.50e-08)**	5.36e-03 (8.04e-08)	4.73e-03 (5.50e-08)
	Comp $\ddot{\mathbf{A}}$	**1.06e-03 (2.39e-08)**	3.16e-03 (1.87e-07)	1.06e-03 (2.39e-08)
$\eta_M = 0.001$	Comp $\mathbf{B}$	**2.03e-03 (1.25e-07)**	3.00e-03 (1.66e-07)	3.03e-03 (1.25e-07)
$\eta_T = 0.1$	Comp $\mathbf{C}$	**2.15e-03 (6.21e-08)**	3.10e-03 (3.68e-08)	3.15e-03 (6.21e-08)
	Comp $\mathbf{D}$	**2.20e-03 (1.02e-07)**	3.23e-03 (1.01e-07)	3.20e-03 (1.02e-07)
	λ	1.52e-04 (7.07e-09)	**1.46e-04 (6.09e-09)**	1.52e-04 (7.07e-09)
	$\mathcal{T}$	**3.88e-04 (5.55e-10)**	5.35e-04 (6.41e-10)	4.88e-04 (5.55e-10)
	Comp $\ddot{\mathbf{A}}$	**1.74e-04 (3.79e-10)**	3.21e-04 (8.24e-10)	1.74e-04 (3.82e-10)
$\eta_M = 0.01$	Comp $\mathbf{B}$	**2.17e-04 (9.18e-10)**	3.14e-04 (1.10e-09)	3.17e-04 (9.18e-10)
$\eta_T = 0.001$	Comp $\mathbf{C}$	**2.16e-04 (1.13e-09)**	3.16e-04 (1.44e-09)	3.16e-04 (1.13e-09)
	Comp $\mathbf{D}$	**2.07e-04 (8.39e-10)**	3.02e-04 (8.70e-10)	3.07e-04 (8.39e-10)
	λ	**1.49e-05 (7.21e-11)**	1.53e-05 (6.63e-11)	**1.49e-05 (7.21e-11)**
	$\mathcal{T}$	9.75e-04 (1.60e-08)	**5.37e-04 (1.36e-09)**	1.28e-03 (1.60e-08)
	Comp $\ddot{\mathbf{A}}$	1.39e-03 (2.27e-08)	**3.17e-04 (1.16e-09)**	1.39e-03 (2.27e-08)
$\eta_M = 0.1$	Comp $\mathbf{B}$	**2.20e-04 (1.11e-09)**	3.09e-04 (1.02e-09)	3.21e-04 (1.12e-09)
$\eta_T = 0.001$	Comp $\mathbf{C}$	**2.29e-04 (1.30e-09)**	3.19e-04 (1.01e-09)	3.23e-04 (1.32e-09)
	Comp $\mathbf{D}$	**2.24e-04 (1.20e-09)**	3.12e-04 (1.27e-09)	3.25e-04 (1.20e-09)
	λ	**1.26e-05 (7.94e-11)**	1.27e-05 (7.62e-11)	**1.26e-05 (7.94e-11)**

in the coupling and therefore makes the tensor completion problem harder than when the matrix is completed omitted from the model. Finally, an interesting phenomenon is that the noise level of the error matrix η_M only affects the estimation error of the shared component but not those of the non-shared components. To see it, in the last two settings in Table 3, when η_T is fixed and η_M increases, only the recovery accuracy of the shared component $\mathbf{A}$ significantly drops, but those of the non-shared components have no significant changes. However, in the first two settings in Table 3, when η_M is fixed and η_T increases, the recovery accuracy of both shared and non-shared components significantly drops. These findings agree well with our theoretical results in Theorem 2.

6 Real Data Analysis

We apply our COSTCO method to an advertisement (ad) data to showcase its practical advantages. COSTCO makes use of multiple sources of ad data to extract the ad latent component which is a comprehensive representation of ads. We demonstrate that the obtained ad latent components are able to deliver interesting ad clustering results that are not achievable by a stand-alone method.

Online advertising is a type of marketing strategy which uses internet to promote a given product to potential customers. Extracting patterns in data gathered from online advertisement allows ad platforms and companies to churn data into knowledge which is then used to improve customer satisfaction. Clustering algorithms have been applied to the ad data to discover ad or user clusters for better ad targeting. After computing the similarity between the new ad and each ad cluster, the ad agency can determine whether a new ad should be assigned to a specific user group. Most ad-user clustering research focuses on a single correlation data. What makes our method different is that we not only have a third-order user-by-ad-by-device click tensor data but we also possess additional information which describe specific features of ads. Our COSTCO algorithm uses both click tensor data and ad matrix data to extract the ad latent component for better ad clustering.

The data we analyze in this section is advertising data collected from a major internet company for 4 weeks in May-June 2016. A user preference tensor was obtained by tracking the behavior of 1000 users on 140 ads accessed through 3 different devices. The $1000 \times 140 \times 3$ tensor is formed by computing the click-through-rate (CTR) of each (user, ad, device) triplet over the four weeks period; which is the number of times a user has clicked an ad from a certain device divided by the number of times the user has seen that ad from the specific device. As illustrated in Figure 3, this ad CTR tensor has 96% missing entries and is highly sparse with only 40% of the revealed entries being nonzero. A missing entry in the ad CTR data occurs when a given user is not presented with a certain ad from a specific device, while zeros (sparsity) in the ad CTR data are used to represent user choosing not to interact with an ad that was presented to them on a specific device.

Beside the ad CTR tensor, we also have access to the ad text raw data that store the content of all ads. We use Latent Dirichlet Allocation (LDA) (Blei et al., 2003) to process the ad text data. LDA is an unsupervised topic modeling algorithm that attempts to describe a set of text observations as a mixture of different topics. We first follow Blei et al. (2003) to tune the parameters of LDA such as the number of topics and the Dirichlet distribution parameter that give the best
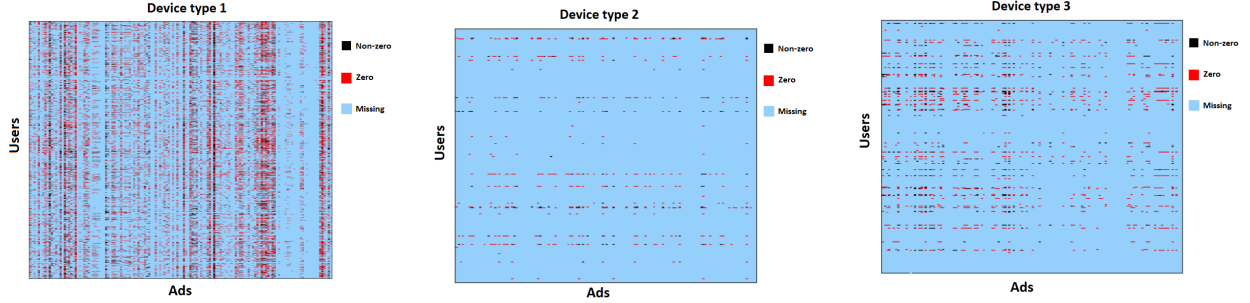
Figure 3: Illustration of missing data and sparsity in our ad CTR tensor.

trade-off between low perplexity value and efficient computing time. The best perplexity is obtained for 20 topics. This means that all the 140 advertisement data can be considered as a combination of 20 topics. Due to space constraints, we illustrate an example of 7 out of 20 topics in Table 4, and only display the top 10 words for each of the 7 topics returned by LDA. Each topic column was labeled based on overall meaning of the top words. Once trained, LDA returns a matrix that contains the proportion of topics in each ad. We use this matrix of proportions of dimension $\mathbb{R}^{140 \times 20}$ as the ad covariate matrix that will be used jointly with the ad CTR tensor to obtain ad latent components in our COSTCO algorithm.

Table 4: Top ten words for 7 chosen topics. Top words were obtained through LDA.

Topics	Ride	Gaming	Security	Mortgage	Insurance	Online dating	Fashion retail
	uber	game	vivint	mortgage	get	single	buy
	pay	controller	home	apr	insurance	pic	sale
	car	experience	front	payment	less	man	gilt
	people	gameplay	security	free	see	profile	zulily
Top Words	weekly	accessory	smart	new	month	click	lulus
	fare	ebay	call	arm	drive	meet	charlotterusse
	ride	level	control	quotes	day	browse	neimanmarcus
	give	time	camera	calculate	miles	look	maurices
	work	joystick	adt	easy	low	free	lastcall
	drive	wide	look	process	qualify	pay	spring

We first evaluate the tensor recovery error by randomly splitting the observed tensor entries into 80% training and 20% testing. Let $\widehat{\mathcal{T}}$ indicate the recovered tensor from the training set. We use $\widehat{\mathcal{T}}$ for training and compute the recovery error on the testing set. The metrics used to access the recovery error of the tensor is defined as $\|P_{\Omega_{Test}}(\mathcal{T} - \widehat{\mathcal{T}})\|_F / \|P_{\Omega_{Test}}(\mathcal{T})\|_F$, where $P_{\Omega_{Test}}(\mathcal{T}) = \mathbf{\Omega}_{Test} * \mathcal{T}$ with $\mathbf{\Omega}_{Test}$ being a binary tensor of the same size as $\mathcal{T}$ that has ones on the test entries and zeros elsewhere. The tensor recovery error for COSTCO is 0.825, leading to 23% accuracy improvement

over the baseline `tenALSsparse` whose error is 1.083. This again highlights the benefit of fusing the ad content matrix to the ad CTR tensor. The `OPT` algorithm was not used for comparison as the algorithm optimization package failed with error messages after multiple trials on this data. We conjecture this is due to the unstable performance of the all at once optimization when the missing percentage is very high.

We then compare the ad latent components returned from `COSTCO` and `tenALSsparse` in Figure 4. As a comparison, we also include the result of SVD which directly decomposes the ad covariate matrix data. The ad clusters shown in Figure 4 are obtained by applying the K-means clustering algorithm to the ad latent component data from each method. As shown in Figure 4, the first two columns of the latent components returned from our `COSTCO` show a clear clustering structure with 5 clusters. On the other hand, the ad components extracted from `tenALSsparse` are all clustered around zeros. This is because the ad CTR tensor is highly sparse and the latent components based on decomposing the tensor itself contain many small values. Therefore, ad clusters generated using `tenALSsparse` tend to have very large and very small clusters.
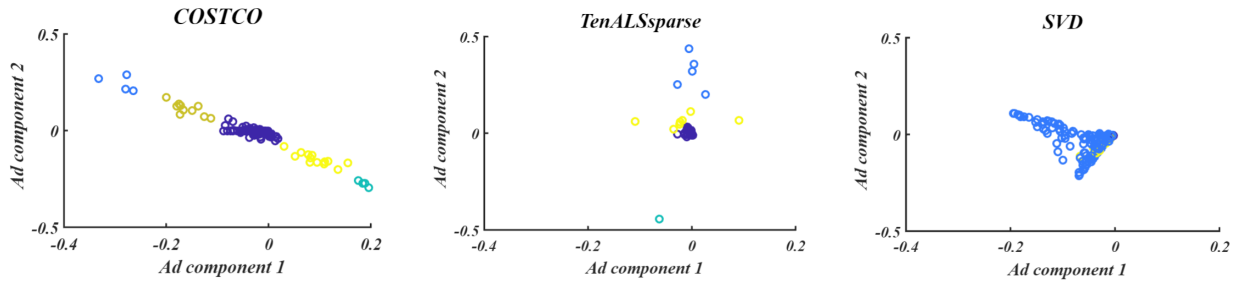
Figure 4: Scatter plot of the ad latent components obtained from three methods. Different clusters are represented via different colors.

Finally, Figure 5 demonstrates some interesting ad clustering results obtained from our `COSTCO` algorithm which links different ad industries into the same cluster. For example based on cluster 1 from `COSTCO`, ads about male and female online dating are clustered together with ads about women retail stores and man clothing accessories. In cluster 2 from `COSTCO`, ads about weight lost and weight lost surgery are clustered together with ads about gourmet cuisine and restaurant which indicates that users who interact with weight loss ads are also interested in nutrition related ads. Cluster 3 of `COSTCO` contains ads about house mortgage, home security devices, auto, home and auto insurance, house weather control devices which indicates that users that are homeowners tend
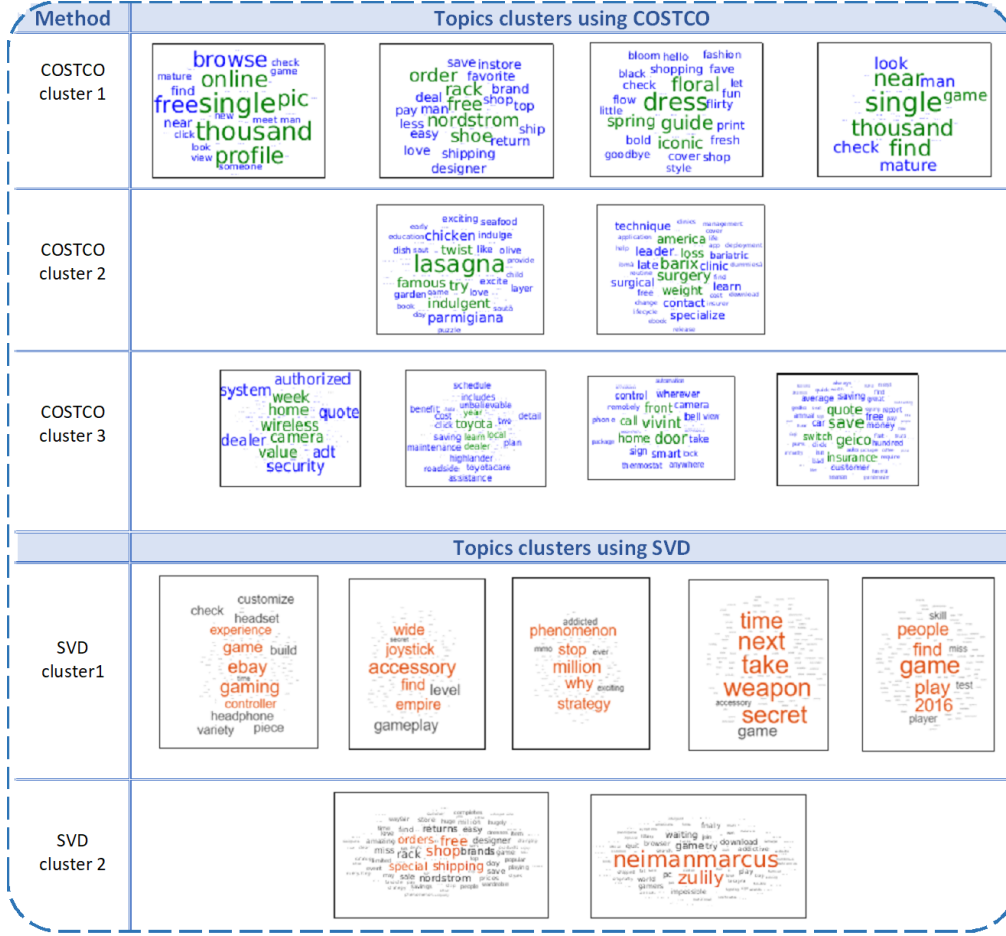
Figure 5: Result of ad clusters obtained using different methods

to be interested in home and auto related things. These interesting clusters are not obtained in the SVD method nor the `tenALSsparse` method. The clusters from SVD are solely related to the topic of each ad as shown in Figure 5 and the clusters from `tenALSsparse` are highly unbalanced and do not contain any understandable relationship between ads. These clustering results illustrate the practical value of our `COSTCO` method. By incorporating ad covariate matrix into the completion of the ad CTR tensor, we are able to obtain a more synthetic description of ads and find interesting links between different advertising industries, which directly helps the marketing team to strategize the ad planing procedure accordingly for better ad targeting.

References

ACAR, E., KOLDA, T. G. and DUNLAVY, D. M. (2011). All-at-once optimization for coupled matrix and tensor factorizations. *arXiv preprint arXiv:1105.3422* .

ACAR, E., RASMUSSEN, M. A., SAVORANI, F., NÆS, T. and BRO, R. (2013). Understanding data fusion within the framework of coupled matrix and tensor factorizations. *Chemometrics and Intelligent Laboratory Systems* **129** 53–63.

ALLEN, G. (2012). Sparse higher-order principal components analysis. In *International Conference on Artificial Intelligence and Statistics*.

ANANDKUMAR, A., GE, R., HSU, D., KAKADE, S. M. and TELGARSKY, M. (2014a). Tensor decompositions for learning latent variable models. *Journal of Machine Learning Research* **15** 2773–2832.

ANANDKUMAR, A., GE, R. and JANZAMIN, M. (2014b). Guaranteed non-orthogonal tensor decomposition via alternating rank-1 updates. *arXiv preprint arXiv:1402.5180* .

BI, X., QU, A., SHEN, X. ET AL. (2018). Multilayer tensor factorization with applications to recommender systems. *Annals of Statistics* **46** 3308–3333.

BI, X., TANG, X., YUAN, Y., ZHANG, Y. and QU, A. (2020). Tensors in statistics. *Annual Review of Statistics and Its Application* **8**.

BLEI, D. M., NG, A. Y. and JORDAN, M. I. (2003). Latent dirichlet allocation. *Journal of machine Learning research* **3** 993–1022.

CAI, C., LI, G., POOR, H. V. and CHEN, Y. (2019). Nonconvex low-rank tensor completion from noisy data. In *Advances in Neural Information Processing Systems* (H. Wallach, H. Larochelle, A. Beygelzimer, F. d Alch e-Buc, E. Fox and R. Garnett, eds.), vol. 32. Curran Associates, Inc.

CAI, C., POOR, H. V. and CHEN, Y. (2020). Uncertainty quantification for nonconvex tensor completion: Confidence intervals, heteroscedasticity and optimality. In *Proceedings of the 37th International Conference on Machine Learning* (H. D. III and A. Singh, eds.), vol. 119 of *Proceedings of Machine Learning Research*. PMLR.

CHEN, R., YANG, D. and ZHANG, C.-H. (2019). Factor models for high-dimensional tensor time series. *arXiv preprint arXiv:1905.07530* .

CHOI, D., JANG, J. G. and KANG, U. (2019). S3cmtf: Fast, accurate, and scalable method for incomplete coupled matrix-tensor factorization. *PLoS ONE* **14**.

HAGHIGHAT, M., ABDEL-MOTTALEB, M. and ALHALABI, W. (2016). Discriminant correlation analysis: Real-time feature level fusion for multimodal biometric recognition. *IEEE* .

HAO, B., ZHANG, A. R. and CHENG, G. (2020). Sparse and low-rank tensor estimation via cubic sketchings. In *Proceedings of the Twenty Third International Conference on Artificial Intelligence and Statistics* (S. Chiappa and R. Calandra, eds.), vol. 108 of *Proceedings of Machine Learning Research*. PMLR.

HOFF, P. (2015). Multilinear tensor regression for longitudinal relational data. *Ann. Appl. Stat.* **9** 1169–1193.

HUANG, H., LIU, Y. and ZHU, C. (2020). A unified framework for coupled tensor completion. *arXiv preprint arXiv:2001.02810* .

Ipsen, C. F. (1998). Relative perturbation results for matrix eigenvalues and singular values. *Acta Numerica* **7** 151–201.

Jain, P. and Oh, S. (2014). Provable tensor factorization with missing data. In *Advances in Neural Information Processing Systems*.

Jing, B.-Y., Li, T., Lyu, Z. and Xia, D. (2020). Community detection on mixture multi-layer networks via regularized tensor decomposition. *arXiv preprint arXiv:2002.04457* .

Karatzoglou, A., Amatriain, X., Baltrunas, L. and Oliver, N. (2010). Multiverse recommendation: n-dimensional tensor factorization for context-aware collaborative filtering. *ACM Recommender Systems* .

Kishan, W., Makoto, Y. and Hiroshi, M. (2018). Convex coupled matrix and tensor completion. *arXiv preprint arXiv:1705.05197* .

Kolda, T. G. and Bader, B. W. (2009). Tensor decompositions and applications. *SIAM review* **51** 455–500.

Koren, Y., Bell, R., Volinsky, C. et al. (2009). Matrix factorization techniques for recommender systems. *Computer* **42** 30–37.

Li, L., Kang, J., Lockhart, S. N., Adams, J. and Jagust, W. J. (2018). Spatially adaptive varying correlation analysis for multimodal neuroimaging data. *IEEE transactions on medical imaging* **38** 113–123.

Li, L., Zeng, J. and Zhang, X. (2020). Generalized liquid association analysis for multimodal data integration. *arXiv preprint arXiv:2008.03733* .

Li, L. and Zhang, X. (2017). Parsimonious tensor response regression. *Journal of the American Statistical Association* **112** 1131–1146.

Lin, Y.-R., Sun, J., Castro, P., Konuru, R., Sundaram, H. and Kelliher, A. (2009). Metafac: community discovery via relational hypergraph factorization. In *Proceedings of the 15th ACM SIGKDD international conference on Knowledge discovery and data mining*. ACM.

Luo, Y., Ahmad, F. S. and Shah, S. J. (2017). Tensor factorization for precision medicine in heart failure with preserved ejection fraction. *Journal of Cardiovascular Translational Research* **10**.

Montanari, A. and Sun, N. (2018). Spectral algorithms for tensor completion. *Communications on Pure and Applied Mathematics* **71**.

Pan, Y., Mai, Q. and Zhang, X. (2019). Covariate-adjusted tensor classification in high dimensions. *Journal of the American Statistical Association* **114** 1305–1319.

Papalexakis, E. E., Faloutsos, C. and Sidiropoulos, N. D. (2016). Tensors for data mining and data fusion: Models, applications, and scalable algorithms. *ACM Transactions on Intelligent Systems and Technology* **8**.

Sidiropoulos, N. D., Lathauwer, L. D., Fu, X., Huang, K., Papalexakis, E. E. and Faloutsos, C. (2017). Tensor decomposition for signal processing and machine learning. *IEEE Transactions on Signal Processing* **65**.

SONG, Q., GE, H., CAVERLEE, J. and HU, X. (2019). Tensor completion algorithms in big data analytics. *ACM Transactions on Knowledge Discovery from Data* **13**.

STEWART, G. W. (1990). Perturbation theory for the singular value decomposition. In *SVD and Signal ProcessingPart II: Algorithms Analysis and Applications*.

SUN, W. W., LU, J., LIU, H. and CHENG, G. (2017). Provable sparse tensor decomposition. *Journal of the Royal Statistical Society. Series B: Statistical Methodology* **79**.

SYMEONIDIS, P., NANOPOULOS, A. and MANOLOPOULOS, Y. (2008). Tag recommendations based on tensor dimensionality reduction.

TANG, X., BI, X. and QU, A. (2020). Individualized multilayer tensor learning with an application in imaging analysis. *Journal of the American Statistical Association* **115** 836–851.

TOMASI, G. and BRO., R. (2006). A comparison of algorithms for fitting the parafac model. *Computational Statistics and Data Analysis* **50** 1700–1734.

WANG, H., ZHANG, Q., CHEN, F. Y., MAN LEUNG, E. Y., YI WONG, E. L. and YEOH, E.-K. (2019). Tensor factorization-based prediction with an application to estimating the risk of chronic diseases. *bioRxiv* .

WANG, X., ZHU, H. and INITIATIVE, A. D. N. (2017). Generalized scalar-on-image regression models via total variation. *Journal of the American Statistical Association* **112** 1156–1168.

WANG, Z., GU, Q., NING, Y. and LIU, H. (2014a). High dimensional expectation-maximization algorithm: Statistical optimization and asymptotic normality. *arXiv preprint arXiv:1412.8729* .

WANG, Z., LIU, H. and ZHANG, T. (2014b). Optimal computational and statistical rates of convergence for sparse nonconvex learning problems. *Annals of statistics* **42** 2164.

XIA, D. and YUAN, M. (2019). On polynomial time methods for exact low-rank tensor completion. *Foundations of Computational Mathematics* **19**.

XIA, D. and YUAN, M. (2021). Effective tensor sketching via sparsification. *IEEE Transactions on Information Theory* **67** 1356–1369.

XIA, D., YUAN, M. and ZHANG, C.-H. (2021). Statistically optimal and computationally efficient low rank tensor completion from noisy entries. *Ann. Statist.* **49** 76–99.

XUE, F. and QU, A. (2020). Integrating multisource block-wise missing data in model selection. *Journal of the American Statistical Association* 1–14.

YUAN, M. and ZHANG, C. H. (2017). Incoherent tensor norms and their applications in higher order tensor completion. *IEEE Transactions on Information Theory* **63**.

ZHANG, A. (2019). Cross: Efficient low-rank tensor completion. *Annals of Statistics* **47**.

ZHANG, A. and HAN, R. (2019). Optimal sparse singular value decomposition for high-dimensional high-order data. *Journal of the American Statistical Association* **114** 1708–1725.

ZHOU, H., LI, L. and ZHU, H. (2013). Tensor regression with applications in neuroimaging data analysis. *Journal of the American Statistical Association* **108** 540–552.

ZHOU, T., QIAN, H., SHEN, Z., ZHANG, C. and XU, C. (2017). Tensor completion with side information: A riemannian manifold approach. In *IJCAI*.

Supplementary Material for
Covariate-assisted Sparse Tensor Completion

This supplementary material contains four parts. Section S.1 provides proofs of two main theorems, Section S.2 proves main lemmas, Section S.3 lists auxiliary lemmas and their proofs, and Section S.4 discusses additional simulation results.

S.1 Proof of Main Theorem

In this section we provide the proofs of the main theoretical results presented in 1 and 2. As elaborated in the discussion paragraphs in section 4 proving first the particular case in theorem 1 allows for a better presentation and explanation for the proof technique used for the general case in theorem 2. For simplicity, in the following proofs we consider the case where all tensor and matrix modes have the same dimensions n that is $n_1 = n_2 = n_3 = n_v = n$. We also assume that the sparsity parameters for each mode are equal ($d_1 = d_2 = d_3 = d_v = d$). It follows from the two simplification aforementioned that in Algorithm 1 we let $s_1 = s_2 = s_3 = s_v = s$. Proving the case, in which the dimensions of the tensor and matrix' modes are allowed to be unequal is a trivial yet notation heavy extension of the technique we use in the proof of Theorem 1 and Theorem 2. As defined in equation (S1), we use the euclidean distance between the component estimates and true components to measure the error for component recovery. We also use the relative absolute difference between estimated and true weights to capture the recovery error for the weights as defined in equation (S2). Define $\mathbf{d}_{u_r}$ to be,

$$\mathbf{d}_{u_r} =: \mathbf{u}_r - \mathbf{u}_r^*, \quad \text{and} \quad \|\mathbf{d}_{u_r}\|_2 = \|\mathbf{u}_r - \mathbf{u}_r^*\|_2, \tag{S1}$$

and

$$\Delta_{\lambda_r} := |\frac{\lambda_r - \lambda_r^*}{\lambda_r^*}| \quad \text{and} \quad \Delta_{\sigma_r} := |\frac{\sigma_r - \sigma_r^*}{\sigma_r^*}|, \tag{S2}$$

where $\mathbf{u}_r$ could be any of $\mathbf{a}_r, \mathbf{b}_r, \mathbf{c}_r, \mathbf{v}_r, \forall r \in [R]$.

S.1.1 Proof of Theorem 1

Theorem 1 provides the sufficient conditions which guarantee that the shared tensor components $\mathbf{a}_r$ and non-shared components $\mathbf{b}_r, \mathbf{c}_r$ recovered in Algorithm 1 converge to the truth $\mathbf{a}_r^*$ and $\mathbf{b}_r^*, \mathbf{c}_r^*$ respectively with the assumption that the tensor and matrix are dense and their decomposition weights are equal in each mode i.e $\lambda_r^* = \sigma_r^* \quad \forall r \in [R]$. The theorem also provides the explicit convergence rates for the tensor components in Algorithm 1 and highlights the difference in rates between the shared and non-shared components.

Our proof consists of three steps. In Step 1 we use Lemma 1 to derive the close form for the optimization problem presented in equation (7). This step is only specific to the dense tensor and equal weights case as it makes it possible to derive a close form solution to the optimization formula presented in equation (7). In Step 2, we derive a general bound for the share and non-shared tensor estimates by proving Lemmas 2 and 3 given that the components obtained from the initialization method satisfy a specific error constraint. In Step 3, we simplify the error bound obtained in Lemma 2 and 3 to ensure that the share and non-shared tensor component estimate contract at a geometric rate in one iteration. Theorem 1 is then completed by showing that after enough iterations the contraction error vanishes to only leave a statistical error.

Step 1: The next lemma accomplishes the first step in proving Theorem 1. Since the tensor and matrix weights are assumed to be equal, without loss of generality we use λ_r^* and $\lambda_r \; \forall r \in [R]$ to represent true and estimated weights respectively for both tensor and matrix.

Lemma 1. *Let $res_M = \mathbf{M} - \sum\limits_{m \neq r} \lambda_m \mathbf{a}_m \otimes \mathbf{v}_m$ and $res_T = P_\Omega(\mathcal{T}) - P_\Omega(\sum\limits_{m \neq r} \lambda_m \mathbf{a}_m \otimes \mathbf{b}_m \otimes \mathbf{c}_m)$ be the residual matrix and residual tensor, respectively defined on line (7) of Algorithm 1. In each ALS update of Algorithm 1, the solution to the optimization problem in equation (7) for the shared and non-shared components of the tensor and matrix in the rth iteration of the inner loop are,*

Share Components: $\mathbf{a}_r = \frac{\lambda_r \, res_T(\mathbf{I}, \mathbf{b}_r, \mathbf{c}_r) + \sigma_r \, res_M \mathbf{v}_r}{\lambda_r^2 P_\Omega(\mathbf{I}, \mathbf{b}_r^2, \mathbf{c}_r^2) + \sigma_r^2}$, $\qquad\qquad$ (S3)

Tensor non-shared components: $\mathbf{b}_r = \widetilde{\mathbf{b}}_r / \|\widetilde{\mathbf{b}}_r\|_2$, $\quad \mathbf{c}_r = \widetilde{\mathbf{c}}_r / \|\widetilde{\mathbf{c}}_r\|_2$, $\quad \lambda_r = \|\widetilde{\mathbf{c}}_r\|_2$, $\qquad$ (S4)

Matrix non-shared components: $\mathbf{v}_r = \widetilde{\mathbf{v}}_r / \|\widetilde{\mathbf{v}}_r\|_2$ *and* $\quad \sigma_r = \|\widetilde{\mathbf{v}}_r\|_2$, $\qquad\qquad$ (S5)

where $\widetilde{\mathbf{b}}_r$, $\widetilde{\mathbf{c}}_r$, $\widetilde{\mathbf{v}}_r$ have the following form

$$\widetilde{\mathbf{b}}_r = \frac{res_T(\mathbf{a}_r, \mathbf{I}, \mathbf{c}_r)}{P_\Omega(\mathbf{a}_r^2, \mathbf{I}, \mathbf{c}_r^2)} \quad \widetilde{\mathbf{c}}_r = \frac{res_T(\mathbf{a}_r, \mathbf{b}_r, \mathbf{I})}{P_\Omega(\mathbf{a}_r^2, \mathbf{b}_r^2, \mathbf{I})} \; and \; \widetilde{\mathbf{v}}_r = res_T \mathbf{a}_r. \tag{S6}$$

Note that the horizontal double lines in the expressions above indicate element-wise fraction and the squares in the denominator represent the element-wise squaring. The proof of Lemma 1 is provided in Section S.2. It involves deriving the close form of the optimization problem presented in equation (7) in the non-sparse tensor case.

Step 2: The second step builds the error contraction results in one iteration of Algorithm 1. We achieve step two through Lemmas 2 and 3 which address the non-shared and shared component cases respectively.

Lemma 2. *Assume Assumption 1 holds and $p \geq \frac{C\mu^3(1+\gamma/3)\log_2(n^{10})}{n^{3/2}\gamma^2}$ for some positive γ. Also assume estimates $\mathbf{a}_r$, $\mathbf{b}_r$, λ_r of our algorithm with $s_i = n_i$, $i = 1, 2, 3, v$, satisfy $\max\{\|\mathbf{d}_{a_r}\|, \|\mathbf{d}_{b_r}\|, \lambda_r^* \Delta_{\lambda_r}\} \leq$*

2

$\epsilon_T \ \forall r \in [R]$ *with* $\mathbf{d}_{a_r}, \mathbf{d}_{b_r}, \Delta_{\lambda_r}$ *defined in* (S1). *Then, the update for the non-shared tensor component* $\mathbf{c}_r$ *satisfies with probability* $1 - 2n^{-9}$,

$$\max_{r \in [R]} \|\mathbf{c}_r - \mathbf{c}_r^*\|_2 \leq \frac{16R\lambda_{max}^* \max\left(c_0/\sqrt{n} + 3\epsilon_T, \gamma\right)\epsilon_T + (1+\gamma)\|\mathcal{E}\|}{\lambda_{min}^*(1-\gamma)}. \tag{S7}$$

The detailed proof of Lemma 2 is presented in Section S.2. We later show in step 3 of the proof of Theorem 1 that the upper bound in (S7) can we written as the sum of a contracting term and a non contracting statistical error term.

Lemma 3. *Assume Assumption 1 holds and* $p \geq \frac{C\mu^3(1+\gamma/3)\log_2(n^{10})}{n^{3/2}\gamma^2}$ *for some positive* γ. *In addition, assume estimators* $\mathbf{c}_r$, $\mathbf{b}_r$, $\mathbf{v}_r$, λ_r, σ_r *of our algorithm with* $s_i = n_i$, $i = 1, 2, 3, v$, *satisfy* $\max\{\|\mathbf{d}_{c_r}\|, \|\mathbf{d}_{b_r}\|, \lambda_r^*\Delta_{\lambda_r}\} \leq \epsilon_T$ *and* $\{\|\mathbf{d}_{v_r}\|, \sigma_r^*\Delta_{\sigma_r}\} \leq \epsilon_M \ \forall r \in [R]$. *Then the update for the shared tensor component* $\mathbf{a}_r$ *satisfies with probability* $1 - 2n^{-9}$,

$$\max_{r \in [R]} \|\mathbf{a}_r - \mathbf{a}_r^*\|_2 \leq g(p, \epsilon_T, \zeta, R)\epsilon_T + f(\epsilon_M, \zeta, R)\epsilon_M + \frac{1}{\lambda_{min}^*}\frac{p(1+\gamma)\|\mathcal{E}_T\| + \|\mathcal{E}_M\|}{p(1-\gamma) + 1} \tag{S8}$$

with $g(p, \epsilon_T, \zeta, R) := \frac{16pR\lambda_{max}^*(\zeta + 3\epsilon_T, \gamma)}{\lambda_{min}^*(p(1-\gamma)+1)}$; $f(\epsilon_M, \zeta, R) := \frac{6R\lambda_{max}^*(\zeta + 3\epsilon_M)\epsilon_M}{\lambda_{min}^*(p(1-\gamma)+1)}$, *and* $\zeta = c_0/\sqrt{n}$.

The proof of Lemma 2 and Lemma 3 show that each iteration of Algorithm 1 results in an error contraction for the estimates of the non-shared ($\mathbf{b}_r$ and $\mathbf{c}_r$) and shared ($\mathbf{a}_r$) tensor components respectively. Such results imply that after a sufficient number of iterations, Algorithm 1 can yield good estimates for these components. The detailed proof of Lemma 3 is discussed in Section S.2.

Step 3: To complete the proof of the theorem, we carefully employ the assumptions on the initialization in order to guarantee that expressions (S7) and (S8) in Lemmas 2 and 3 can be written in the form $\epsilon_R + q\epsilon_0$ with $q \leq \frac{1}{2}$. This entails showing that for $f(\epsilon_M, \zeta, R)$ and $g(\epsilon_M, \zeta, R)$ in the Lemma 3 adds up to less than $\frac{1}{2}$ given the assumptions in Theorem 1.

Denote $\epsilon_0 := \max\{\epsilon_{T_0}, \epsilon_{M_0}\}$, $q_1 := \frac{16R\lambda_{max}^*(\zeta + 3\epsilon_0)(p + \frac{6}{16})}{\lambda_{min}^*(p(1-\gamma)+1)}$ and $q_2 := \frac{16R\lambda_{max}^*(p\gamma + \frac{6}{16}(\zeta + 3\epsilon_0))}{\lambda_{min}^*(p(1-\gamma)+1)}$. Set $\gamma := \frac{\lambda_{min}^*}{64R\lambda_{max}^*}$. According to Assumption 3, we get that $q_1 \leq \frac{p + 6/16}{2p+2} \leq \frac{1}{2}$. Also $q_2 \leq \frac{p}{4(\frac{63}{64}p + 1)} + \frac{3}{16} \leq \frac{1}{4} + \frac{3}{16} < \frac{1}{2}$ since $p \leq 1$. This implies that $q := \max\{q_1, q_2\} \leq 1/2$.

Finally, we bound the error term of $\max_{r \in [R]} \|\mathbf{a}_r - \mathbf{a}_r^*\|_2$ by showing that it can be written as a sum of a contracting term and a constant non-contracting term. Specifically, according to (S8) in each iteration we have,

$$\max_{r \in [R]} \|\mathbf{a}_r - \mathbf{a}_r^*\|_2 \leq g(p, \epsilon_{T_0}, \zeta, R)\epsilon_{T_0} + f(\epsilon_{M_0}, \zeta, R)\epsilon_{M_0} + \frac{1}{\lambda_{min}^*}\frac{p(1+\gamma)\|\mathcal{E}_T\| + \|\mathcal{E}_M\|}{p(1-\gamma) + 1}$$

$$\leq \max\{q_1, q_2\}\epsilon_0 + \frac{1}{\lambda_{min}^*}\frac{p(65/64)\|\mathcal{E}_T\| + \|\mathcal{E}_M\|}{p(63/64) + 1}$$

$$\leq q\epsilon_0 + \frac{1}{\lambda_{min}^*}\frac{p(65/64)\|\mathcal{E}_T\| + \|\mathcal{E}_M\|}{p(63/64) + 1}, \tag{S9}$$

3

where $q\epsilon_0$ is a contracting term and the term after it is non contracting. By iteratively applying the above inequality, after $\tau = \Omega\left(\log_2\left(\frac{(p(63/64)+1)\epsilon_0}{(65/64)p\|\mathcal{E}_T\|+\|\mathcal{E}_M\|}\right)\right)$, we get

$$\max_{r\in[R]}\|\mathbf{a}_r - \mathbf{a}_r^*\|_2 \leq \mathcal{O}\left(\frac{1}{\lambda_{min}^*}\frac{(65/64)p\|\mathcal{E}_T\| + \|\mathcal{E}_M\|}{p(63/64)+1}\right).$$

Similar derivation can be applied on the upper bound of $\max_{r\in[R]}\|\mathbf{c}_r - \mathbf{c}_r^*\|_2$ in (S7) to get a contracting and non contracting term. Then taking the maximun over all non-shared components and tensor weights lead to getting after running $\tau = \Omega\left(\log_2\left(\frac{(63/64)\lambda_{min}^*\epsilon_0}{(65/64)\|\mathcal{E}_T\|}\right)\right)$ iterations of Algorithm 1,

$$\max_{r\in[R]}\left(\|\mathbf{b}_r - \mathbf{b}_r^*\|_2, \|\mathbf{c}_r - \mathbf{c}_r^*\|_2, \frac{|\lambda_r - \lambda_r^*|}{\lambda_r^*}\right) \leq \mathcal{O}\left(\frac{(65/64)\|\mathcal{E}_T\|}{(63/64)\lambda_{min}^*}\right),$$

which completes the proof of Theorem 1. $\qquad\square$

S.1.2   Proof of Theorem 2

In this section we establish the results for the analysis of Theorem 2 which is the general and sparse case where the matrix and tensor weights are not assumed to be equal. In order to prove the general case we make use of some of the intermediate results derived in the analysis of Theorem 1. Namely, we follow the 3 three steps analysis approach introduced in the analysis of Theorem 1 and highlight the key difference which makes the analysis of Theorem 2 non trivial in comparison. As presented in the formulation of the optimization problem in (7) we use the ℓ^0 norm regularization as a mean to introduce sparsity in the model. However, deriving a close form solution to this sparse optimization problem becomes very difficult with this choice of regularization function. In step 1 of the analysis, we circumvent this issue by using a greedy truncation method defined on lines (9) and (11) of Algorithm 1 to approximate the sparse solution to the optimization problem in (7). We show that using the truncation method to only preserve the s largest entries of the components with the condition that $s \geq d$ is suitable for accurate components recovery. In practice for Algorithm 1 the parameter s can be tuned in a data-driven manner following the sequential tuning schema presented in Algorithm 3.2.2. In step 2 of the analysis, we derive a general bound for the shared tensor component through Lemma 4. In step 3 we simplify the general bound derived in step 2 to show that one iteration of the algorithm results in a geometric error contraction. Theorem 2 is then completed by showing that after enough iterations the contraction error vanished to only leave a statistical error.

Lemma 4. *Assume Assumptions 4, 5 and 6 hold, and that $s \geq d$. In addition, assume estimators $\mathbf{c}_r$, $\mathbf{b}_r$, $\mathbf{v}_r$, λ_r, σ_r of our algorithm satisfy $\max\{\|\mathbf{d}_{c_r}\|, \|\mathbf{d}_{b_r}\|, \lambda_r^*\Delta_{\lambda_r}\} \leq \epsilon_T$ and $\{\|\mathbf{d}_{v_r}\|, \sigma_r^*\Delta_{\sigma_r}\} \leq \epsilon_M$*

4

$\forall r \in [R]$ and $s_i \geq d_i$ for $i = 1, 2, 3, v$. Then the update for the shared tensor component $\mathbf{a}_r$ satisfies with probability $1 - 2n^{-9}$,

$$\max_{r \in [R]} \|\mathbf{a}_r - \mathbf{a}_r^*\|_2 \leq g(p, \epsilon_T, \zeta, R)\epsilon_T + f(\epsilon_M, \zeta, R)\epsilon_M$$

$$+ \frac{\lambda_{max}^* p(1+\gamma)\|\mathcal{E}_T\|_{<d+s>} + \sigma_{max}^*\|\mathcal{E}_M\|_{<d+s>}}{\lambda_{min}^{*2} p(1-\gamma) + \sigma_{min}^{*2}}, \tag{S10}$$

with $g(p, \epsilon_T, \zeta, R) \leq \frac{24pR\lambda_{max}^{*2} \max(\zeta + 3\epsilon_T, \gamma)}{\lambda_{min}^{*2} p(1-\gamma) + \sigma_{min}^{*2}}$; $f(\epsilon_M, \zeta, R) \leq \frac{9R\sigma_{max}^{*2}(\zeta + 3\epsilon_M)}{\lambda_{min}^{*2} p(1-\gamma) + \sigma_{min}^{*2}}$ and where $\zeta = c_0/\sqrt{d}$.

The detailed proof of Lemma 4 is discussed in Section S.2.

Step 3: The last step in the proof of Theorem 2, consists in using the assumptions on the initialization error in order to guarantee that expression (S10) in Lemmas 4 can be written in the form $\epsilon_R + q\epsilon_0$ with $q \leq \frac{1}{2}$. Just like was the case in the proof of Theorem 1, this entails showing that for $f(\epsilon_M, \zeta, R)$ and $g(\epsilon_M, \zeta, R)$ adds up to less than $\frac{1}{2}$ given the assumptions in Theorem 2.

Given the initialization condition in Assumption 6 we get

$$g(p, \epsilon_T, \zeta, R) \leq \frac{24pR\lambda_{max}^{*2} \max(\zeta + 3\epsilon_T, \gamma)}{\lambda_{min}^{*2} p(1-\gamma) + \sigma_{min}^{*2}}; \quad f(\epsilon_M, \zeta, R) \leq \frac{9R\sigma_{max}^{*2}(\zeta + 3\epsilon_M)}{\lambda_{min}^{*2} p(1-\gamma) + \sigma_{min}^{*2}}$$

Denote $\epsilon_0 := \max\{\epsilon_{T_0}, \epsilon_{M_0}\}$, $q_1 := \frac{24R(\zeta + 3\epsilon_0)(\lambda_{max}^{*2}p + \frac{9}{24}\sigma_{max}^{*2})}{\lambda_{min}^{*2} p(1-\gamma) + \sigma_{min}^{*2}}$ and $q_2 := \frac{24R(\lambda_{max}^{*2}p\gamma + \frac{9}{24}\sigma_{max}^{*2}(\zeta + 3\epsilon_0))}{\lambda_{min}^{*2} p(1-\gamma) + \sigma_{min}^{*2}}$. We choose $\gamma = \frac{1/2\lambda_{min} + 1/2\sigma_{min}}{96R\lambda_{max}}$. According to Assumption 6 we get that $q_1 \leq \frac{p\lambda_{max}^{*2} + 3/8\sigma_{max}^{*2}}{2(p\lambda_{max}^{*2} + \sigma_{max}^{*2})} \leq \frac{1}{2}$. Also $q_2 \leq \frac{p\min\{\lambda_{min}^{*2}, \sigma_{min}^{*2}\}}{4(\lambda_{min}^{*2}p\frac{95}{96} + \sigma_{min}^{*2})} + \frac{3\sigma_{max}^{*2}}{16(p\lambda_{max}^{*2} + \sigma_{max}^{*2})} \leq \frac{p}{4(p\frac{95}{96} + 1)} + \frac{3}{16}$. Hence $q_2 \leq \frac{1}{4} + \frac{3}{16} < \frac{1}{2}$ since $p \leq 1$. This implies that $q := \max\{q_1, q_2\} \leq 1/2$.

Finally, we bound the error term of $\max_{r \in [R]} \|\mathbf{a}_r - \mathbf{a}_r^*\|_2$ by showing that it can be written as a sum of a contracting term and a constant non-contracting term. Specifically, according to (S8) in each iteration we have,

$$\max_{r \in [R]} \|\mathbf{a}_r - \mathbf{a}_r^*\|_2 \leq g(p, \epsilon_{T_0}, \zeta, R)\epsilon_{T_0} + f(\epsilon_{M_0}, \zeta, R)\epsilon_{M_0}$$

$$+ \frac{(\lambda_{max}^* + \epsilon_T)p(1+\gamma)\|\mathcal{E}_T\|_{<d+s>} + (\sigma_{max}^* + \epsilon_T)\|\|\mathcal{E}_M\|_{<d+s>}}{(\lambda_{min}^* + \epsilon_T)^2 p(1-\gamma) + (\sigma_{min}^* + \epsilon_M)^2}$$

$$\leq \max\{q_1, q_2\}\epsilon_0 + \frac{(97/96)p\lambda_{max}^*\|\mathcal{E}_T\|_{<d+s>} + \sigma_{max}^*\|\mathcal{E}_M\|_{<d+s>}}{\frac{95}{96}p\lambda_{min}^{*2} + \sigma_{min}^{*2}}$$

$$\leq q\epsilon_0 + \frac{(97/96)p\lambda_{max}^*\|\mathcal{E}_T\|_{<d+s>} + \sigma_{max}^*\|\mathcal{E}_M\|_{<d+s>}}{\frac{95}{96}p\lambda_{min}^{*2} + \sigma_{min}^{*2}}, \tag{S11}$$

where $q\epsilon_0$ is a contracting term. By iteratively applying the above inequality, after the number of iterations stated in Theorem 2, we get

$$\max_{r \in [R]} \|\mathbf{a}_r - \mathbf{a}_r^*\|_2 \leq \mathcal{O}\left(\frac{(97/96)p\lambda_{max}^*\|\mathcal{E}_T\|_{<d+s>} + \sigma_{max}^*\|\mathcal{E}_M\|_{<d+s>}}{(95/96)p\lambda_{min}^{*2} + \sigma_{min}^{*2}}\right),$$

5

The proof for the non-shared component in Theorem 2 is very similar to that of the non-share component in Theorem 1 we therefore leave it out. This completes the proof of Theorem 2. $\qquad\square$

S.2 Proofs of Lemmas 1, 2, 3 and 4

In this section we provide details of the derivation for the proofs of Lemmas 1-4.

S.2.1 Proof of Lemma 1

The dense version of the optimization problem in (7) can be formulated as follows:

Optimization: Non-Sparse formulation

$$\min_{\mathbf{A},\mathbf{B},\mathbf{C},\mathbf{V}} \left\{ \|P_\Omega(\mathcal{T}) - P_\Omega\big(\sum_{r\in[R]} \lambda_r \mathbf{a}_r \otimes \mathbf{b}_r \otimes \mathbf{c}_r \big)\|_F^2 + \|\mathbf{M} - \sum_{r\in[R]} \sigma_r \mathbf{a}_r \otimes \mathbf{v}_r\|_F^2 \right\} \qquad \text{(S12)}$$

subject to $\sigma_r, \lambda_r \in \mathbb{R}^+$,

Given $\mathrm{res}_M = \mathbf{M} - \sum_{m \neq r} \sigma_m \mathbf{a}_m \otimes \mathbf{v}_m$ and $\mathrm{res}_T = P_\Omega(\mathcal{T}) - P_\Omega\big(\sum_{m \neq r} \lambda_r \mathbf{a}_m \otimes \mathbf{b}_m \otimes \mathbf{c}_m \big)$ the residual matrix and residual tensor, respectively. In each ALS update of Algorithm 1 we need to solve the following least squares optimizations problem.

$$\min_{\mathbf{a}_r} \left\{ \|\mathrm{res}_M - \sigma_r \mathbf{a}_r \otimes \mathbf{v}_r\|_F^2 + \|\mathrm{res}_T - P_\Omega(\lambda_r \mathbf{a}_r \otimes \mathbf{b}_r \otimes \mathbf{c}_r)\|_F^2 \right\}. \qquad \text{(S13)}$$

The optimization problem in (S13) is convex in $\mathbf{a}_r$. Therefore, we can find $\mathbf{a}_r$ by taking its derivative and setting it to zero. In order to do this we first derive the equivalent of the optimization function in (S13) explicitly in terms of the entries of the tensor and matrix components:

$$\min_{\mathbf{a}_r} \left\{ \sum_{i,j} \big(\mathrm{res}_{Mi,l} - \sigma_r \mathbf{a}_r(i) \times \mathbf{v}_r(l) \big)^2 + \sum_{\{i,j,k\}\in\Omega} \big(\mathrm{res}_{Ti,j,k} - \lambda_r \mathbf{a}_r(i) \times \mathbf{b}_r(j) \times \mathbf{c}_r(k) \big)^2 \right\}, \qquad \text{(S14)}$$

where $\mathrm{res}_{Ti,j,k}$ is the $(i,j,k)^{\text{th}}$ entry of res_T and $\mathrm{res}_{Mi,l}$ is the $(i,l)^{\text{th}}$ entry of res_M. The notation $\{i,j,k\} \in \Omega$ with Ω defines in (3), guarantees that the summation only applies on the observed entries of tensor res_T; $\mathbf{a}_r(i)$ is the ith component of $\mathbf{a}_r$ where $i \in [n]$.

Taking the derivative of (S14) with respect to $\mathbf{a}_r(i)$ for all $i \in [n]$ and setting it to zero we get:

$$\mathbf{a}_r(i) = \frac{\lambda_r \sum_{j,k}(\mathrm{res}_{Ti,j,k}\mathbf{b}_r(j)\mathbf{c}_r(k)) + \sigma_r \sum_j \mathrm{res}_{Mi,l}\mathbf{v}_r(l)}{\lambda_r^2 \sum_{j,k} \mathbf{b}_r^2(j)\mathbf{c}_r^2(k) + \sigma_r^2 \sum_l \mathbf{v}_r^2(l)} \qquad \text{(S15)}$$

for all $i \in [n]$. The first summation in the numerator of equation (S15) is the definition of the modes 2 and 3 tensor matrix product of res_T with the matrix obtained from $\mathbf{b}_r \otimes \mathbf{c}_r$. Following the notation provided in section 2 this product can be rewritten as:

$$\text{res}_T(\mathbf{I}, \mathbf{b}_r, \mathbf{c}_r) = \text{res}_T \times_2 \mathbf{b}_r \times_3 \mathbf{c}_r, \tag{S16}$$

for all $i \in [n]$, where $\mathbf{I}$ is the identity matrix. It is worth noting that the vector tensor product in (S16) is a vector of length n. We can write the second term in the numerator as a matrix vector left multiplication. The vector $\mathbf{a}_r$ can therefore be written as:

$$\mathbf{a}_r = \frac{\lambda_r \text{res}_T(\mathbf{I}, \mathbf{b}_r, \mathbf{c}_r) + \sigma_r \text{res}_M \mathbf{v}_r}{\lambda_r^2 P_\Omega(\mathbf{I}, \mathbf{b}_r^2, \mathbf{c}_r^2) + \sigma_r^2}, \tag{S17}$$

where the double line fraction indicates element-wise division and $(\cdot)^2$ denotes elements-wise power.

In order to solve the optimization problem for components other than the first component that are not shared with the matrix we proceed similarly. We start from:

$$\min_{\mathbf{b}_r} \left\{ \|\text{res}_T - P_\Omega(\lambda_r \mathbf{a}_r \otimes \mathbf{b}_r)\|_F^2 \right\}, \tag{S18}$$

which is equivalent to

$$\sum_{\{i,j,k\} \in \Omega} \left(\text{res}_{T\,i,j,k} - \lambda_r \mathbf{a}_r(i) \times \mathbf{b}_r(j) \times \mathbf{c}_r(k) \right)^2. \tag{S19}$$

Taking the derivative of (S19) with respect to $\mathbf{b}_r(j)$ or $\mathbf{c}_r(k)$ then setting to them to zero and solving for $\mathbf{b}_r(j)$ or $\mathbf{c}_r(k)$ we get the following update:

$$\widetilde{\mathbf{b}}_r(j) := \lambda_r \mathbf{b}_r(j) = \frac{\sum\limits_{\{i,.,k\} \in \Omega} (\text{res}_{T\,i,j,k} \mathbf{a}_r(i) \mathbf{c}_r(k))}{\sum\limits_{\{i,.,k\} \in \Omega} \mathbf{a}_r^2(i) \mathbf{c}_r^2(k)}, \quad \widetilde{\mathbf{c}}_r(k) := \lambda_r \mathbf{c}_r(k) = \frac{\sum\limits_{\{i,j,.\} \in \Omega} (\text{res}_{T\,i,j,k} \mathbf{a}_r(i) \mathbf{b}_r(j))}{\sum\limits_{\{i,j,.\} \in \Omega} \mathbf{a}_r^2(i) \mathbf{b}_r^2(j)}, \tag{S20}$$

respectively. In vector form this is written as,

$$\widetilde{\mathbf{b}}_r = \frac{\text{res}_T(\mathbf{a}_r, \mathbf{I}, \mathbf{c}_r)}{P_\Omega(\mathbf{a}_r^2, \mathbf{I}, \mathbf{c}_r^2)} \quad \text{and} \quad \widetilde{\mathbf{c}}_r = \frac{\text{res}_T(\mathbf{a}_r, \mathbf{b}_r, \mathbf{I})}{P_\Omega(\mathbf{a}_r^2, \mathbf{b}_r^2, \mathbf{I})}. \tag{S21}$$

These are the un-normalized updates in line 10 of Algorithm 1. Since by definition $\mathbf{b}_r$ and $\mathbf{c}_r$ are unit vectors then $\|\widetilde{\mathbf{c}}_r\|_2 = \|\lambda_r \mathbf{c}_r\|_2 = |\lambda_r|$ as defined in line 12 of Algorithm 1 and $\mathbf{c}_r = \widetilde{\mathbf{c}}_r / \|\widetilde{\mathbf{c}}_r\|_2$ as in line 13 of the main algorithm. The update for $\mathbf{b}$ is obtained in a similar manner. The above derivation corresponds to the non-sparse scenario, i.e., Algorithm 1 without the truncation steps on lines 9 and 11. However for the sparse case, to incorporate sparsity in the resulting update equations, we use the truncation scheme proposed in Sun et al. (2017). We get the estimate of the matrix component $\mathbf{v}_r$, using a similar derivation and get,

$$\widetilde{\mathbf{v}}_r := \sigma_r \mathbf{v}_r = \text{res}_T \mathbf{a}_r, \tag{S22}$$

and since $\mathbf{v}_r$ is a unit vector we get $\sigma_r = \|\widetilde{\mathbf{v}}_r\|_2$ and $\mathbf{v}_r = \widetilde{\mathbf{v}}_r/\|\widetilde{\mathbf{v}}_r\|_2$ as in lines 12 and 13 of Algorithm 1. This complete the proof of Lemma 1. $\qquad\square$

S.2.2 Proof of Lemma 2

The main challenge in the proof of Lemma 2 lies in finding a tight upper bound for the error of c_r. In the following derivation only provide the analysis for the non-shared tensor components $\mathbf{c}_r$ since the proof of the other non-shared component $\mathbf{b}_r$ is very similar.

In (S4) we derived the close form formula for the update $\mathbf{c}_r$ to be $\widetilde{\mathbf{c}}_r/\|\widetilde{\mathbf{c}}_r\|_2$. To bound the expression $\|\mathbf{c}_r - \mathbf{c}_r^*\|_2$, we make use of the intermediate estimate $\widetilde{\mathbf{c}}_r$ which is define in (S6) as,

$$\widetilde{\mathbf{c}}_r = \frac{\operatorname{res}_T(\mathbf{a}_r, \mathbf{b}_r, \mathbf{I})}{P_\Omega(\mathbf{a}_r^2, \mathbf{b}_r^2, \mathbf{I})}. \tag{S23}$$

From Lemma 1, notice that $\widetilde{\mathbf{c}}_r$ can be written as $\lambda_r \mathbf{c}_r$. That is, $\widetilde{\mathbf{c}}_r$ can be thought of as the un-normalized version of the estimate $\mathbf{c}_r$. Proving Lemma 2 therefore consists in deriving an error bound for $\|\widetilde{\mathbf{c}}_r - \lambda_r^* \mathbf{c}_r^*\|_2$, followed by using Lemma 9 which shows that $\|\mathbf{c}_r - \mathbf{c}_r^*\|_2 \leq \frac{2}{\lambda_r^*}\|\widetilde{\mathbf{c}}_r - \lambda_r^* \mathbf{c}_r^*\|_2$.

Let $\mathbf{D}$, $\mathbf{E}$, $\mathbf{F}$, $\mathbf{G}$, be $n \times n$ diagonal matrices with the following diagonal elements,

$$\mathbf{D}_{kk} = \sum_{i,j} \delta_{ijk} \mathbf{a}_r^2(i) \mathbf{b}_r^2(j) ; \quad \mathbf{E}_{kk} = \sum_{i,j} \delta_{ijk} \mathbf{a}_r^*(i) \mathbf{b}_r^*(j) \mathbf{a}_r(i) \mathbf{b}_r(j);$$

$$\mathbf{F}_{kk} = \sum_{i,j} \delta_{ijk} \mathbf{a}_m^*(i) \mathbf{b}_m^*(j) \mathbf{a}_r(i) \mathbf{b}_r(j) ; \quad \mathbf{G}_{kk} = \sum_{i,j} \delta_{ijk} \mathbf{a}_m(i) \mathbf{b}_m(j) \mathbf{a}_r(i) \mathbf{b}_r(j),$$

where δ_{ijk} is a Bernoulli random variable with success probability p and indicates whether the ijk_{th} tensor entry is observed or not. Then the vector $\widetilde{\mathbf{c}}_r$ obtained after one pass of the inner loop of Algorithm 1 can be written as

$$\widetilde{\mathbf{c}}_r = \mathbf{D}^{-1} \left(\lambda_r^* \mathbf{E} \mathbf{c}_r^* + \sum_{m \in [R] \backslash r} (\lambda_m^* \mathbf{F} \mathbf{c}_m^* - \lambda_m \mathbf{G} \mathbf{c}_m) + \mathcal{E}_T(\mathbf{a}_r, \mathbf{b}_r, \mathbf{I}) \right). \tag{S24}$$

We make use of the fact that $\|\widetilde{\mathbf{c}}_r - \lambda_r^* \mathbf{c}_r^*\|_2 = \|\widetilde{\mathbf{c}}_r - \lambda_r^* \mathbf{D}^{-1} \mathbf{D} \mathbf{c}_r^*\|_2$, to yield,

$$\|\widetilde{\mathbf{c}}_r - \lambda_r^* \mathbf{c}_r^*\|_2 = \| \underbrace{\lambda_r^* \mathbf{D}^{-1}(\mathbf{E} - \mathbf{D})\mathbf{c}_r^*}_{err_1} + \underbrace{\mathbf{D}^{-1} \sum_{m \in [R] \backslash r} (\lambda_m^* \mathbf{F} \mathbf{c}_m^* - \lambda_m \mathbf{G} \mathbf{c}_m)}_{err_2} + \underbrace{\mathbf{D}^{-1} \mathcal{E}_T(\mathbf{a}_r, \mathbf{b}_r, \mathbf{I})}_{err_3} \|_2$$

Applying the triangle inequality to the above expression is very convenient as it breaks its into the three different error terms shown below, each characterizing different sources of error affecting the non-shared component update,

$$\|\widetilde{\mathbf{c}}_r - \lambda_r^* \mathbf{c}_r^*\|_2 \leq \|err_1\|_2 + \|err_2\|_2 + \|err_3\|_2, \tag{S25}$$

where $err_1 = \lambda_r^* \mathbf{D}^{-1}(\mathbf{E} - \mathbf{D})\mathbf{c}_r^*$ can be characterized as the error due to the power method. This error is well understood and does not require meticulous bound control in order to yield the desire result. Also if $\mathcal{T}^*$ was a rank 1 and noiseless tensor, the proof of Lemma 2 would reduce to bounding this error term.

Unlike err_1 discussed above, bounding $err_2 = \mathbf{D}^{-1} \sum\limits_{m \in [R] \backslash r} (\lambda_m^* \mathbf{F}\mathbf{c}_m^* - \lambda_m \mathbf{G}\mathbf{c}_m)$ represents the main challenge in the proof. It is worth noting that err_2 is the error due to the deflation method applied in Algorithm 1. Two issues arises with bounding this error, the first resides in the non-orthogonality of the tensor $\mathcal{T}^*$. If the tensor $\mathcal{T}^*$ was orthogonal then a deflation algorithm would have little to no difficulty differentiating between the ranks of the tensor. However with the non-orthogonality assumption we are left with a non disappearing residual due to fact that for example two component vectors of the tensor $\mathbf{c}_r$ and $\mathbf{c}_j$ could be close to parallel making it difficult for the algorithm to differentiate between the two. Moreover err_2 exposes the relationship that exists between recovering a component $\mathbf{c}_r$ and the error for the other mode components $\mathbf{a}_j, \mathbf{b}_j$ and with $j \neq r$. If not carefully controlled, err_2 could cause the estimate $\mathbf{c}_r$ to diverge from $\mathbf{c}_r^*$. Assumption $(1.iii)$ is therefore used and required to control the magnitude of err_2.

The third error term $err_3 = \mathbf{D}^{-1}\mathcal{E}_T(\mathbf{a}_r, \mathbf{b}_r, \mathbf{I})$ is simply the error due to the noise of the tensor and can be easily bounded after standard assumptions are made about the spectral norm of $\mathcal{E}_T$. Another challenge in bounding the error of the $\mathbf{c}_r$ update comes from the fact that the tensor has missing entries. As represented in equation (S23) the operations involved in computing the update $\mathbf{c}_r$ is only carried on the observed entries of the tensor. This computation caveat forces the use of concentration inequalities in the analysis of the error bound of the component. Choosing the right concentration inequality becomes therefore very important in order to guarantee a given convergence rate while allowing some reasonable constraints on the tensor entry reveal probability to p. The rest of the proof consists in finding a bound for each of the three errors discussed above. We start with bounding the first error term. Using the fact that $\|\mathbf{c}_r^*\|_2 = 1$ and since $\mathbf{D}^{-1}(\mathbf{E} - \mathbf{D})$ is a diagonal matrix its spectral norm is the maximum absolute value of its diagonal elements, we get

$$
\begin{aligned}
\|err_1\|_2 &\leq \|\lambda_r^* \mathbf{D}^{-1}(\mathbf{E} - \mathbf{D})\|_2 \\
&= \lambda_r^* \max_k |\mathbf{D}^{-1}(\mathbf{E} - \mathbf{D})|_{kk} \\
&\leq \lambda_r^* \max_k |\mathbf{D}^{-1}|_{kk} \max_k |(\mathbf{E} - \mathbf{D})|_{kk}.
\end{aligned}
$$

Next is finding an upper bound for the maximum of each of the random elements in the equation above with high probability. To do that we first get an upper bound for each of the diagonal

elements with high probability and make use of the union bound method. This is derived as:

$$|(\mathbf{E} - \mathbf{D})_{kk}| = |\sum_{ij} \delta_{ijk} \mathbf{a}_r^*(i) \mathbf{b}_r^*(j) \mathbf{a}_r(i) \mathbf{b}_r(j) - \sum_{jk} \delta_{ijk} \mathbf{a}_r^2(i) \mathbf{b}_r^2(j)|$$

$$= |\sum_{ij} \delta_{ijk} \mathbf{a}_r^*(i) \mathbf{d}_{b_r}(j) \mathbf{a}_r(i) \mathbf{b}_r(j) - \sum_{ij} \delta_{ijk} \mathbf{d}_{a_r}(i) \mathbf{b}_r^*(j) \mathbf{a}_r(i) \mathbf{b}_r(j)$$

$$- \sum_{ij} \delta_{ijk} \mathbf{d}_{a_r}(i) \mathbf{d}_{b_r}(j) \mathbf{a}_r(i) \mathbf{b}_r(j)|.$$

The expression on the right side of the equality are obtained from the fact that $\mathbf{a}_r(i) = \mathbf{a}_r^*(i) + \mathbf{d}_{a_r}(i)$ and $\mathbf{b}_r(j) = \mathbf{b}_r^*(j) + \mathbf{d}_{b_r}(j)$. Next Lemma 6 is used to bound the three random elements inside the absolute value. Combined with the triangle inequality and the fact that $|\langle \mathbf{d}_{a_r}, \mathbf{a}_r^* \rangle| = \frac{1}{2} \|\mathbf{d}_{a_r}\|_2^2$ (Lemma 11) yields the following,

$$|(\mathbf{E} - \mathbf{D})_{kk}| \leq p \left(|\langle \mathbf{a}_r^*, \mathbf{a}_r \rangle \langle \mathbf{d}_{b_r}, \mathbf{b}_r \rangle| + |\langle \mathbf{d}_{a_r}, \mathbf{a}_r \rangle \langle \mathbf{b}_r^*, \mathbf{b}_r \rangle| + |\langle \mathbf{d}_{a_r}, \mathbf{a}_r \rangle \langle \mathbf{d}_{b_r}, \mathbf{b}_r \rangle| \right)$$

$$+ p\gamma \left(\|\mathbf{d}_{a_r}\|_2 + \|\mathbf{d}_{b_r}\|_2 + \|\mathbf{d}_{a_r}\|_2 \|\mathbf{d}_{b_r}\|_2 \right)$$

$$\leq 6p \left(\max_{\mathbf{u}_r \in \{a_r, b_r\}} \{ \sqrt{1 - \frac{\|d_{u_r}\|_2}{2}} \|\mathbf{d}_{u_r}\|_2^2, \|\mathbf{d}_{u_r}\|_2^4, \gamma \|\mathbf{d}_{u_r}\|_2 \} \right)$$

$$= 6p \max_{\mathbf{u}_r \in \{a_r, b_r\}} \left(\sqrt{1 - \frac{\|d_{u_r}\|_2}{2}} \|\mathbf{d}_{u_r}\|_2, \|\mathbf{d}_{u_r}\|_2^3, \gamma \right) \|\mathbf{d}_{u_r}\|_2. \tag{S26}$$

The above inequality holds with probability $1 - 2n^{-10}$ provided the reveal probability $p \geq \frac{C\mu^3(1+\gamma/3)\log^2(n^{10})}{n^{3/2}\gamma^2}$. Using (S26) and the bound from Lemma 5, we get

$$\|err_1\|_2 \leq \frac{6p\lambda_r^* \max_{\mathbf{u}_r \in \{a_r, b_r\}} \left(\sqrt{1 - \frac{\|d_{u_r}\|_2}{2}} \|\mathbf{d}_{u_r}\|_2, \|\mathbf{d}_{u_r}\|_2^3, \gamma \right) \|\mathbf{d}_{u_r}\|_2}{p(1-\gamma)}, \tag{S27}$$

with probability $1 - 2n^{-9}$.

Next we work on bounding err_2. Note that

$$\|err_2\| = \|\mathbf{D}^{-1} \sum_{m \in [R] \backslash r} (\lambda_m^* \mathbf{F} \mathbf{c}_m^* - \lambda_m \mathbf{G} \mathbf{c}_m)\|_2$$

$$\leq \max_{kk} |\mathbf{D}^{-1}|_{kk} \sum_{m \in [R] \backslash r} \|(\lambda_m^* \mathbf{F} \mathbf{c}_m^* - \lambda_m \mathbf{G} \mathbf{c}_m)\|_2$$

$$= \lambda_m^* \max_{kk} |\mathbf{D}^{-1}|_{kk} \sum_{m \in [R] \backslash r} \|\mathbf{F} \mathbf{c}_m^* - \mathbf{G} \mathbf{c}_m + \Delta_{\lambda_m} \mathbf{G} \mathbf{c}_m\|_2$$

$$\leq \lambda_m^* \max_{kk} |\mathbf{D}^{-1}|_{kk} \sum_{m \in [R] \backslash r} \|(\mathbf{F} - \mathbf{G}) \mathbf{c}_m^*\|_2 + \|\mathbf{G} \mathbf{d}_{c_m}\|_2 + \|\Delta_{\lambda_m} \mathbf{G} \mathbf{c}_m\|_2. \tag{S28}$$

We focus on bounding each of the four components in the last inequality above as

$$\|\mathbf{F}\mathbf{c}_m^* - \mathbf{G}\mathbf{c}_m\|_2 \leq \|(\mathbf{F}-\mathbf{G})\mathbf{c}_m^*\| + \|\mathbf{G}\mathbf{d}_{\mathbf{c}_m}\|_2$$
$$= \max_i |\mathbf{F}_{ii} - \mathbf{G}_{kk}|\|\mathbf{c}_m^*\|_2 + \max_i |\mathbf{G}_{kk}|\|\mathbf{d}_{\mathbf{c}_m}\|_2. \tag{S29}$$

Just like we did for err_1 we bound each element $|\mathbf{F}_{kk} - \mathbf{G}_{kk}|$ then apply the union bound to get the bound its maximum,

$$|\mathbf{F}_{kk} - \mathbf{G}_{kk}| = |\sum_{jk}\delta_{ijk}\mathbf{a}_m^*(i)\mathbf{b}_m^*(j)\mathbf{a}_r(i)\mathbf{b}_r(j) - \sum_{jk}\delta_{ijk}\mathbf{a}_m(i)\mathbf{b}_m(j)\mathbf{a}_r(i)\mathbf{b}_r(j)|$$
$$\leq |\sum_{jk}\delta_{ijk}\mathbf{d}_{a_m}(i)\mathbf{b}_m^*(j)\mathbf{a}_r(i)\mathbf{b}_r(j)| + |\sum_{jk}\delta_{ijk}\mathbf{a}_m^*(i)\mathbf{d}_{b_m}(j)\mathbf{a}_r(i)\mathbf{b}_r(j)|$$
$$+ |\sum_{jk}\delta_{ijk}\mathbf{d}_{a_m}(i)\mathbf{d}_{b_m}(j)\mathbf{a}_r(i)\mathbf{b}_r(j)|$$
$$\leq p\left(|\langle\mathbf{d}_{a_m},\mathbf{a}_r\rangle\langle\mathbf{b}_m^*,\mathbf{b}_r\rangle| + |\langle\mathbf{a}_m^*,\mathbf{a}_r\rangle\langle\mathbf{d}_{b_m},\mathbf{b}_r\rangle| + |\langle\mathbf{d}_{a_m},\mathbf{a}_r\rangle\langle\mathbf{d}_{b_m},\mathbf{b}_r\rangle|\right)$$
$$+ \gamma(\|\mathbf{d}_{a_m}\|_2 + \|\mathbf{d}_{b_m}\|_2 + \|\mathbf{d}_{a_m}\|_2\|\mathbf{d}_{b_m}\|_2)$$
$$\leq 6p \max_{\mathbf{u}\in\{\mathbf{a}_m,\mathbf{b}_m,\mathbf{a}_r,\mathbf{b}_r,\}} \left((\frac{c_0}{\sqrt{(n)}} + \|\mathbf{d_u}\|_2)\|\mathbf{d_u}\|_2, \gamma\|\mathbf{d_u}\|_2\right).$$

The last inequality above holds with probability $1 - 2n^{-10}$ provided the reveal probability $p \geq \frac{C\mu^3(1+\gamma/3)\log^2(n^{10})}{n^{3/2}\gamma^2}$. The second inequality is obtained by using Lemma 7 and the last inequality is obtained using the incoherence assumption (1.iii) to get that $\max\{|\langle\mathbf{a}_m^*,\mathbf{a}_r\rangle|, |\langle\mathbf{b}_m^*,\mathbf{b}_r\rangle|\} \leq \frac{c_0}{\sqrt{(n)}} + \max\{\|\mathbf{d}_{\mathbf{a}_r}\|_2, \|\mathbf{d}_{\mathbf{b}_r}\|_2\}$. Using the union bound we get that

$$\max_k |\mathbf{F}_{kk} - \mathbf{G}_{kk}| \leq 6p \max_{\mathbf{u}\in\{\mathbf{a}_m,\mathbf{b}_m,\mathbf{a}_r,\mathbf{b}_r,\}} \left((\frac{c_0}{\sqrt{(n)}} + \|\mathbf{d}_u\|_2), \gamma\right)\|\mathbf{d}_u\|_2, \tag{S30}$$

with probability $1 - 2n^{-9}$.

Similarly using Lemma 7, and applying the union bound and the fact that,

$$|\langle\mathbf{a}_m,\mathbf{a}_r\rangle\langle\mathbf{b}_m,\mathbf{b}_r\rangle| \leq \max\{\langle\mathbf{a}_m,\mathbf{a}_r\rangle^2, \langle\mathbf{b}_m,\mathbf{b}_r\rangle^2\} \tag{S31}$$
$$\leq \left(\frac{c_0}{\sqrt{(n)}} + \max_{\mathbf{u}_r\in\{\mathbf{a}_r,\mathbf{b}_r\}} 3\|\mathbf{d}_{u_r}\|_2\right)^2, \tag{S32}$$

yields the following inequality,

$$\max_k |\mathbf{G}_{kk}| \leq p \max_{\mathbf{u}_r\in\{\mathbf{a}_r,\mathbf{b}_r,\mathbf{a}_m,\mathbf{b}_m\}} \left((\frac{c_0}{\sqrt{(n)}} + 3\|\mathbf{d}_{u_r}\|_2)^2, \gamma\right), \tag{S33}$$

with probability $1 - 2n^{-9}$.

Putting equations (S28), (S29), (S33) and using Lemma 5 to bound $\mathbf{D}^{-1}$ yields,

$$\|err_2\|_2 \leq \frac{8p \sum\limits_{m\in[R]\backslash r} \lambda_m^* \max\limits_{\mathbf{u}\in\{\mathbf{a}_m,\mathbf{b}_m,\mathbf{a}_r,\mathbf{b}_r,\}} \left((\frac{c_0}{\sqrt{(n)}} + \|\mathbf{d}_\mathbf{u}\|_2), (\frac{c_0}{\sqrt{(n)}} + 3\|\mathbf{d}_\mathbf{u}\|_2)^2, \gamma \right) \|\mathbf{d}_\mathbf{u}\|_2}{p(1-\gamma)}, \quad (S34)$$

with probability $1 - 2n^{-9}$ provided $p \geq \frac{C\mu^3(1+\gamma/3)\log^2(n^{10})}{n^{3/2}\gamma^2}$.

Next we use Lemma 10, combined with Lemma 5 and apply the union bound to get the bound on the tensor noise $\|err_3\|_2$ as

$$\|err_3\|_2 \leq \frac{p(1+\gamma)\|\mathcal{E}_T\|}{p(1-\gamma)}, \quad (S35)$$

with probability $1 - 2n^{-9}$ provided $p \geq \frac{C\mu^3(1+\gamma/3)\log^2(n^{10})}{n^{3/2}\gamma^2}$. Combining the error bounds results of $\|err_1\|_2$, $\|err_2\|_2$, $\|err_3\|_2$ in equations (S27), (S34) and (S35) respectively, yields

$$\|\widetilde{\mathbf{c}}_r - \lambda_r^*\mathbf{c}_r^*\|_2$$

$$\leq \frac{8pR\lambda_{max}^* \max\limits_{\mathbf{u}\in\{\mathbf{a}_m,\mathbf{b}_m,\mathbf{a}_r,\mathbf{b}_r,\}} \left(\sqrt{1 - \frac{\|d_u\|_2}{2}}\|\mathbf{d}_u\|_2, (\frac{c_0}{\sqrt{(n)}} + \|\mathbf{d}_u\|_2), (\frac{c_0}{\sqrt{(n)}} + 3\|\mathbf{d}_u\|_2)^2, \|\mathbf{d}_u\|_2^3, \gamma \right) \|\mathbf{d}_u\|_2}{p(1-\gamma)}$$

$$+ \frac{p(1+\gamma)\|\mathcal{E}\|}{p(1-\gamma)}, \quad (S36)$$

with probability $1 - 2n^{-9}$. The proof of Lemma 2 is then completed by applying the results of Lemma 9 which shows that $\|\mathbf{c}_r - \mathbf{c}_r^*\|_2 \leq \frac{2}{\lambda_r^*}\|\widetilde{\mathbf{c}}_r - \lambda_r^*\mathbf{c}_r^*\|_2$ and Lemma 8 ($|\lambda_r - \lambda_r^*| \leq \|\widetilde{\mathbf{c}}_r - \lambda_r^*\mathbf{c}_r^*\|_2$) and by letting $\max\{\|\mathbf{d}_\mathbf{u}\|_2\} = \epsilon_T$. $\qquad\square$

S.2.3 Proof of Lemma 3

We now prove the contraction result in one iteration of Algorithm 1 for the shared components of the tensor and matrix $\mathbf{a}_r$ in the special case where the tensor and matrix weights are equal and both tensor and matrix are dense. When the tensor and matrix weight are assumed to be equal, the close form solution for the update of the shared tensor component derived in Lemma 1 simplifies to $\mathbf{a}_r = \frac{(\mathrm{res}_T(\mathbf{I},\mathbf{b}_r,\mathbf{c}_r)+\mathrm{res}_M\mathbf{v}_r)}{\lambda_r(P_\Omega(\mathbf{I},(\mathbf{b}_r).^2,(\mathbf{c}_r).^2)+1)}$. In this special case we can still employ the same technique used in bounding the non-shared components by using the intermediate step of bounding the expression $\|\widetilde{\mathbf{a}}_r - \lambda_r^*\mathbf{a}_r^*\|_2$ where $\widetilde{\mathbf{a}}_r = \frac{(\mathrm{res}_T(\mathbf{I},\mathbf{b}_r,\mathbf{c}_r)+\mathrm{res}_M\mathbf{v}_r)}{P_\Omega(\mathbf{I},(\mathbf{b}_r).^2,(\mathbf{c}_r).^2)+1}$.
This is the main advantage of restricting the problem to the equal tensor matrix weight case as it allows the proof technique derived for the non-shared component to be easily extended to the case of the shared component. As we will show in the analysis of Lemma 4 this advantage disappears when the weight of the tensor ans matrix are allowed to be different.

Let $\mathbf{D}$, $\mathbf{E}$, $\mathbf{F}$, $\mathbf{G}$, $\mathbf{H}$, $\mathbf{J}$, $\mathbf{P}$ be $n \times n$ diagonal matrices with diagonal elements,

$$\mathbf{D}_{ii} = \sum_{j,k} \delta_{ijk} \mathbf{b}_r^2(j) \mathbf{c}_r^2(k) + 1 \; ; \quad \mathbf{E}_{ii} = \sum_{j,k} \delta_{ijk} \mathbf{b}_r^*(j) \mathbf{c}_r^*(k) \mathbf{b}_r(j) \mathbf{c}_r(k);$$

$$\mathbf{F}_{ii} = \sum_{j,k} \delta_{ijk} \mathbf{b}_m^*(j) \mathbf{c}_m^*(k) \mathbf{b}_r(j) \mathbf{c}_r(k) \; ; \quad \mathbf{G}_{ii} = \sum_{j,k} \delta_{ijk} \mathbf{b}_m(j) \mathbf{c}_m(k) \mathbf{b}_r(j) \mathbf{c}_r(k);$$

$$\mathbf{H}_{ii} = \sum_{l} \mathbf{v}_r^*(l) \mathbf{v}_r(l) \; ; \quad \mathbf{J}_{ii} = \sum_{l} \mathbf{v}_m^*(l) \mathbf{v}_r(l) \; ; \quad \mathbf{P}_{ii} = \sum_{l} \mathbf{v}_m(l) \mathbf{v}_r(l).$$

Then the vector $\widetilde{\mathbf{a}}_r$ obtained after one pass of the inner loop of Algorithm 1 can be written as

$$\widetilde{\mathbf{a}}_r = \mathbf{D}^{-1} \left(\lambda_r^* \mathbf{E} \mathbf{a}_r^* + \sum_{m \in [R] \backslash r} (\lambda_m^* \mathbf{F} \mathbf{a}_m^* - \lambda_m \mathbf{G} \mathbf{a}_m) + P_\Omega(\mathcal{E}_T(\mathbf{I}, \mathbf{b}_r, \mathbf{c}_r)) \right)$$

$$+ \mathbf{D}^{-1} \left(\lambda_r^* \mathbf{H} \mathbf{a}_r^* + \sum_{m \in [R] \backslash r} (\lambda_m^* \mathbf{J} \mathbf{a}_m^* - \lambda_m \mathbf{P} \mathbf{a}_m) + \mathcal{E}_M \mathbf{v}_r \right). \tag{S37}$$

In the next steps we bound

$$\|\widetilde{\mathbf{a}}_r - \lambda_r^* \mathbf{a}_r^*\|_2 \le \| \underbrace{\lambda_r^* \mathbf{D}^{-1} (\mathbf{E} + \mathbf{H} - \mathbf{D}) a_r^*}_{err_1} \|_2 + \| \underbrace{\mathbf{D}^{-1} \sum_{m \in [R] \backslash r} (\lambda_m^* \mathbf{F} a_m^* - \lambda_m \mathbf{G} a_m)}_{err_2} \|_2$$

$$+ \| \underbrace{\mathbf{D}^{-1} \sum_{m \in [R] \backslash r} (\lambda_m^* \mathbf{J} a_m^* - \lambda_m \mathbf{P} a_m)}_{err_3} \|_2 + \| \underbrace{\mathbf{D}^{-1}(P_\Omega(\mathcal{E}_T(\mathbf{I}, \mathbf{b}_r, \mathbf{c}_r)) + \mathcal{E}_M \mathbf{v}_r)}_{err_4} \|_2. \tag{S38}$$

In the shared component case, the right hand side of equation (S38) can be characterized as the sum of 4 sources of errors, where $err_1 = \lambda_r^* \mathbf{D}^{-1} (\mathbf{E} + \mathbf{H} - \mathbf{D}) a_r^*$ can be characterized as the error due to the power method applied to both the tensor and matrix. This error is similar to err_1 discussed in the proof of Lemma 2 with the exception that it factors in the contribution of the matrix. Again, if $\mathcal{T}^*$ was a rank 1, noiseless tensor, then proving Lemma 3 would reduce to bounding this term. The second and third sources of error $err_2 = \mathbf{D}^{-1} \sum_{m \in [R] \backslash r} (\lambda_m^* \mathbf{F} a_m^* - \lambda_m \mathbf{G} a_m)$ and $err_3 = \mathbf{D}^{-1} \sum_{m \in [R] \backslash r} (\lambda_m^* \mathbf{J} a_m^* - \lambda_m \mathbf{P} a_m)$ again represents the main challenge in the proof. The challenge in bounding these two errors are very similar to those exposed for err_2 in the analysis of Lemma 2 in addition to the fact that we have an extra residual due to the matrix. If both the tensor and matrix components were orthogonal this error would be non existent. We therefore partly control these errors magnitude through the bound imposed on the components vector inner product namely Assumption $(1.iii)$ the incoherence assumption. The fourth error term $err_4 = \mathbf{D}^{-1}(P_\Omega(\mathcal{E}_T(\mathbf{I}, \mathbf{b}_r, \mathbf{c}_r)) + \mathcal{E}_M \mathbf{v}_r$ is simply the error due to the noise of the tensor and the

matrix and can be easily bounded after standard Assumptions are made about the spectral norms of $\mathcal{E}_T$ and $\mathcal{E}_M$. At first glance it might seem that right hand-side of the inequalities in equation (S38) is larger than that found in equation (S25) making therefore the bound on the shared component larger than that of the that of the non-shared component. However as we demonstrate in the proof below, the component $\mathbf{D}^{-1}$ plays the role of a weight which averages the tensor and matrix sources of error in equation (S38).

We start with bounding the first error term,

$$\|err_1\|_2 = \|\lambda_r^* \mathbf{D}^{-1} (\mathbf{E} + \mathbf{H} - \mathbf{D}) a_r^*\|_2$$
$$\leq \lambda_r^* \|\mathbf{D}^{-1} (\mathbf{E} + \mathbf{H} - \mathbf{D})\|_2 \|a_r^*\|_2$$
$$\leq \lambda_r^* \max_i |\mathbf{D}_{ii}^{-1}| |(\mathbf{E} + \mathbf{H} - \mathbf{D})_{ii}|,$$

where last inequality above is obtained by observing that $\mathbf{D}^{-1} (\mathbf{E} + \mathbf{H} - \mathbf{D})$ is a diagonal matrix whose spectral norm is the maximum absolute value of its diagonal elements and that $\|a_r^*\|_2 = 1$. We proceed to getting an upper bound for each of the maximum of each of the random variable elements in the equation above with high probability. To do that we first get an upper bound on each of the diagonal elements with high probability and make use of the union bound method to get a high probability bound on the maximums.

$$|(\mathbf{E} + \mathbf{H} - \mathbf{D})_{ii}| \leq |\langle \mathbf{v}_r^*, \mathbf{v}_r \rangle - 1| + |\sum_{jk} \delta_{ijk} \mathbf{b}_r^*(j) \mathbf{c}_r^*(k) \mathbf{b}_r(j) \mathbf{c}_r(k) - \sum_{jk} \delta_{ijk} \mathbf{b}_r^2(j) \mathbf{c}_r^2(k)|$$
$$= \frac{1}{2} \|\mathbf{d}_v\|_2^2 + |\sum_{ij} \delta_{ijk} \mathbf{a}_r^*(i) \mathbf{d}_{b_r}(j) \mathbf{a}_r(i) \mathbf{b}_r(j) - \sum_{ij} \delta_{ijk} \mathbf{d}_{a_r}(i) \mathbf{b}_r^*(j) \mathbf{a}_r(i) \mathbf{b}_r(j)$$
$$- \sum_{ij} \delta_{ijk} \mathbf{d}_{c_r}(i) \mathbf{d}_{b_r}(j) \mathbf{c}_r(i) \mathbf{b}_r(j)|$$
$$\leq \frac{1}{2} \|\mathbf{d}_v\|_2^2 + p \left(|\langle \mathbf{c}_r^*, \mathbf{c}_r \rangle \langle \mathbf{d}_{b_r}, \mathbf{b}_r \rangle| + |\langle \mathbf{d}_{c_r}, \mathbf{c}_r \rangle \langle \mathbf{b}_r^*, \mathbf{b}_r \rangle| + |\langle \mathbf{d}_{c_r}, \mathbf{c}_r \rangle \langle \mathbf{d}_{b_r}, \mathbf{b}_r \rangle|\right)$$
$$+ p\gamma \left(\|\mathbf{d}_{c_r}\|_2 + \|\mathbf{d}_{b_r}\|_2 + \|\mathbf{d}_{c_r}\|_2 \|\mathbf{d}_{b_r}\|_2\right).$$

The expression on the right side of the equality is obtained by combining the triangle inequality to the fact that $\mathbf{c}_r(i) = \mathbf{c}_r^*(i) + \mathbf{d}_{c_r}(i)$ $\mathbf{b}_r(j) = \mathbf{b}_r^*(j) + \mathbf{d}_{b_r}(j)$ and using the results from Lemma 11. We then use Lemma 6 to bound the three random elements inside the absolute value. Hence, provided the reveal probability $p \geq \frac{C\mu^3(1+\gamma/3)\log^2(n^{10})}{n^{3/2}\gamma^2}$ we get,

$$|(\mathbf{E} + \mathbf{H} - \mathbf{D})_{ii}| |(\mathbf{E} + \mathbf{H} - \mathbf{D})_{ii}| \leq \frac{1}{2} \|\mathbf{d}_v\|_2^2 + 6p \left(\max_{\mathbf{u}_r \in \{c_r, b_r\}} \left\{\sqrt{1 - \frac{\|d_{u_r}\|_2}{2}} \|\mathbf{d}_{u_r}\|_2^2, \|\mathbf{d}_{u_r}\|_2^4, \gamma \|\mathbf{d}_{u_r}\|_2\right\}\right)$$
$$\leq \frac{1}{2} \|\mathbf{d}_v\|_2^2 + 6p \max_{\mathbf{u}_r \in \{c_r, b_r\}} \left(\sqrt{1 - \frac{\|d_{u_r}\|_2}{3}} \|\mathbf{d}_{u_r}\|_2, \|\mathbf{d}_{u_r}\|_2^3, \gamma\right) \|\mathbf{d}_{u_r}\|_2,$$

(S39)

with probability $1 - 2n^{-10}$. Using the union bound on the result in equation (S39) combined with the results of Lemma 5. We get,

$$\|err_1\|_2 \leq \frac{\lambda_r^* \left(6p \max_{\mathbf{u}_r \in \{a_r, b_r\}} \left(\sqrt{1 - \frac{\|d_{u_r}\|_2}{2}} \|\mathbf{d}_{u_r}\|_2, \|\mathbf{d}_{u_r}\|_2^3, \gamma \right) \|\mathbf{d}_{u_r}\|_2 + 1/2 \|\mathbf{d}_v\|_2^2 \right)}{p(1-\gamma) + 1} \tag{S40}$$

with probability $1 - 2n^{-9}$.

Next we proceed to bound $\|err_3\|_2$ before coming back to $\|err_2\|_2$,

$$\|err_3\|_2 = \|\mathbf{D}^{-1} \sum_{m \in [R] \setminus r} (\lambda_m^* \mathbf{J} a_m^* - \lambda_m \mathbf{P} a_m)\|_2.$$

We start by bounding the component inside the summation.

$$\|\lambda_m^* \mathbf{J} a_m^* - \lambda_m \mathbf{P} a_m\|_2 = \|\lambda_m^* \langle \mathbf{v}_m^*, \mathbf{v}_r \rangle \mathbf{a}_m^* - \lambda_m \langle \mathbf{v}_m, \mathbf{v}_r \rangle \mathbf{a}_m\|_2$$

$$= \lambda_m^* \|(\langle \mathbf{v}_m^*, \mathbf{v}_r \rangle - \langle \mathbf{v}_m, \mathbf{v}_r \rangle)\mathbf{a}_m^* + \langle \mathbf{v}_m, \mathbf{v}_r \rangle \mathbf{d}_{a_m} + \Delta_{\lambda_m} \langle \mathbf{v}_m, \mathbf{v}_r \rangle \mathbf{a}_m\|_2$$

$$\leq 3\lambda_m^* \max \left(\|\mathbf{d}_{\mathbf{v}_m}\|_2, \frac{c_0}{\sqrt{(n)}} + 3\|\mathbf{d}_{v_r}\|_2 \right) \|\mathbf{d}_{v_r}\|_2, \tag{S41}$$

where the last inequality is due to the fact that $\langle \mathbf{v}_m, \mathbf{v}_r \rangle \leq (\frac{c_0}{\sqrt{(n)}} + 3\|\mathbf{d}_{v_r}\|_2)$. This, combined with the results of Lemma 5 to bound $|\mathbf{D}^{-1}|$ yields,

$$\|err_3\|_2 \leq \frac{3 \sum_{m \in [R] \setminus r} \lambda_m^* \max(\|\mathbf{d}_{\mathbf{v}_m}\|_2, \frac{c_0}{\sqrt{(n)}} + 3\|\mathbf{d}_{v_r}\|_2) \|\mathbf{d}_{v_r}\|_2}{p(1-\gamma) + 1}, \tag{S42}$$

with probability $1 - 2n^{-9}$.

The technique used to bound $\|err_2\|_2$ in this section is very similar to the one used to bound expression in section. We therefore provide the bound and incite the reader to review the section mention to understand the process involved. The main difference recedes in substituting the components $\mathbf{c}$ for $\mathbf{a}$ and finding a lower bound for D^{-1} using Lemma 5. This yields,

$$\|err_2\|_2 \leq \frac{8p \sum_{m \in [R] \setminus r} \lambda_m^* \max_{\mathbf{u} \in \{c_m, b_m, c_r, b_r,\}} \left((\frac{c_0}{\sqrt{(n)}} + \|\mathbf{d}_u\|_2), (\frac{c_0}{\sqrt{(n)}} + 3\|\mathbf{d}_u\|_2)^2\|, \gamma \right) \|\mathbf{d}_u\|_2}{p(1-\gamma) + 1}, \tag{S43}$$

with probability $1 - 2n^{-9}$.

Next $\|err_4\|_2$ is bounded using Lemma 10, combined with Lemma 5 and the fact that $\|\mathcal{E}_M \mathbf{v}_r\|_2 \leq \|\mathcal{E}_M\|$ since $\|\mathbf{v}_r\|_2 = 1$ and by definition $\|\mathcal{E}_M\| = \sup_{\|\mathbf{u}\|=1} \|\mathcal{E}_M \mathbf{u}\|_2$. This therefore yields

$$\|err_4\|_2 \leq \frac{p(1+\gamma)\|\mathcal{E}_T\| + \|\mathcal{E}_M\|}{p(1-\gamma) + 1} \tag{S44}$$

with probability $1 - 2n^{-9}$.

Combining the error bounds results of $\|err_1\|_2$, $\|err_3\|_2$, $\|err_2\|_2$, $\|err_4\|_2$ in equations (S40), (S43), (S42) and (S44) respectively, we get

$$\|\widetilde{\mathbf{a}}_r - \lambda_r^* \mathbf{a}_r^*\|_2$$

$$\leq \frac{8pR\lambda_{max}^* \max\limits_{\mathbf{u} \in \{\mathbf{c}_m, \mathbf{b}_m, \mathbf{c}_r, \mathbf{b}_r,\}} \left(\sqrt{1 - \frac{\|d_u\|_2}{2}} \|\mathbf{d}_u\|_2, (\frac{c_0}{\sqrt{(n)}} + \|\mathbf{d}_u\|_2), (\frac{c_0}{\sqrt{(n)}} + 3\|\mathbf{d}_u\|_2)^2, \|\mathbf{d}_u\|_2^3, \gamma \right) \|\mathbf{d}_u\|_2}{p(1 - \gamma) + 1}$$

$$+ \frac{3R\lambda_{max}^* \max \left(\|\mathbf{d}_{v_r}\|_2, \frac{c_0}{\sqrt{(n)}} + 3\|\mathbf{d}_{v_r}\|_2 \right) \|\mathbf{d}_{v_r}\|_2 + p(1 + \gamma)\|\mathcal{E}_T\| + \|\mathcal{E}_M\|}{p(1 - \gamma) + 1} \tag{S45}$$

with probability $1 - 2n^{-9}$.

The proof of Lemma 3 is then completed by applying the results of Lemma 9 which shows that $\|\mathbf{a}_r - \mathbf{a}_r^*\|_2 \leq \frac{2}{\lambda_r^*}\|\widetilde{\mathbf{a}}_r - \lambda_r^*\mathbf{a}_r^*\|_2$ and letting $\max\{\|\mathbf{d}_\mathbf{u}\|_2\} = \epsilon_T$ and $\max\{\|\mathbf{d}_\mathbf{v}\|_2\} = \epsilon_M$. $\square$

S.2.4 Proof of Lemma 4

We now prove Lemma 4 which establishes an error contraction result for the shared tensor components in one iteration of Algorithm 1 when the input tensor and matrix are assumed to be sparse and their respective components weight are allowed to differ. First, we introduce some notation below in order reveal how we address the sparse components in the analysis .

Define $F_a := \text{supp}(\mathbf{a}_r^*) \cup \text{supp}(\mathbf{a}_r)$, $F_b := \text{supp}(\mathbf{b}_r^*) \cup \text{supp}(\mathbf{b}_r)$, $F_c := \text{supp}(\mathbf{c}_r^*) \cup \text{supp}(\mathbf{c}_r)$ and $F_v := \text{supp}(\mathbf{v}_r^*) \cup \text{supp}(\mathbf{v}_r)$ where $\text{supp}(\mathbf{u})$ refers to the set of indices in a vector $\mathbf{u}$ that are nonzero. Then let F and F' be compositions of support sets defined as $F := F_a \circ F_b \circ F_c$ and $F' := F_1 \circ F_v$ respectively. We use the notation $\mathcal{T}^{\backslash r} := \sum_{m \in [R] \backslash r} \lambda_m \mathbf{a}_m \otimes \mathbf{b}_m \otimes \mathbf{c}_m$ to represent the CP decomposition of the tensor $\mathcal{T}$ minus its rth rank 1 tensor element $(\lambda_r \mathbf{a}_r \otimes \mathbf{b}_r \otimes \mathbf{c}_r)$.

Denote the truncated vectors $\mathbf{u}_r^*$ and $\mathbf{u}_r$ to be $\bar{\mathbf{u}}_r^* = \text{Truncate}(\mathbf{u}_r^*, F_\mathbf{u})$ and $\bar{\mathbf{u}}_r = \text{Truncate}(\mathbf{u}_r, F_\mathbf{u})$ with $\mathbf{u} \in \{\mathbf{a}, \mathbf{b}, \mathbf{c}, \mathbf{v}\}$ and $r = 1, \ldots, R$.

Note that in the update of a_r in our algorithm, we first obtain non-sparse estimator $\mathbf{a}_r$ in line (8) of algorithm 1 then update it by applying the truncation method and normalization method in (9). We let $\dot{\mathbf{a}}_r$ be the update on line (8) of algorithm 1 before the truncation and $\mathbf{a}_r$ be the truncated update on line (9) of the algorithm. That is $\mathbf{a}_r = \frac{\dot{\mathbf{a}}_r}{\|\dot{\mathbf{a}}_r\|_2}$ with,

$$\dot{\mathbf{a}}_r = \frac{(\lambda_r \text{res}_{T_F}(\mathbf{I}, \mathbf{b}_r, \mathbf{c}_r) + \sigma_r \text{res}_{M_{F'}} \mathbf{v}_r)}{(\lambda_r^2 P_\Omega(\mathbf{I}, (\mathbf{b}_r).^2, (\mathbf{c}_r).^2) + \sigma_r^2)}$$

where res_{T_F} denotes the restriction of the residual tensor res_T on the three modes indexed by F_a,

16

F_b and F_c and res_{T_F} is the equivalent for the residual matrix res_M. That is

$$\mathrm{res}_{T_F} = \sum_{m\in[R]} \lambda_m^* \bar{\mathbf{a}}_m^* \otimes \bar{\mathbf{b}}_m^* \otimes \bar{\mathbf{c}}_m^* - \sum_{m\in[R]\backslash r} \lambda_m \bar{\mathbf{a}}_m \otimes \bar{\mathbf{b}}_m \otimes \bar{\mathbf{c}}_m,$$

$$\mathrm{res}_{M_F'} = \sum_{m\in[R]} \sigma_m^* \bar{\mathbf{a}}_m^* \otimes \bar{\mathbf{v}}_m^* - \sum_{m\in[R]\backslash r} \lambda_m \bar{\mathbf{a}}_m \otimes \bar{\mathbf{v}}_m.$$

Proving Lemma 4 involves bounding $\|\mathbf{a}_r - \mathbf{a}_r^*\|_2$ which we do in two steps. First we notice that $\|\mathbf{a}_r - \mathbf{a}_r^*\|_2 \le \|\mathbf{a}_r - \dot{\mathbf{a}}_r\|_2 + \|\dot{\mathbf{a}}_r - \mathbf{a}_r^*\|_2$ using the triangle inequality. Then we bound each of the two norms in the expression above. As will be demonstrated in the proof,

$$\|\mathbf{a}_r - \mathbf{a}_r^*\|_2 \le \|\mathbf{a}_r - \dot{\mathbf{a}}_r\|_2 + \|\dot{\mathbf{a}}_r - \mathbf{a}_r^*\|_2 \le 2\|\dot{\mathbf{a}}_r - \mathbf{a}_r^*\|_2.$$

While bounding $\|\mathbf{a}_r - \mathbf{a}_r^*\|_2$ directly is a challenge, getting relatively tight upper bounds for $\|\mathbf{a}_r - \dot{\mathbf{a}}_r\|_2$ and $\|\dot{\mathbf{a}}_r - \mathbf{a}_r^*\|_2$ although challenging is feasible.

Step1: We begin with bounding $\|\dot{\mathbf{a}}_r - \mathbf{a}_r^*\|_2$.

Let $\mathbf{D}$, $\mathbf{E}$, $\mathbf{F}$, $\mathbf{G}$, $\mathbf{H}$, $\mathbf{J}$, $\mathbf{P}$ be $n \times n$ diagonal matrices with diagonal elements,

$$\mathbf{D}_{ii} = \lambda_r^2 \sum_{j,k} \delta_{ijk} \mathbf{b}_r^2(j)\mathbf{c}_r^2(k) + \sigma_r^2 \ ; \quad \mathbf{E}_{ii} = \sum_{j,k} \delta_{ijk} \bar{\mathbf{b}}_r^*(j)\bar{\mathbf{c}}_r^*(k)\mathbf{b}_r(j)\mathbf{c}_r(k);$$

$$\mathbf{F}_{ii} = \sum_{j,k} \delta_{ijk} \bar{\mathbf{b}}_m^*(j)\bar{\mathbf{c}}_m^*(k)\mathbf{b}_r(j)\mathbf{c}_r(k) \ ; \quad \mathbf{G}_{ii} = \sum_{j,k} \delta_{ijk} \bar{\mathbf{b}}_m(j)\bar{\mathbf{c}}_m(k)\mathbf{b}_r(j)\mathbf{c}_r(k);$$

$$\mathbf{H}_{ii} = \sum_{l} \bar{\mathbf{v}}_r^*(l)\mathbf{v}_r(l) \ ; \quad \mathbf{J}_{ii} = \sum_{l} \bar{\mathbf{v}}_m^*(l)\mathbf{v}_r(l) \ ; \quad \mathbf{P}_{ii} = \sum_{l} \bar{\mathbf{v}}_m(l)\mathbf{v}_r(l).$$

Then the vector $\mathbf{a}_r$ obtained after one pass of the inner loop of Algorithm 1 and before normalization can be written as

$$\dot{\mathbf{a}}_r = \lambda_r \mathbf{D}^{-1} \left(\lambda_r^* \mathbf{E}\bar{\mathbf{a}}_r^* + \sum_{m\in[R]\backslash r} (\lambda_m^* \mathbf{F}\bar{\mathbf{a}}_m^* - \lambda_m \mathbf{G}\bar{\mathbf{a}}_m) + \mathcal{E}_{T_F} \times_2 \mathbf{b}_r \times_3 \mathbf{c}_r \right)$$

$$+ \sigma_r \mathbf{D}^{-1} \left(\sigma_r^* \mathbf{H}\bar{\mathbf{a}}_r^* + \sum_{m\in[R]\backslash r} (\sigma_m^* \mathbf{J}\bar{\mathbf{a}}_m^* - \sigma_m \mathbf{P}\bar{\mathbf{a}}_m) + \mathcal{E}_{M_F'} \mathbf{v}_r \right). \tag{S46}$$

This means that

$$\|\dot{\mathbf{a}}_r - \mathbf{a}_r^*\|_2 = \| \underbrace{\mathbf{D}^{-1}\left(\lambda_r \lambda_r^* \mathbf{E} + \sigma_r \sigma_r^* \mathbf{H} - \mathbf{DI}\right)\bar{\mathbf{a}}_r^*}_{err_1} \|_2 + \| \underbrace{\lambda_r \mathbf{D}^{-1} \sum_{m\in[R]\backslash r} (\lambda_m^* \mathbf{F}\bar{\mathbf{a}}_m^* - \lambda_m \mathbf{G}\bar{\mathbf{a}}_m)}_{err_2} \|_2$$

$$+ \| \underbrace{\sigma_r \mathbf{D}^{-1} \sum_{m\in[R]\backslash r} (\sigma_m^* \mathbf{J}\mathbf{a}_m^* - \sigma_m \mathbf{P}\bar{\mathbf{a}}_m)}_{err_3} \|_2 + \| \underbrace{\mathbf{D}^{-1}(\lambda_r \mathcal{E}_{T_F} \times_2 \mathbf{b}_r \times_3 \mathbf{c}_r + \sigma_r \mathcal{E}_{M_F'} \mathbf{v}_r)}_{err_4} \|_2.$$

$$\tag{S47}$$

The right hand side of the inequality above is split into four sources of errors where err_2 and err_3 are due to tensor rank being greater than one, err_3 is the error associated tot the tensor and matrix noise and err_1 is the error from the power iteration used in the algorithm. We notice in the case where the tensor and matrix have different weight expression of $\mathbf{a}_r$ contains the estimated weights unlike when the tensor weights can be assumed to be equal. This main difference requires careful derivation of the error bound for the update of the shared components.

We start with bounding the first error term

$$
\begin{aligned}
\|err_1\|_2 &= \|\mathbf{D}^{-1}\left(\lambda_r \lambda_r^* \mathbf{E} + \sigma_r \sigma_r^* \mathbf{H} - \mathbf{DI}\right)\bar{\mathbf{a}}_r^*\|_2 \\
&\leq \|\mathbf{D}^{-1}\left(\lambda_r \lambda_r^* \mathbf{E} + \sigma_r \sigma_r^* \mathbf{H} - \mathbf{DI}\right)\|_2 \|\bar{\mathbf{a}}_r^*\|_2 \\
&\leq \max_i \underbrace{|\mathbf{D}_{ii}^{-1}|}_{err_{11}} \underbrace{|\left(\lambda_r \lambda_r^* \mathbf{E} + \sigma_r \sigma_r^* \mathbf{H} - \mathbf{DI}\right)_{ii}|}_{err_{12}},
\end{aligned}
$$

where the third inequality is due to the fact that $\|\bar{\mathbf{a}}_r^*\|_2 \leq \|\mathbf{a}_r^*\|_2 = 1$ and since, $\mathbf{D}^{-1}\left(\lambda_r \lambda_r^* \mathbf{E} + \sigma_r \sigma_r^* \mathbf{H} - \mathbf{DI}\right)$ is a diagonal matrix hence its spectral norm is obtained by taking the maximum absolute value of its diagonal elements. We therefore proceed to getting an upper bound each of the maximum of each of the random variable elements in the equation above with high probability. To do that we first get an upper bound on each of the diagonal elements with high probability and make use of the union bound method to get a high probability bound on the maximums.

$$
\begin{aligned}
err_{12} &= |\lambda_r \lambda_r^* \sum_{jk} \delta_{ijk} \bar{\mathbf{b}}_r^*(j)\bar{\mathbf{c}}_r^*(k)\mathbf{b}_r(j)\mathbf{c}_r(k) + \sigma_r \sigma_r^* \langle \bar{\mathbf{v}}_r^*, \mathbf{v}_r \rangle - (\lambda_r^2 \sum_{jk} \delta_{ijk} \mathbf{b}_r^2(j)\mathbf{c}_r^2(k) + \sigma_r^2)| \\
&\leq \underbrace{|\lambda_r \lambda_r^* \sum_{jk} \delta_{ijk} \bar{\mathbf{b}}_r^*(j)\bar{\mathbf{c}}_r^*(k)\mathbf{b}_r(j)\mathbf{c}_r(k) - \lambda_r^2 \sum_{jk} \delta_{ijk} \mathbf{b}_r^2(j)\mathbf{c}_r^2(k)|}_{I_{121}} + \underbrace{|\sigma_r \sigma_r^* \langle \bar{\mathbf{v}}_r^*, \mathbf{v}_r \rangle - \sigma_r^2)|}_{I_{122}}.
\end{aligned}
$$

We can bound I_{121} and I_{122} next

$$
\begin{aligned}
I_{122} &= |\sigma_r \sigma_r^* \langle \bar{\mathbf{v}}_r^*, \mathbf{v}_r \rangle - \sigma_r^2)| \\
&\leq \sigma_r \sigma_r^* (|\langle \mathbf{v}_r^*, \mathbf{v}_r \rangle - 1| + \Delta_{\sigma_r}) \\
&\leq \sigma_r \sigma_r^* (\frac{1}{2}\|d_v\|_2^2, +\Delta_{\sigma_r})
\end{aligned}
\tag{S48}
$$

where the first inequality is due to using the triangle inequality, the fact that $\sigma_r = \sigma_r - \sigma_r^* + \sigma_r^*$ and Lemma 12 by noting that $supp(\mathbf{v}_r) \subseteq F_b$. The second inequality is obtained from the results of

18

Lemma 11. Next we also bound I_{121}.

$$I_{121} = |\lambda_r \lambda_r^* \sum_{jk} \delta_{ijk} \bar{\mathbf{b}}_r^*(j) \bar{\mathbf{c}}_r^*(k) \mathbf{b}_r(j) \mathbf{c}_r(k) - \lambda_r^2 \sum_{jk} \delta_{ijk} \mathbf{b}_r^2(j) \mathbf{c}_r^2(k)|$$

$$\leq \lambda_r \lambda_r^* (|\sum_{jk} (\delta_{ijk} \bar{\mathbf{b}}_r^*(j) \bar{\mathbf{c}}_r^*(k) \mathbf{b}_r(j) \mathbf{c}_r(k) - \delta_{ijk} \mathbf{b}_r^2(j) \mathbf{c}_r^2(k))| + \Delta_{\lambda_r} \sum_{jk} \delta_{ijk} \mathbf{b}_r^2(j) \mathbf{c}_r^2(k))$$

$$\leq |\sum_{jk} \delta_{ijk} \mathbf{b}_r^*(j) \mathbf{d}_{c_r}^*(k) \mathbf{b}_r(j) \mathbf{c}_r(k)| + |\sum_{jk} \delta_{ijk} \mathbf{d}_{b_r}^*(j) \mathbf{c}_r^*(k) \mathbf{b}_r(j) \mathbf{c}_r(k)|$$

$$+ |\sum_{jk} \delta_{ijk} \mathbf{d}_{b_r}^*(j) \mathbf{d}_{c_r}^*(k) \mathbf{b}_r(j) \mathbf{c}_r(k)|,$$

where the last inequality is obtained using the triangle inequality and the fact that $\mathbf{b}_r(j) = \mathbf{b}_r^*(j) + \mathbf{d}_{b_r}(j)$ and $\mathbf{c}_r(j) = \mathbf{c}_r^*(j) + \mathbf{d}_{c_r}(j)$ combined with the fact that $F_b = supp(\mathbf{b}_r^*) \subseteq supp(\bar{\mathbf{b}}_r^*) = F$ and $F_c = supp(\mathbf{c}_r^*) \subseteq supp(\bar{\mathbf{c}}_r^*) = F$ which means that $\bar{\mathbf{b}}_r^*(k) - \mathbf{b}_r^*(k) = 0$ and $\bar{\mathbf{c}}_r^*(k) - \mathbf{c}_r^*(k) = 0$. Next applying the results of Lemma 5 and Lemma 8, we get

$$I_{121} \leq \lambda_r^* \lambda_r p (|\langle \mathbf{b}_r^*, \mathbf{b}_r \rangle \langle \mathbf{d}_{c_r}, \mathbf{c}_r \rangle| + |\langle \mathbf{d}_{b_r}, \mathbf{b}_r \rangle \langle \mathbf{c}_r^*, \mathbf{c}_r \rangle| + |\langle \mathbf{d}_{b_r}, \mathbf{b}_r \rangle \langle \mathbf{d}_{c_r}, \mathbf{c}_r \rangle| + \Delta_{\lambda_r})$$

$$+ p\gamma (\|\mathbf{d}_{c_r}\|_2 + \|\mathbf{d}_{b_r}\|_2 + \|\mathbf{d}_{c_r}\|_2 \|\mathbf{d}_{b_r}\|_2 + \Delta_{\lambda_r})$$

$$\leq 8\lambda_r^* \lambda_r p \left(\max_{\mathbf{u}_r \in \{c_r, b_r\}} \{ \sqrt{1 - \frac{\|d_{u_r}\|_2}{2}} \|\mathbf{d}_{u_r}\|_2^2, \|\mathbf{d}_{u_r}\|_2^4, \Delta_{\lambda_r}, \gamma \|\mathbf{d}_{u_r}\|_2, \gamma \Delta_{\lambda_r} \} \right), \qquad \text{(S49)}$$

where the last inequality above holds with probability $1 - 2d^{-10}$ provided the reveal probability $p \geq \frac{C\mu^3(1+\gamma/3)\log^2(d^{10})}{d^{3/2}\gamma^2}$. Combining equations (S48) and (S49) followed by making use of lemma (5) to bound the denominator of $\|err_1\|_2$, we get

$$\|err_1\|_2 \leq \frac{8\lambda_r^* \lambda_r p \left(\max_{\mathbf{u}_r \in \{c_r, b_r\}} \{ \sqrt{1 - \frac{\|d_{u_r}\|_2}{2}} \|\mathbf{d}_{u_r}\|_2^2, \|\mathbf{d}_{u_r}\|_2^4, \Delta_{\lambda_r}, \gamma \|\mathbf{d}_{u_r}\|_2, \gamma \Delta_{\lambda_r} \} \right) + \sigma_r \sigma_r^* (\frac{1}{2}\|d_v\|_2^2 + \Delta_{\sigma_r})}{\lambda_r^2 p(1-\gamma) + \sigma_r^2},$$

$$\text{(S50)}$$

with probability $1 - 2d^{-9}$.

We now move on to bounding the expression $\|err_3\|_2$.

$$\|err_3\|_2 \leq \sigma_r \|\mathbf{D}^{-1} \sum_{m \in [R] \setminus r} (\sigma_m^* \mathbf{J} \bar{\mathbf{a}}_m^* - \sigma_m \mathbf{P} \bar{\mathbf{a}}_m)\|_2$$

$$\leq \sigma_r \max_i |\mathbf{D}_{ii}^{-1}| \sum_{m \in [R] \setminus r} \|\sigma_m^* \langle \bar{\mathbf{v}}_m^*, \mathbf{v}_r \rangle \bar{\mathbf{a}}_m^* - \sigma_m \langle \bar{\mathbf{v}}_m, \mathbf{v}_r \rangle \bar{\mathbf{a}}_m\|_2$$

$$\leq \sigma_r \max_i |\mathbf{D}_{ii}^{-1}| \sum_{m \in [R] \setminus r} \sigma_m^* (|\langle \bar{\mathbf{v}}_m^*, \mathbf{v}_r \rangle - \langle \bar{\mathbf{v}}_m, \mathbf{v}_r \rangle| \|\bar{\mathbf{a}}_m^*\|_2 + |\langle \bar{\mathbf{v}}_m, \mathbf{v}_r \rangle| \|\mathbf{d}_{a_m}\|_2)$$

$$+ \sigma_r \max_i |\mathbf{D}_{ii}^{-1}| \sum_{m \in [R] \setminus r} \sigma_m^* (\Delta_{\sigma_m} |\langle \bar{\mathbf{v}}_m, \mathbf{v}_r \rangle| \|\bar{\mathbf{a}}_m\|_2), \qquad \text{(S51)}$$

19

where for inequality three, we use the fact that $\|\langle \bar{\mathbf{v}}_m^*, \mathbf{v}_r \rangle \bar{\mathbf{a}}_m^* \|_2 \leq \|\langle \mathbf{v}_m^*, \mathbf{v}_r \rangle \mathbf{a}_m^* \|_2$ since $\|\bar{\mathbf{a}}_m^*\|_2 \leq 1$ and that the truncation process is invariant to scaling. We also used the fact that $\sigma_r = \sigma_r - \sigma_r^* + \sigma_r^*$. Next, since $\{\text{supp}(\mathbf{v}_m^*), \text{supp}(\mathbf{v}_m)\} \subseteq F$ it follows that $\langle \bar{\mathbf{v}}_m^*, \mathbf{v}_r \rangle - \langle \bar{\mathbf{v}}_m, \mathbf{v}_r \rangle = \langle \mathbf{d}_{\mathbf{v}_m}, \mathbf{v}_r \rangle$. Then noticing that $\langle \mathbf{v}_m, \mathbf{v}_r \rangle \leq (\frac{c_0}{\sqrt{d}} + 3\|\mathbf{d}_{v_r}\|_2)$ and using the results of Lemma 5 to bound $\max_i |\mathbf{D}_{ii}^{-1}|$ yields

$$\|err_3\|_2 \leq \frac{\sigma_r \sum\limits_{m \in [R] \backslash r} \sigma_m^* \left(\|\mathbf{d}_{\mathbf{v}_m}\|_2 + (\frac{c_0}{\sqrt{d}} + 3\|\mathbf{d}_{v_r}\|_2)\|\mathbf{d}_{\mathbf{a}_m}\|_2 + \Delta_{\sigma_m}(\frac{c_0}{\sqrt{d}} + 3\|\mathbf{d}_{v_r}\|_2) \right)}{\lambda_r^2 p(1 - \gamma) + \sigma_r^2}, \tag{S52}$$

with probability $1 - 2d^{-9}$ provided the reveal probability $p \geq \frac{C\mu^3(1+\gamma/3)\log^2(d^{10})}{d^{3/2}\gamma^2}$.

Next we bound the expression $\|err_2\|_2$ as

$$\|err_2\|_2 = \|\lambda_r \mathbf{D}^{-1} \sum_{m \in [R] \backslash r} \lambda_m^* (\mathbf{F}\bar{\mathbf{a}}_m^* - \mathbf{G}\bar{\mathbf{a}}_m + \Delta_{\lambda_m}\mathbf{G}\bar{\mathbf{a}}_m)\|_2$$

$$\leq \lambda_r \|\mathbf{D}^{-1}\|_2 \sum_{m \in [R] \backslash r} \lambda_m^* (\|(\mathbf{F} - \mathbf{G})\bar{\mathbf{a}}_m^*\|_2 + \|\mathbf{G}\mathbf{d}_{a_m}\|_2 + \|\Delta_{\lambda_m}\mathbf{G}\bar{\mathbf{a}}_m\|_2)$$

$$\leq \lambda_r \|\mathbf{D}^{-1}\|_2 \sum_{m \in [R] \backslash r} \lambda_m^* \left(\underbrace{\max_i |(\mathbf{F} - \mathbf{G})_{ii}|}_{I_{21}} + (\|\mathbf{d}_{a_m}\|_2 + \Delta_{\lambda_m}) \underbrace{\max_i |\mathbf{G}_{ii}|}_{I_{22}} \right), \tag{S53}$$

where the second inequality is due to the triangle inequality and the third inequality is due to the fact that $\|\bar{\mathbf{a}}_m^*\|_2 \leq \|\mathbf{a}_m^*\|_2 = 1$ and $\|\bar{\mathbf{a}}_m\|_2 \leq \|\mathbf{a}_m\|_2 = 1$ as well as the fact that the matrices $\|\mathbf{F} - \mathbf{G}\|_2$ and $\|\mathbf{G}\|_2$ are diagonal matrices hence there spectral norm is their maximum absolute diagonal value. We focus on bounding bounding I_{21} and I_{22} next.

$$I_{21} = |\sum_{jk} \delta_{ijk}\bar{\mathbf{c}}_m^*(k)\bar{\mathbf{b}}_m^*(j)\mathbf{c}_r(k)\mathbf{b}_r(j) - \sum_{jk} \delta_{ijk}\bar{\mathbf{c}}_m(k)\bar{\mathbf{b}}_m(j)\mathbf{c}_r(k)\mathbf{b}_r(j)|$$

$$\leq |\sum_{jk} \delta_{ijk}\mathbf{d}_{c_m}(k)\bar{\mathbf{b}}_m^*(j)\mathbf{c}_r(k)\mathbf{b}_r(j)| + |\sum_{jk} \delta_{ijk}\bar{\mathbf{c}}_m^*(k)\mathbf{d}_{b_m}(j)\mathbf{c}_r(k)\mathbf{b}_r(j)|$$

$$+ |\sum_{jk} \delta_{ijk}\mathbf{d}_{c_m}(k)\mathbf{d}_{b_m}(j)\mathbf{c}_r(k)\mathbf{b}_r(j)|$$

$$\leq p \left(|\langle \mathbf{d}_{c_m}, \mathbf{c}_r \rangle \langle \bar{\mathbf{b}}_m^*, \mathbf{b}_r \rangle| + |\langle \bar{\mathbf{c}}_m^*, \mathbf{c}_r \rangle \langle \mathbf{d}_{b_m}, \mathbf{b}_r \rangle| + |\langle \mathbf{d}_{c_m}, \mathbf{c}_r \rangle \langle \mathbf{d}_{b_m}, \mathbf{b}_r \rangle| \right)$$

$$+ \gamma(\|\mathbf{d}_{c_m}\|_2 + \|\mathbf{d}_{b_m}\|_2 + \|\mathbf{d}_{c_m}\|_2\|\mathbf{d}_{b_m}\|_2)$$

$$\leq 6p \max_{\mathbf{u} \in \{\mathbf{c}_m, \mathbf{b}_m, \mathbf{c}_r, \mathbf{b}_r,\}} \left((\frac{c_0}{\sqrt{d}} + \|\mathbf{d}_u\|_2), \|\mathbf{d}_u\|_2, \gamma \right) \|\mathbf{d}_u\|_2. \tag{S54}$$

The last inequality above holds with probability $1 - 2d^{-10}$ provided the reveal probability $p \geq \frac{C\mu^3(1+\gamma/3)\log^2(d^{10})}{d^{3/2}\gamma^2}$. The third inequality is due to Lemma 6 by noting that since $\text{supp}(\mathbf{b}_m^*) \subseteq F_b$ then $\bar{\mathbf{b}}_m^*(j) \leq \frac{\mu}{\sqrt{d}}$. Similarly using Lemma 7, and applying the union bound and the fact that

20

$|\langle \mathbf{c}_m, \mathbf{c}_r \rangle \langle \mathbf{b}_m, \mathbf{b}_r \rangle| \leq \max\{\langle \mathbf{c}_m, \mathbf{c}_r \rangle^2, \langle \mathbf{b}_m, \mathbf{b}_r \rangle^2\}, \leq \left(\frac{c_0}{\sqrt{d}} + \max_{\mathbf{u}_r \in \{\mathbf{c}_r, \mathbf{b}_r\}} 3\|\mathbf{d}_{u_r}\|_2 \right)^2$ yields the following inequality

$$I_{22} \leq p \max_{\mathbf{u}_r \in \{\mathbf{c}_r, \mathbf{b}_r, \mathbf{c}_m, \mathbf{b}_m\}} \left((\frac{c_0}{\sqrt{d}} + 3\|\mathbf{d}_{u_r}\|_2)^2, \gamma \right), \tag{S55}$$

with probability $1 - 2d^{-9}$.

Putting equations (S53), (S54),(S55), and Lemma 5 together yields

$$\|err_2\|_2 \leq \frac{\lambda_r 8p \sum_{m \in [R] \backslash r} \lambda_m^* \max_{\mathbf{u} \in \{\mathbf{a}_m, \mathbf{b}_m, \mathbf{a}_r, \mathbf{b}_r,\}} \left((\frac{c_0}{\sqrt{d}} + \|\mathbf{d}_u\|_2), (\frac{c_0}{\sqrt{d}} + 3\|\mathbf{d}_u\|_2)^2, \|\mathbf{d}_u\|_2, \gamma \right) \|\mathbf{d}_u\|_2}{\lambda_r^2 p(1 - \gamma) + \sigma_r^2}, \tag{S56}$$

with probability $1 - 2d^{-9}$ provided $p \geq \frac{C\mu^3(1+\gamma/3)\log^2(d^{10})}{d^{3/2}\gamma^2}$.

Next, we bound the error matrix and error matrix through $\|err_4\|_2$ which is bounded by applying Lemma10, combined with Lemma 5 and the fact that $\|\mathcal{E}_M \mathbf{v}_r\|_2 \leq \|\mathcal{E}_M\|$ since $\|\mathbf{v}_r\|_2 = 1$ and by definition $\|\mathcal{E}_M\| = \sup_{\|\mathbf{u}\|=1} \|\mathcal{E}_M \mathbf{u}\|_2$ yields,

$$\|err_4\|_2 \leq \frac{\lambda_r p(1 + \gamma)\|\mathcal{E}_T\|_{<d+s>} + \sigma_r\|\mathcal{E}_M\|_{<d+s>}}{\lambda_r^2 p(1 - \gamma) + \sigma_r^2}, \tag{S57}$$

with probability $1 - 2d^{-9}$ provided $p \geq \frac{C\mu^4(1+\gamma/3)\log^2(d^{10})}{d^2\gamma^2}$. Combining the error bounds results of $\|err_1\|_2, \|err_3\|_2, \|err_2\|_2, \|err_4\|_2$ in equations (S50), (S56), (S52) and (S57), lettings $\|\mathbf{d_u}\|_2 = \epsilon_T$, for $\mathbf{u} \in \{\mathbf{a}_r, \mathbf{b}_r, \mathbf{c}_r\}$, $\|\mathbf{d}_v\|_2 = \epsilon_M$, $\Delta_{\lambda_r} = \frac{\epsilon_T}{\lambda_r^*}$ and $\Delta_{\sigma_r} = \frac{\epsilon_M}{\sigma_r^*}$ $\forall r \in [R]$ and using the fact that $\lambda_r^* - \epsilon_T \leq \lambda_r \leq \lambda_r^* + \epsilon_T$ and $\sigma_r^* - \epsilon_T \leq \sigma_r \leq \lambda_r^* + \epsilon_T$ for all $r \in [R]$, yields

$\|\dot{\mathbf{a}}_r - \mathbf{a}_r^*\|_2$

$$\leq \frac{8pR\lambda_{max}^*(\lambda_r^* + \epsilon_T) \max_{\mathbf{u} \in \{\mathbf{c}_m, \mathbf{b}_m, \mathbf{c}_r, \mathbf{b}_r,\}} \left(\sqrt{1 - \frac{\epsilon_T}{2}}\epsilon_T, (\frac{c_0}{\sqrt{d}} + \epsilon_T), (\frac{c_0}{\sqrt{d}} + 3\epsilon_T)^2, \epsilon_T, \gamma, 1/\lambda_{min}^* \right) \epsilon_T}{(\lambda_{min}^* - \epsilon_T)^2 p(1 - \gamma) + (\sigma_{min}^* - \epsilon_M)^2}$$

$$+ \frac{3R\sigma_{max}(\sigma_r^* + \epsilon_M) \max \left(\epsilon_M, 1/\sigma_{min}^*, \frac{c_0}{\sqrt{d}} + 3\epsilon_M \right) \epsilon_M}{(\lambda_{min}^* - \epsilon_T)^2 p(1 - \gamma) + (\sigma_{min}^* - \epsilon_M)^2}$$

$$+ \frac{(\lambda_r^* + \epsilon_T)p(1 + \gamma)\|\mathcal{E}_T\|_{<d+s>} + (\sigma_r^* + \epsilon_T)\|\mathcal{E}_M\|_{<d+s>}}{(\lambda_{min}^* - \epsilon_T)^2 p(1 - \gamma) + (\sigma_{min}^* - \epsilon_M)^2}, \tag{S58}$$

with probability $1 - 2d^{-9}$. Simplifying the expression completes the proof for step 1 of the Lemma 4.

Step2: We now get an upper bound for $\|\mathbf{a}_r - \dot{\mathbf{a}}_r\|_2$. Note that

$$\|\mathbf{a}_r - \dot{\mathbf{a}}_r\|_2 = \|\frac{\dot{\mathbf{a}}_r}{\|\dot{\mathbf{a}}_r\|_2} - \dot{\mathbf{a}}_r\|_2 = \|\frac{\dot{\mathbf{a}}_r}{\|\dot{\mathbf{a}}_r\|}\|_2 |1 - \|\dot{\mathbf{a}}_r\|_2| = |1 - \|\dot{\mathbf{a}}_r\|_2|.$$

Hence bounding $\|\mathbf{a}_r - \dot{\mathbf{a}}_r\|_2$ simplifies to bounding $|1 - \|\dot{\mathbf{a}}_r\|_2|$. Using the expression of $\dot{\mathbf{a}}_r$ in (S46) and applying the triangle inequality we get,

$$|1 - \|\dot{\mathbf{a}}_r\|_2| \leq \underbrace{|1 - \|\lambda_r \mathbf{D}^{-1}\lambda_r^* \mathbf{E}\bar{\mathbf{a}}_r^* + \sigma_r \mathbf{D}^{-1}\sigma_r^* \mathbf{H}\bar{\mathbf{a}}_r^*\|_2|}_{I} + \underbrace{\|\lambda_r \mathbf{D}^{-1} \sum_{m \in [R] \setminus r} (\lambda_m^* \mathbf{F}\bar{\mathbf{a}}_m^* - \lambda_m \mathbf{G}\bar{\mathbf{a}}_m)\|_2}_{II}$$

$$+ \underbrace{\|\sigma_r \mathbf{D}^{-1} \sum_{m \in [R] \setminus r} (\sigma_m^* \mathbf{J}\bar{\mathbf{a}}_m^* - \sigma_m \mathbf{P}\bar{\mathbf{a}}_m)\|_2}_{III} + \underbrace{\|\mathcal{E}_{T_F} \times_2 \mathbf{b}_r \times_3 \mathbf{c}_r + \mathcal{E}_{M_{F'}} \mathbf{v}_r\|_2}_{IV}. \tag{S59}$$

Bounds for elements (II) (III) and (IV) in the equation above are derived in (S56), (S52) and (S57) respectively. Hence we only focus on bounding elements (I).

$$I = |\|\mathbf{a}_r^*\|_2 - \|\lambda_r \mathbf{D}^{-1}\lambda_r^* \mathbf{E}\bar{\mathbf{a}}_r^* + \sigma_r \mathbf{D}^{-1}\sigma_r^* \mathbf{H}\bar{\mathbf{a}}_r^*\|_2|$$

$$\leq \|\mathbf{a}_r^* - \mathbf{D}^{-1}(\lambda_r \lambda_r^* \mathbf{E} + \sigma_r \sigma_r^* \mathbf{H})\bar{\mathbf{a}}_r^*\|_2$$

$$= \|\mathbf{D}^{-1}(\lambda_r \lambda_r^* \mathbf{E} + \sigma_r \sigma_r^* \mathbf{H} - \mathbf{D}\mathbf{I})\bar{\mathbf{a}}_r^*\|_2$$

$$= \|err_1\|_2, \tag{S60}$$

where err_1 is the error component defined in (S47) and bounded in (S50). The first equality is obtained by using the fact that $\|\mathbf{a}_r^*\|_2 = 1$, vector norm property is then use to get the first inequality and finally second equality is due to $\mathbf{a}_r^* = \mathbf{D}^{-1}\mathbf{D}\mathbf{a}_r^*$ and the fact that $\bar{\mathbf{a}}_r^* = \mathbf{a}_r^*$ since $F_a = supp(\mathbf{a}_r^*) \subseteq supp(\bar{\mathbf{a}}_r^*) = F$. Hence combining the results in equations (??) and (S59) yields,

$$\|\mathbf{a}_r - \dot{\mathbf{a}}_r\|_2 \leq I + II + III + III + IV$$

$$\leq \|\dot{\mathbf{a}}_r - \mathbf{a}_r^*\|_2, \tag{S61}$$

which ends step 2 of the proof. The proof of Lemma 4 is completed by combining results of step 1 and step 2 which shows that $\|\mathbf{a}_r - \mathbf{a}_r^*\|_2 \leq 2\|\dot{\mathbf{a}}_r - \mathbf{a}_r^*\|_2$, and taking the maximum over all r. $\square$

S.3   Auxillary Lemmas

Lemma 5. *Let $\mathbf{u}$ and $\mathbf{w}$ be unit vectors in $\mathbb{R}^n$ such that $|\mathbf{u}(i)| \leq \frac{\mu}{\sqrt{d}}$ and $|\mathbf{w}(j)| \leq \frac{\beta}{\sqrt{d}}$. Also let $\delta_{i,j,k}$ be i.i.d. Bernoulli random variables with $P(\delta_{ijk} = 1) = p$ and $1 \leq i \leq n$, $1 \leq j \leq n$, $1 \leq k \leq n$. Then provided $p \geq \frac{C\mu^2\beta^2(1+\gamma/3)\log(d^{10})}{d^2\gamma^2}$ we have*

$$|\sum_{j,k} \delta_{ijk}\mathbf{u}_r^2(j)\mathbf{w}_r^2(k)| \leq p\langle\mathbf{u},\mathbf{u}\rangle\langle\mathbf{w},\mathbf{w}\rangle - p\gamma,$$

with probability $1 - d^{-10}$.

Proof: Let $X_{jk} = \frac{1}{p}\left(\delta_{ijk}\mathbf{u}^2(j)\mathbf{w}^2(k) - E(\delta_{ijk}\mathbf{u}^2(j)\mathbf{w}^2(k))\right)$. Using the bound on the elements of $\mathbf{u}$ and $\mathbf{w}$, we have $|X_{jk}| = |\frac{1}{p}(\delta_{ijk} - p)\mathbf{u}^2(j)\mathbf{w}^2(k)| \leq \frac{\mu^2\beta^2}{pd^2}$. Also

$$\sum_{j,k} E[X_{jk}^2] = \frac{1}{p}(1-p)\sum_{j,k}\mathbf{u}_r^4(j)\mathbf{w}_r^4(k) \leq \frac{\mu^2\beta^2}{pd^2}.$$

Applying Bernstein tail bound inequality we get:

$$P\left(|\sum_{j,k}\delta_{ijk}\mathbf{u}_r^2(j)\mathbf{w}_r^2(k) - p\langle\mathbf{u},\mathbf{u}\rangle\langle\mathbf{w},\mathbf{w}\rangle| \geq pt\right) \leq \exp\left(\frac{-d^2pt^2/2}{\mu^2\beta^2(1+\frac{1}{3}t)}\right).$$

Setting the right side of the inequality to be less than q yields:

$$P\left(|\sum_{j,k}\delta_{ijk}\mathbf{u}_r^2(j)\mathbf{w}_r^2(k)| \leq p\langle\mathbf{u},\mathbf{u}\rangle\langle\mathbf{w},\mathbf{w}\rangle - p\gamma\right) \geq 1-q,$$

for $p \geq \frac{\mu^2\beta^2(1+\gamma/3)\log(1/q)}{d^2\gamma^2}$. Choosing $q \leq d^{-10}$ completes the proof of Lemma 5. $\square$

Lemma 6. *Let $\mathbf{u}^*$, $\mathbf{u}$ and $\mathbf{w}$ be unit vectors in $\mathbb{R}^n$ such that $|\mathbf{u}_i^*| \leq \frac{\mu}{\sqrt{d}}$, $|\mathbf{u}|$ and $|\mathbf{w}| \leq \frac{\beta}{\sqrt{d}}$. Let $\mathbf{d}$ be another vector with $\|\mathbf{d}\|_2 \leq 1$. Also let $\delta_{i,j,k}$ be i.i.d. Bernoulli random variables with $P(\delta_{ijk} = 1) = p$ and $1 \leq i \leq n$, $1 \leq j \leq n$, $1 \leq k \leq n$. Provided $p \geq \frac{C\mu\beta^2(1+\gamma/3)\log^2(\frac{1}{2}d^{10})}{d^{3/2}\gamma^2}$, with probability greater than $1 - 2d^{-10}$, we have*

$$|\sum_{j,k}\delta_{ijk}\mathbf{u}^*(j)\mathbf{d}(k)\mathbf{u}(j)\mathbf{w}(k) - p\langle\mathbf{u}^*,\mathbf{u}\rangle\langle\mathbf{d},\mathbf{w}\rangle| \leq p\gamma\|\mathbf{d}\|_2.$$

Proof: Let $X_{jk} = \frac{1}{p}\left(\delta_{ijk}\mathbf{u}^*(j)\mathbf{d}(k)\mathbf{u}(j)\mathbf{w}(k) - E(\delta_{ijk}\mathbf{u}^*(j)\mathbf{d}(k)\mathbf{u}(j)\mathbf{w}(k))\right)$. Then we have That is $|X_{jk}| = \frac{1}{p}(\delta_{ijk} - p)\mathbf{u}^*(j)\mathbf{d}(k)\mathbf{u}(j)\mathbf{w}(k) \leq \frac{1}{p}(1-p)\frac{\mu\beta^2}{d^{3/2}}\|\mathbf{d}\|_2$. Also,

$$\sum_{j,k} E[X_{jk}^2] = \frac{1}{p}\sum_{j,k}(\mathbf{u}(j)^2\mathbf{d}(k)^2\mathbf{u}(j)^2\mathbf{w}(k)^2) \leq \frac{\mu\beta^2\|d\|_2^2}{pd^{3/2}}.$$

Applying Bernstein tail bound inequality we get:

$$P\left(|\sum_{j,k}\delta_{ijk}\mathbf{u}^*(j)\mathbf{d}(k)\mathbf{u}(j)\mathbf{w}(k) - p\langle\mathbf{u}^*,\mathbf{u}\rangle\langle\mathbf{d},\mathbf{w}\rangle| \geq pt\right) \leq 2\exp\left(\frac{-d^{3/2}pt^2}{\mu\beta^2\|\mathbf{d}\|_2(\|\mathbf{d}\|_2 + \frac{1}{3}t)}\right). \quad \text{(S62)}$$

Setting the right side of the inequality to be less than q and choosing $t \leq \gamma\|\mathbf{d}\|_2$ then solving for p yields:

$$P\left(|\sum_{j,k}\delta_{ijk}\mathbf{u}^*(j)\mathbf{d}(k)\mathbf{u}(j)\mathbf{w}(k) - p\langle\mathbf{u}^*,\mathbf{u}\rangle\langle\mathbf{d},\mathbf{w}\rangle| \leq p\gamma\|b\|_2\right) \geq 1-2q,$$

for $p \geq \frac{\mu\beta^2(1+\gamma/3)\log(\frac{1}{q})}{d^{3/2}\gamma^2}$. Choosing $q \leq d^{-10}$ completes the proof of Lemma 6. $\hfill\square$

Lemma 7. *Let $\mathbf{u}^*$, $\mathbf{w}^*$, $\mathbf{u}$ and $\mathbf{w}$ be unit vectors in $\mathbb{R}^n$ such that $|\mathbf{u}^*(i)|$ and $|\mathbf{w}^*(j)| \leq \frac{\mu}{\sqrt{d}}$, $|\mathbf{u}_i|$ and $|\mathbf{w}_i| \leq \frac{\beta}{\sqrt{d}}$. Let $\delta_{i,j,k}$ be i.i.d. Bernoulli random variables with $P(\delta_{ijk} = 1) = p$ and $1 \leq i, j, k \leq n$. Provided $p \geq \frac{C\mu^2\beta^2(1+\gamma/3)\log(\frac{1}{2}d^{10})}{d^2\gamma^2}$, with probability greater than $1 - 2d^{-10}$, we have*

$$|\sum_{j,k} \delta_{ijk}\mathbf{u}^*(j)\mathbf{w}^*(k)\mathbf{u}(j)\mathbf{w}(k)| \leq p|\langle\mathbf{u}^*,\mathbf{u}\rangle\langle\mathbf{w}^*\mathbf{w}\rangle| + p\gamma.$$

Proof: Let $X_{jk} = \frac{1}{p}\left(\delta_{ijk}\mathbf{u}^*(j)\mathbf{w}^*(k)\mathbf{u}(j)\mathbf{w}(k) - E(\delta_{ijk}\mathbf{u}^*(j)\mathbf{w}^*(k)\mathbf{u}(j)\mathbf{w}(k))\right)$. Then we have $|X_{jk}| = \frac{1}{p}(\delta_{ijk} - p)\mathbf{u}^*(j)\mathbf{w}^*(k)\mathbf{u}(j)\mathbf{w}(k) \leq \frac{1}{p}(1-p)\frac{\mu^2\beta^2}{d^2}$.Also

$$\sum_{j,k} E[X_{jk}^2] = \frac{1}{p}(1-p)\sum_{j,k}(\mathbf{u}(j)^{2*}\mathbf{w}(k)^{*2}\mathbf{u}(j)^2\mathbf{w}(k)^2) \leq \frac{1}{p}(1-p)\frac{\mu^2\beta^2}{d^2}.$$

Applying Bernstein tail bound inequality we get:

$$P\left(|\sum_{j,k} \delta_{ijk}\mathbf{u}^*(j)\mathbf{d}(k)\mathbf{u}(j)\mathbf{w}(k) - p\langle\mathbf{u}^*,\mathbf{u}\rangle\langle\mathbf{d},\mathbf{w}\rangle| \geq pt\right) \leq 2\exp\left(\frac{-d^2pt^2}{\mu^2\beta^2(1-p)(1+\frac{1}{3}t)}\right).$$

Setting the right side of the inequality to be less than q and choosing $t \leq \gamma$ then solving for p yields:

$$P\left(|\sum_{j,k} \delta_{ijk}\mathbf{u}^*(j)\mathbf{w}^*(k)\mathbf{u}(j)\mathbf{w}(k) - \langle\mathbf{u}^*,\mathbf{u}\rangle\langle\mathbf{w}^*\mathbf{w}\rangle| \leq p\gamma\right) \geq 1 - 2q,$$

and $p \geq \frac{\mu^2\beta^2(1+\gamma/3)\log(\frac{1}{q})}{d^2\gamma^2}$. Letting $q \leq d^{-10}$ completes the proof of Lemma 7. $\hfill\square$

Lemma 8. *Let λ_r be the update of the rth weight of the tensor after one iteration of Algorithm 1 and let λ_r^* be the true r^{th} weight of the tensor decomposition in the dense tensor and dense matrix case. Let $\widetilde{\mathbf{c}}$ be as defined in (S6) and $\mathbf{c}$ as defined in (S4) then with probability greater than $1 - 2n^{-9}$ we have*

$$|\lambda_r - \lambda_r^*| \leq \|\widetilde{\mathbf{c}}_r - \lambda_r^*\mathbf{c}_r^*\|_2.$$

Proof: We know that $\|\mathbf{c}_r^*\|_2 = \|\mathbf{c}_r\|_2 = 1$ hence we can write,

$$\begin{aligned}|\lambda_r - \lambda_r^*| &= |\|\lambda_r\mathbf{c}_r\|_2 - \|\lambda_r^*\mathbf{c}_r^*\|_2| \\ &\leq \|\lambda_r\mathbf{c}_r - \lambda_r^*\mathbf{c}_r^*\|_2 \\ &= \|\widetilde{\mathbf{c}}_r - \lambda_r^*\mathbf{c}_r^*\|_2\end{aligned}$$

The last equality above is obtained by observing that $\widetilde{\mathbf{c}}_r = \lambda_r \mathbf{c}_r$ as shown in the proof of Lemma1. This complete the proof of the Lemma. Notice that the above Lemma can also be applied on σ_r to obtain $|\sigma_r - \sigma_r^*| \leq \|\widetilde{\mathbf{v}_r} - \sigma_r^* \mathbf{v}_r^*\|_2$. $\square$

Lemma 9. *Let $\widetilde{\mathbf{c}}$ be as defined in* (S6) *and $\mathbf{c}$ as defined in* (S4). *Also let λ_r be the update of the rth weight of the tensor after one iteration of Algorithm* 1 *and let λ_r^* be the true r^{th} weight of the tensor decomposition in the dense tensor and dense matrix case. Then with probability greater than $1 - 2n^{-9}$ we have*

$$\|\mathbf{c}_r - \mathbf{c}_r^*\|_2 \leq \frac{2}{\lambda_r^*} \|\widetilde{\mathbf{c}}_r - \lambda_r^* \mathbf{c}_r^*\|_2,$$

$$\|\mathbf{c}_r - \mathbf{c}_r^*\|_2 + \Delta_{\lambda_r} \leq \frac{3}{\lambda_r^*} \|\widetilde{\mathbf{c}}_r - \lambda_r^* \mathbf{c}_r^*\|_2,$$

where Δ_{λ_r} is as defined in (S2).

Proof:

$$
\begin{aligned}
\lambda_r^* \|\mathbf{c}_r - \mathbf{c}_r^*\|_2 &= \|\lambda_r^* \mathbf{c}_r - \lambda_r^* \mathbf{c}_r^*\|_2 \\
&= \|\lambda_r \mathbf{c}_r - \lambda_r^* \mathbf{c}_r^* - \epsilon_{\lambda_r} \mathbf{c}_r\|_2 \leq \|\lambda_r \mathbf{c}_r - \lambda_r^* \mathbf{c}_r^*\|_2 + \|\epsilon_{\lambda_r} \mathbf{c}_r\|_2 \\
&= \|\widetilde{\mathbf{c}}_r - \lambda_r^* \mathbf{c}_r^*\|_2 + |\lambda_r - \lambda_r^*| \\
&\leq 2\|\widetilde{\mathbf{c}}_r - \lambda_r^* \mathbf{c}_r^*\|_2, &\text{(S63)}
\end{aligned}
$$

which proves the first inequality of the Lemma. The proof of the second inequality in the lemma is obtained by combining (S63) with the results of Lemma 8. $\square$

Lemma 10. *For any tensor $\mathcal{E}_T \in \mathbb{R}^{n \times n \times n}$ and any vectors $\mathbf{u}$ and $\mathbf{v} \in \mathbb{R}^n$ with $\|\mathbf{u}\|_2 = \|\mathbf{v}\|_2 = 1$, we have*

$$\|\mathcal{E}_T \times_1 \mathbf{u} \times_2 \mathbf{v}\|_2 \leq \|\mathcal{E}_T\|,$$

where $\|\mathcal{E}_T\|$ represents the spectral norm of the tensor defined in (1).

Proof:

$$\|\mathcal{E}_T \times_1 \mathbf{u} \times_2 \mathbf{v}\|_2 = \frac{\|\mathcal{E}_T \times_1 \mathbf{u} \times_2 \mathbf{v}\|_2^2}{\|\mathcal{E}_T \times_1 \mathbf{u} \times_2 \mathbf{v}\|_2}$$

$$= \left| \mathcal{E}_T \times_1 \mathbf{u} \times_2 \mathbf{v} \times_3 \left(\frac{\mathcal{E}_T \times_1 \mathbf{u} \times_2 \mathbf{v}}{\|\mathcal{E}_T \times_1 \mathbf{u} \times_2 \mathbf{v}\|_2} \right) \right|$$

$$\geq \sup_{\|\mathbf{u}\|=\|\mathbf{v}\|=\|\mathbf{w}\|=1} \left| \mathcal{E}_T \times_1 \mathbf{u} \times_2 \mathbf{v} \times_3 \mathbf{w} \right|$$

$$= \|\mathcal{E}_T\|.$$

The first inequality is due to $\|\mathbf{u}\|_2 = \|\mathbf{v}\|_2 = 1$ and the fact that $\frac{\mathcal{E}_T \times_1 \mathbf{u} \times_2 \mathbf{v}}{\|\mathcal{E}_T \times_1 \mathbf{u} \times_2 \mathbf{v}\|_2} = 1$. The last equality is obtained by applying the definition of the tensor spectral norm provided in (1). $\qquad \square$

Lemma 11. *Let* $\mathbf{u}$ *and* $\mathbf{w}$ *be unit vectors and let* $\mathbf{d}$ *be a vector such that* $\mathbf{d} = \mathbf{u} - \mathbf{w}$ *then*

$$|\langle \mathbf{w}, \mathbf{d} \rangle| = \frac{1}{2} \|\mathbf{d}\|_2^2.$$

Proof: Note that $\|\mathbf{u}\|_2^2 = \sum (\mathbf{w}(i) + \mathbf{d}(i))^2$. Hence given that $\mathbf{u}$ is a unit vector we get

$$\sum \mathbf{w}(i)^2 + 2 \sum \mathbf{w}(i)\mathbf{d}(i) + \sum \mathbf{d}(i)^2 = 1$$

$$2 \sum \mathbf{w}(i)\mathbf{d}(i) + \sum \mathbf{d}(i)^2 = 0$$

$$2 \sum \mathbf{w}(i)\mathbf{d}(i) = -\sum \mathbf{d}(i)^2$$

$$|\langle \mathbf{w}, \mathbf{d} \rangle| = \frac{1}{2} \|\mathbf{d}\|_2^2,$$

Which completes the proof of the lemma. $\qquad \square$

Lemma 12. *Let* $\mathbf{u}$ *and* $\mathbf{w}$ *be unit vectors define* $F_1 := supp(\mathbf{u})$, $F_2 := supp(\mathbf{w})$ *be the support sets for* $\mathbf{u}$ *and* $\mathbf{w}$ *respectively with* $F_i \subseteq \{1, \cdots d\}$ *and* $F := F_u \cup F_w$ *be the union of the two vectors' support sets. Let* $\bar{\mathbf{u}} := Truncate(\mathbf{u}, F)$ *then it follows that*

$$\langle \bar{\mathbf{u}}, \mathbf{w} \rangle = \langle \mathbf{u}, \mathbf{w} \rangle.$$

Proof: Since by definition, $\bar{\mathbf{u}} := \text{Truncate}(\mathbf{u}, F)$, then we can write $\langle \bar{\mathbf{u}}, \mathbf{w} \rangle$ explicitly as $\langle \bar{\mathbf{u}}, \mathbf{w} \rangle = \sum_{i \in [d]} \bar{\mathbf{u}}(i)\mathbf{w}(i)$. Since $\bar{\mathbf{u}}(i) \neq 0$ only when $i \in F_1$ and $i \in F_2$, we get $\sum_{i \in [d]} \bar{\mathbf{u}}(i)\mathbf{w}(i) = \sum_{i \in F} \mathbf{u}(i)\mathbf{w}(i)$.
However, we know that $\text{supp}(\mathbf{w}) = F_2 \subseteq F$ hence we get

$$\langle \bar{\mathbf{u}}, \mathbf{w} \rangle = \sum_{i \in F} \mathbf{u}(i)\mathbf{w}(i) = \sum_{i \in [d]} \mathbf{u}(i)\mathbf{w}(i) = \langle \mathbf{u}, \mathbf{w} \rangle.$$

$\qquad \square$

S.4 Additional Simulations

In these two additional simulations, we focus solely on the recovery accuracy of the shared and non-shared tensor components under our `COSTCO` to investigate the practical effect of component dimensions size and the rank on our algorithm.

Component Size: This part of the simulation considers the effect of varying the size of the coupled components $\mathbf{A}^*$ of the true tensor on the tensor recovery. We set the tensor missing entry percentage to be 90%; the noise level parameters are set to be $\eta_T = 0.001$ and $\eta_M = 0.001$ respectively and the sparsity level is kept at 60%. The complete simulation results are presented in Table S5. The tensor completion error improves with increasing size of the shared dimension since there is more information provided by the covariate matrix. With more and more information provided from the covariate matrix, the latent structure of the shared component dominates those of the non-shared components, making it easier to complete the whole tensor.

Table S5: Estimation errors of `COSTCO` with varying coupled dimension d_1.

Coupled Dimension d_1	Estimation Error					
	$\mathcal{T}$	Comp $\ddot{\mathbf{A}}$	Comp $\mathbf{B}$	Comp $\mathbf{C}$	Comp $\mathbf{D}$	$\boldsymbol{\lambda}$
20	5.64e-05	1.77e-05	3.67e-05	3.51e-05	3.68e-05	1.60e-06
	(1.24e-11)	(6.09e-12)	(1.41e-11)	(1.88e-11)	(2.20e-11)	(6.09e-13)
50	3.71e-05	1.72e-05	2.35e-05	2.39e-05	2.44e-05	1.25e-06
	(3.29e-12)	(2.66e-12)	(2.59e-12)	(4.06e-12)	(4.72e-12)	(5.14e-13)
100	2.66e-05	1.73e-05	1.72e-05	1.76e-05	1.77e-05	7.65e-07
	(1.43e-12)	(5.69e-13)	(2.86e-12)	(3.50e-12)	(1.96e-12)	(1.34e-13)

Rank: In this case we investigate the impact of the rank of the tensor and matrix on the tensor recovery performance of our `COSTCO` algorithm. We set the missing percentage of the tensor to 90%, the sparsity to be 60% and the tensor and matrix noise levels η_T and η_M to be both 0.001. We still tune the rank and cardinality using the procedure in Section 3.2.2. As shown in Table S6, the recovery error is an increasing function of the tensor rank. It is well documented that the noisy tensor completion problem in general gets harder as the rank increases (Song et al., 2019).

Table S6: Estimation errors of `COSTCO` with varying rank.

Tensor Rank	Estimation Error					
	$\mathcal{T}$	Comp $\ddot{\mathbf{A}}$	Comp $\mathbf{B}$	Comp $\mathbf{C}$	Comp $\mathbf{D}$	$\boldsymbol{\lambda}$
1	4.78e-05	2.76e-05	1.97e-06	2.77e-05	2.62e-05	5.31e-06
	(1.34e-11)	(1.67e-11)	(6.72e-14)	(7.50e-12)	(1.38e-11)	(1.29e-11)
2	6.50e-05	6.78e-05	1.39e-05	6.63e-05	6.66e-05	1.26e-05
	(1.04e-11)	(6.82e-11)	(4.67e-11)	(5.07e-11)	(7.16e-11)	(3.76e-11)
3	8.57e-05	7.82e-05	2.76e-05	7.99e-05	7.81e-05	1.32e-05
	(2.52e-11)	(5.27e-11)	(1.11e-10)	(8.10e-11)	(5.97e-11)	(4.14e-11)